Sand-Mud Morphodynamics

Colina Alonso, A.

DOI
10.4233/uuid:8bd55ce1-adc7-486d-9bfa-7aa7b929bbe3

Publication date
2024

Document Version
Final published version

Citation (APA)
Colina Alonso, A. (2024). *Sand-Mud Morphodynamics*. [Dissertation (TU Delft), Delft University of Technology]. https://doi.org/10.4233/uuid:8bd55ce1-adc7-486d-9bfa-7aa7b929bbe3

Ana Colina Alonso

SAND-MUD MORPHODYNAMICS

Sand-Mud Morphodynamics

Sand-Mud Morphodynamics

Proefschrift

ter verkrijging van de graad van doctor
aan de Technische Universiteit Delft,
op gezag van de Rector Magnificus Prof. dr. ir. T.H.J.J. van der Hagen,
voorzitter van het College voor Promoties,
in het openbaar te verdedigen op vrijdag 1 maart 2024 om 12:30 uur

door

Ana COLINA ALONSO

Ingenieur in de Civiele Techniek,
Technische Universiteit Delft, Nederland,
geboren te Madrid, Spanje.

Dit proefschrift is goedgekeurd door de promotoren.

Samenstelling promotiecommissie:

Rector Magnificus,	voorzitter
Prof. dr. ir. Z.B. Wang,	Technische Universiteit Delft, promotor
Prof. dr. D.S. van Maren,	East China Normal University, promotor
Onafhankelijke leden:	
Prof. dr. Q. He,	East China Normal University
Prof. dr. S. Fagherazzi,	Boston University
Prof. dr. M.G. Kleinhans,	Utrecht University
Dr. ir. M. van Ledden,	World Bank Consultant
Prof. dr. ir. S.G.J. Aarninkhof,	Technische Universiteit Delft
Prof. dr. ir. A.J.H.M. Reniers,	Technische Universiteit Delft, reservelid

This work is part of the project '*Coping with Deltas in Transition*', which is funded by the Royal Netherlands Academy of Arts and Sciences (KNAW) within the framework of the Programme Strategic Scientific Alliances between China and the Netherlands (PSA-SA-E-02).

Keywords: sand-mud, morphodynamics, tidal basins, Wadden Sea, numerical modeling

Printed by: Ridderprint, www.ridderprint.nl

Front & Back: Design by Ana Colina Alonso, aerial photos by Kevin Krautgartner

ISBN 978-94-6366-816-3

An electronic version of this dissertation is available at http://repository.tudelft.nl/.

You can never cross the ocean until you have
the courage to lose sight of the shore.

André Gide

The earth, the air, the land, and the water are not an
inheritance from our forefathers but on loan from our children.
So we have to handover to them at least as it was handed over to us.

Gandhi

CONTENTS

SUMMARY

The world's coasts and deltas offer a multitude of valuable ecosystem services, providing safety against flooding and economic benefits. Many of these systems are, however, under pressure by climate change and increasing human activities. Protecting these systems and preservation of their multiple functions requires a thorough understanding of their morphodynamic behaviour. The sediment bed in many coastal systems worldwide is composed of two sediment types: sand and mud. While most previous research focused on the individual sediment dynamics of sand and mud, little is still known about how combined sand-mud morphodynamics differs from the sum of individual sediment fractions. In order to assess the impacts of anthropogenic interventions and climate change, we thus need to better understand sand-mud morphodynamics.

This research aims to improve the understanding of large-scale morphodynamics in sand-mud tidal systems. This is done by investigating processes related to long-term deposition, sediment supply, sand-mud interaction, and segregation of sand and mud. We focus on generic idealized cases, as well as on case studies in the Wadden Sea — an example of a heavily-impacted system whose existence is threatened by sea level rise (SLR). Unique long-term data sets of its hydrodynamics, bathymetry and sediment composition are available, making this an excellent area to study the morphological responses to human interventions in detail, and to improve our understanding of sand-mud morphodynamics.

Analysis of the morphological evolution after a closure in the Western Dutch Wadden Sea (Chapter 2) illustrates the importance of distinguishing between the response of sandy and muddy sediments when analyzing the morphodynamic impact of an intervention. Our findings reveal that sand and mud respond on different temporal and spatial scales. Moreover, the results show that the contribution of mud to the total infilling was much larger than the average mud content in the top layer of the bed, because mud preferentially deposits in areas with high net sedimentation rates. This demonstrates that the contribution of sediment types to morphological change is not necessarily reflected by the spatial bed composition.

Up to now, the availability of mud to the Wadden Sea was poorly known, while we know that this availability is crucial for predicting the response to future climate change. Therefore, a first system-wide mud budget of the Wadden Sea has been developed (Chapter 3), revealing a nearly closed balance between the sources and the sinks. This observation implies that disturbing the mud balance at one location will impact downdrift areas. Anthropogenic sediment extraction provides the second largest sink, even surpassing salt marsh deposition. Field data suggest that a mud deficit already exists in some areas of the Wadden Sea, which will only become more pronounced with increased SLR rates. Mud is

thus a finite resource similar to sand, and should be treated as such in sediment management strategies. Furthermore, local interventions may have consequences in downdrift areas, stressing the need for a cross-bordering perspective.

The influence of small-scale sand-mud interaction on large-scale modeled morphodynamic development has been studied by implementing two abiotic interactions (erosion interaction and roughness interaction) in a process-based model (Chapter 4). Model output was converted into metrics that describe the macro-scale configuration of the modeled systems, allowing a quantitative comparison of scenarios. The results demonstrate that sand-mud interaction can significantly impact tidal basin evolution, especially having a large influence on the intertidal flat shape, size and composition.

Lastly, we have seen that the mud content of the sediment bed in tidal systems is often bimodally distributed, indicating a preferential sand-mud segregation (Chapter 5). Bimodality represents the existence of two stable equilibrium conditions, which result from sediment deposition processes (and not erosion processes), and can be expected for a large range of suspended sediment concentrations in sand-mud systems. In order to correctly reproduce this bimodal character in process-based models, and therefore correctly modeling the bed sediment composition, one must account for erosion interaction in the model set-up — despite the role of deposition as a driving mechanism.

In conclusion, this dissertation illustrates the importance of a sand-mud perspective in morphodynamic studies, considering the contribution of both sediment types to the morphodynamic development as well as their interactions. We have seen that advancing our understanding of sand-mud morphodynamics requires combined data-based and modeling approaches, adopting a system-wide perspective, and considering the interactions between the various spatial and temporal scales. Morphological metrics, such as the ones that have been presented, are essential for the evaluation and comparison of model results and coastal morphology worldwide. Enabling successful and sustainable management of coasts and deltas will require further increasing our understanding of sand-mud morphodynamics through additional measurements and modeling studies. Developing a system understanding should be at the heart of all of these studies.

SAMENVATTING

Wereldwijd leveren kusten en delta's waardevolle ecosysteemdiensten, en bieden daarbij onder andere bescherming tegen overstromingen en economische voordelen. Veel van deze systemen staan echter onder grote druk door klimaatverandering en toenemend menselijk ingrijpen. Het beschermen van deze gebieden en het behouden van hun functies vereist een grondig begrip van hun morfodynamisch gedrag. De zeebodem in veel kustsystemen wereldwijd bestaat uit twee soorten sediment: zand en slib. Voorgaand onderzoek richtte zich doorgaans op de sedimentdynamica van de individuele zand en slib fracties, terwijl nog maar weinig bekend is over hoe gecombineerde zand-slib morfodynamica hiervan verschilt. Het bepalen van de impact van antropogene ingrepen en klimaatverandering vereist dus in eerste instantie een beter begrip van zand-slib morfodynamica.

Dit onderzoek heeft tot doel het begrip van grootschalige morfodynamica in zand-slib getijdesystemen te verbeteren. Hiertoe worden processen onderzocht die verband houden met langetermijn afzettingen, sedimentaanvoer, zand-slib interactie en segregatie van zand en slib. We richten ons op generieke geïdealiseerde gevallen, evenals op casestudies in de Waddenzee — een voorbeeld van een sterk beïnvloed systeem en waarvan het voortbestaan bovendien wordt bedreigd door zeespiegelstijging (ZSS). Er zijn unieke datasets beschikbaar over de hydrodynamica, bodemhoogtes en bodemsamenstelling van de Waddenzee, wat het een uiterst geschikt gebied maakt om de morfologische reacties op menselijke ingrepen in detail te bestuderen en om ons begrip van zand-slib morfodynamica te vergroten.

Een analyse van de morfologische ontwikkeling na een afsluiting in de Westelijke Waddenzee (Hoofdstuk 2) heeft aangetoond hoe belangrijk het is om onderscheid te maken tussen de respons van zand en slib bij het bepalen van de morfodynamische impact van een ingreep, aangezien ze op verschillende tijd- en ruimteschalen opereren. Bovendien tonen de resultaten dat de bijdrage van slib aan de totale opvulling veel groter is dan het gemiddelde slibgehalte in de toplaag van de bodem, omdat slib bij voorkeur wordt afgezet in gebieden met hoge sedimentatiesnelheden. Dit bewijst dat de bijdrage van individuele sedimenttypen aan morfologische verandering niet noodzakelijkerwijs wordt weerspiegeld in de ruimtelijke verdeling van de bodemsamenstelling.

Tot nu toe was niet bekend hoeveel slib beschikbaar is voor de Waddenzee, waardoor de impact van toekomstige klimaatverandering moeilijk te voorspellen is. Daarom is een eerste systeembrede slibbalans van de hele Waddenzee opgesteld (Hoofdstuk 3), waaruit is gebleken dat de balans tussen de bronnen en de putten bijna gesloten is. Dit betekent dat een lokale verstoring van de sedimentbalans benedenstrooms invloed zal hebben. Sedimentonttrekking is de op een na grootste put en is zelfs groter dan de afzetting

in kwelders. Velddata suggereren dat er al een slibtekort bestaat in sommige delen van de Waddenzee, dat alleen maar groter zal worden bij versnelde ZSS. Slib is dus net als zand een eindige natuurlijke hulpbron en moet als zodanig worden behandeld in sedimentbeheerstrategieën. Bovendien kunnen lokale ingrepen gevolgen hebben in gebieden stroomafwaarts, wat de noodzaak benadrukt van een grensoverschrijdend perspectief.

De invloed van kleinschalige zand-slib interactie op grootschalige gemodelleerde morfodynamische ontwikkeling is bestudeerd door twee abiotische interacties (erosie- en ruwheidsinteractie) te implementeren in een procesgebaseerd model (Hoofdstuk 4). De modeluitvoer is omgezet in indicatoren die de macroschaalconfiguratie van de gemodelleerde systemen beschrijven. Dit maakt een kwantitatieve vergelijking van scenario's mogelijk. De resultaten tonen aan dat kleinschalige zand-slib interacties de evolutie van getijbekkens aanzienlijk kunnen beïnvloeden. Ze hebben daarbij vooral een grote invloed op de vorm, grootte en samenstelling van intergetijdeplaten.

Tot slot hebben we gezien dat de samenstelling van de zeebodem in getijstelsels vaak bimodaal verdeeld is, wat duidt op een voorkeur voor segregatie van zand en slib (Hoofdstuk 5). Bimodaliteit vertegenwoordigt het bestaan van twee stabiele evenwichtscondities, die het gevolg zijn van de depositiefluxen van zand en slib. Dit fenomeen kan worden verwacht voor een groot scala aan sedimentconcentraties in zand-slib systemen. Om de bimodaliteit correct te reproduceren in procesgebaseerde modellen, en dus de samenstelling van de zeebodem juist te modelleren, moet men rekening houden met erosie-interactie in de modelopstelling.

Samenvattend benadrukt dit proefschrift het belang van een zand-slib perspectief in morfodynamische studies, waarbij zowel de bijdrage van beide sedimentsoorten aan de morfodynamische ontwikkeling als hun interacties worden meegenomen. We hebben gezien dat het verbeteren van ons begrip van zand-slib morfodynamica een combinatie van data analyse en modelleeraanpakken vereist. Hierbij moet een systeembreed perspectief worden gehanteerd, en dient men rekening te houden met de interacties tussen de verschillende ruimte- en tijdschalen. Morfologische indicatoren zijn essentieel voor een systematische evaluatie en vergelijking van modelresultaten en bestaande kustmorfologie wereldwijd. Een succesvol en duurzaam beheer van kusten en delta's vereist verdere vergroting van ons begrip van zand-slib morfodynamica, middels het uitvoeren van aanvullende metingen en modelleerstudies. Het ontwikkelen van systeembegrip zal centraal moeten staan in zulk onderzoek.

Photograph of the Wadden Sea - by Kevin Krautgartner

1

INTRODUCTION

1

1.1. THE WORLD'S COASTS AND DELTAS ARE IN TRANSITION

Where there is water on Earth, there is life. Yet for humans (as well as many other species), our sweet spot lies where water and sediments meet, making deltas and their adjacent coasts invaluable environments. Deltas and coasts play a crucial role in human life, offering a multitude of benefits and serving as vital systems for our well-being. Deltas provide clean freshwater resources and serve as fertile lands for agriculture. Additionally, they comprise essential habitats for various ecosystems, thereby contributing to the balance and resilience of the Earth's biodiversity. Coastal areas provide economic opportunities through tourism, fishing, and trade, supporting local economies and livelihoods. Furthermore, they offer recreational spaces which can significantly contribute to our physical and mental well-being.

However, many of these systems are currently under pressure by climate change and increasing human activities (Syvitski et al., 2009; Ranasinghe et al., 2013; Luijendijk et al., 2018; Nienhuis et al., 2020; Vousdoukas et al., 2020). While climate change is still mostly a slow and continuous process, some of its effects can nowadays already be observed in the form of severe droughts, sea level rise (SLR), extreme storms and river discharges, and ocean acidification (IPCC, 2021). More and especially more severe effects are to be expected in the future, posing unprecedented challenges and threatening our existence (Naumann et al., 2021; Pörtner et al., 2021; IPCC, 2022; Mora et al., 2022). Anthropogenic interventions have already caused many abrupt system transitions worldwide, some of which have irreversibly influenced the morphological development of deltas and coastal systems (Yang et al., 2011; Wang et al., 2015; Nienhuis et al., 2020).

Interventions influence their environment through positive and negative feedback mechanisms. While negative feedback mechanisms are self-regulating such that a system stays in balance, positive feedback mechanisms are self-reinforcing, resulting in a progressively larger impact of the interventions. Such impacts are very difficult to predict, and moreover poorly known for climate change effects. Feedback mechanisms are often regulated by morphodynamic processes.

Preservation of the multiple functions of coasts and deltas requires a thorough understanding of the morphodynamic impacts of human interventions and climate change. Herein, *morphodynamics* is defined as "the adjustment of the seafloor topography through the mutual interaction of coastal morphology with hydrodynamic forcing involving sediment transport". Morphodynamic responses and system transitions are complex: human impacts operate on a wide range of spatial and temporal scales, while internal processes in the natural systems also set specific response timescales (Wang et al., 2015; van Maren et al., 2023). To improve our ability to sustainably manage coasts and deltas in transition, we must understand how processes at different scales shape their resilience.

1.2. A SAND-MUD PERSPECTIVE

The sediment bed in many coastal systems worldwide is composed of two sediment types: sand and mud. Sand is a non-cohesive granular material with a grain size, D, of 63 μm $< D \leq 2$ mm. Mud is a cohesive mixture of clay (here defined as particles with $D < 4$

μm), silt (4 μm $\leq D \leq$ 63 μm) and water, sometimes also including organic material and gas. The bed sediment composition is an important characteristic: it governs sediment mobility and sediment transport, hence morphological evolution. A small amount of mud already influences the development of sandy morphological features in a morphodynamic system, and vice versa. It may also influence hydrodynamics, introducing complex morphodynamic feedback loops (Winterwerp & Wang, 2013; van Maren et al., 2015). Moreover, the bed sediment composition strongly influences biological activity and habitat suitability for many benthic organisms (Brückner et al., 2020), which in turn also affect morphological evolution.

This thesis focuses on sand-mud morphodynamics in tidal systems such as estuaries and tidal basins. Sand-mud morphodynamics in these systems is highly complex as many interacting hydrodynamic, sedimentary and morphological processes play a role — some of which are depicted in Figure 1.1. Most previous research focused on the sediment dynamics of the individual sand and mud fractions, while relatively little is still known about how combined sand-mud morphodynamics differs from it. In order to assess the morphodynamic impacts of anthropogenic interventions and climate change in tidal systems, we thus need to better understand combined sand-mud morphodynamics.

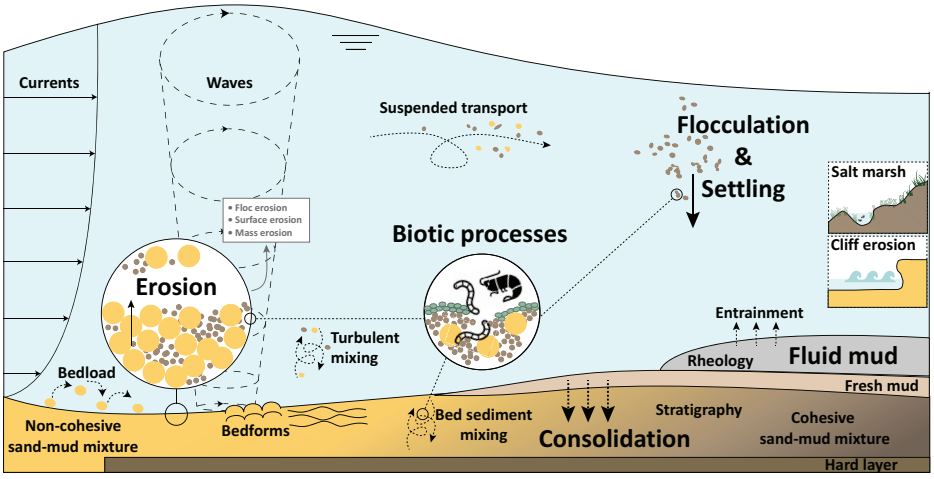

Figure 1.1: Conceptual visualization of the main processes that play a role in the morphodynamics of sand-mud tidal systems.

Although bed sediments often consist of sand and mud mixtures, it is usually not clear what the relative contribution is of the individual sediment fractions to the morphological evolution, and whether this contribution is well-represented by the composition of the upper bed (top cm to dm). These are important unknowns when determining sediment budgets. A *sediment budget* is a balance of volumes for sediments entering (source) and leaving (sink) a selected area, resulting in erosion or accretion (Rosati, 2005). They are often used as coastal management tools to understand and predict morphological change in

a particular coastline over time. For decades, detailed sediment budgets of sandy systems have been established worldwide (Bowen & Inman, 1966; Komar, 1996; Rosati, 2005), but quantitative large-scale analyses of sand-mud systems are scarce. Previous studies however show that mud can largely contribute to the infilling of tidal systems (van Dreumel, 1995; van Ledden et al., 2006). Determining what the contributions of sand and mud to morphological changes tend to be, and especially how these vary in time and space, is essential to predict future change, under the influence of climate change or local human interventions.

The sediment dynamics of sand-mud mixtures can however not be treated as a superposition of the dynamics of separate sand and mud particles. The combined erosive behavior of sand-mud beds has been the subject of several studies (Torfs, 1995; van Ledden, 2003; Jacobs, 2011; van Rijn, 2020). The substrate also introduces feedbacks related to hydraulic roughness — which can be lower in muddy beds (Soulsby & Clarke, 2005) — affecting the erodibility of sand-mud beds as well. We refer to these mechanisms as *sand-mud interaction*. Some sand-mud interaction mechanisms have been addressed in numerical models in the past (e.g., van Ledden et al., 2004b; Le Hir et al., 2011). With several numerical applications, van Ledden (2003) showed that the morphological adaptation timescale of tidal basins to reach (quasi-)equilibrium strongly decreases with the availability of mud. Moreover, results of the simulated bed levels and bed composition profiles showed a good agreement with field observations. Nevertheless, the inclusion of sand-mud interaction in long-term prediction models has remained limited since then. Consequently, despite advances in our understanding of small-scale sand-mud interaction processes, their large-scale morphological implications remain poorly known.

The mechanisms governing the sediment composition are also still poorly understood. Sand and mud can be deposited as mixtures, in alternating vertical layers or in different areas of the system (*sand-mud segregation*). Generally, grain size fractions in the sediment bed are sorted along an energy gradient, with hydrodynamic energy and grain size decreasing from the inlet to the landward side (Flemming & Nyandwi, 1994; Chang et al., 2006). Above a threshold bed shear stress the mud content is generally low ($<10\%$), but the mud content may vary anywhere between 0%–100% below this threshold condition (van Ledden, 2003; Braat, 2019). Apparently, the energy gradient is not the main factor influencing the sediment composition. Previous research has shown that apart from sediment properties that influence the critical shear stress for erosion, the deposition capacity is likely to be a key factor here (van Ledden, 2003). In this thesis, we will further explore what the key factors are using the Wadden Sea as a case study.

1.3. THE WADDEN SEA

The Wadden Sea is the world's largest coherent system of barrier islands and tidal flats, spanning over a distance of nearly 500 km, and providing important habitats for numerous species (Figure 1.2). It contains several examples of sand-mud tidal basins and estuaries that have been heavily impacted by anthropogenic changes for centuries. Moreover, unique and abundant long-term data sets of the hydrodynamics, bathymetry and sediment composition are available, making this an excellent area to study the morpho-

Figure 1.2: Satellite image of the Wadden Sea, from *www.waddensea-secretariat.org*.

logical responses to these interventions in detail, and to improve our understanding of sand-mud morphodynamics.

The low-gradient, yet dynamic landscape of the Wadden Sea is shaped by the intricate interactions between tides, waves, winds, river runoffs, sediments and biological factors. This landscape is, geologically speaking, still relatively young: it was formed after the last glacial period under a temperate climate and rising sea levels. The tidal inlet systems consist of large ebb-tidal delta shoals, narrow and deep inlets, and flood-tidal deltas that cover the entire back-barrier basins, with extensive systems of branching channels and tidal flats, up to the salt marshes and the mainland coast. The bed sediment distribution in the Wadden Sea is characterized by a strong sand-mud segregation (Postma, 1954; van Straaten & Kuenen, 1957; de Glopper, 1967; Flemming & Ziegler, 1995; Zwarts, 2004; Colina Alonso et al., 2022): while central parts mainly consist of sandy channels with low ($<$10%) mud content, the mud content suddenly increases to high values ($>$40%) near the coastlines and the tidal divides.

Since its formation, the development of the Wadden Sea has been influenced by changing environmental conditions (especially SLR) as well as by human interventions. The latter include the closures of the South Sea (*Zuiderzee*, 1932) and the Lauwers Sea (*Lauwerszee*, 1969), land reclamation (dating back to $\sim$1000 AD), mining of gas and salt, dredging and

dumping activities including maintenance of navigation channels, and sand nourishment for the maintenance of the North Sea coast. Especially the closures triggered shifts in the sediment budgets of the Wadden Sea basins, mainly leading to sediment infilling (Elias et al., 2012; van Maren et al., 2023) that is still ongoing. Previous studies elsewhere have demonstrated that the partial closure of tidal basins can result in large accumulation of fines (Williams et al., 2013, 2014; Elias et al., 2016). Studies on the sediment infilling of the Western Wadden Sea basins did not yet differentiate between sand and mud fractions, making this an important unknown when determining its past and present-day sediment budgets.

The future holds a whole new range of challenges for the Wadden Sea, with especially accelerated SLR threatening its existence: if the sediment import cannot keep up with increased SLR rates, this will result in loss or even disappearance of the ecologically valuable intertidal areas (Timmerman et al., 2021; Huismans et al., 2022). Keeping pace with SLR will require sufficient sediment supply, sediment transport capacity and accommodation space (Wang et al., 2018). Predicting the capacity of systems such as the Wadden Sea to keep pace with SLR requires a better understanding of processes during erosion, transport and deposition of sediments in mixed-sediment environments. This thesis aims to advance on this topic by investigating processes related to segregation of sand and mud, sand-mud interaction processes, sediment supply, and long-term deposition.

1.4. RESEARCH SET-UP

The overarching aim of this thesis is:

To improve the understanding of large-scale morphodynamics in sand-mud tidal systems.

Herein, *large-scale* is defined as phenomena and processes on macro and mega scale. Examples of macro scale phenomena are interacting tidal flats and channel systems; relevant processes are e.g., sediment transport, currents and waves. The associated spatial and temporal scales are approximately 100 m – 10 km and 1 month – 10 years. A tidal basin is a phenomenon on mega scale. Here, relevant processes are e.g., sediment supply and climate fluctuations. The associated spatial and temporal scales are >10 km and >10 years (de Vriend, 1991).

This thesis specifically focuses on four main topics that address the aforementioned knowledge gaps within the Wadden Sea and other sand-mud tidal systems worldwide (Sections 1.2 and 1.3). Although the main focus is on the large scale, some of the topics zoom in on meso and even micro scales, and how these relate to and influence larger-scale morphodynamics. The set-up of the research topics and their corresponding research questions (RQs) is as follows:

1. The depositional record

RQ 1: What is the relative role of sand and mud deposition in the morphodynamic evolution of tidal basins in response to human interventions?

2: A system-wide mud budget

RQ 2: How much mud is delivered to the Wadden Sea by marine and fluvial sources, where does it accumulate and how do human interventions influence source and sink terms?

3: Sand-mud interaction

RQ 3: What is the large-scale impact of small-scale sand-mud interactions and how do these interactions influence predictions of the morphodynamic evolution?

4: Composition of the sediment bed

RQ 4: Which processes lead to the spatial segregation of sand and mud, and how can the bed sediment composition be better predicted?

Answering these research questions requires a synthesis of multiple lines of evidence. We therefore opt for an approach in which we combine historical databases and new field measurements with advanced modeling tools. We will use detailed process-based models of the Wadden Sea to interpret available data and to better understand the system, as well as idealized tidal basin models to generalize our findings, which is important for interpreting the impact of sand-mud morphodynamics in a global context.

1.5. OUTLINE

This thesis consists of six chapters. This first chapter has provided an overview of the challenges of understanding sand-mud morphodynamics in tidal systems, and the resulting research set-up. The four research questions are addressed in Chapters 2–5. The remainder of this thesis is structured as follows:

In **Chapter 2**, we combine information on the upper-bed sediment composition and the bed level evolution to better understand the depositional record. We use the Western Wadden Sea for a case study, determining the contribution of sand and mud to the infilling of its basins after closure of the South Sea.

Chapter 3 presents the first mud budget of the Wadden Sea, based on a detailed analysis of sources and sinks. These sinks include sedimentation in the basins, on salt marshes and in offshore parts of the North Sea, but also sediment extraction.

In **Chapter 4**, we investigate the effects of small-scale sand-mud interaction on large-scale morphodynamics of tidal basins. Two sand-mud interaction mechanisms have been included in a process-based model of a schematized tidal basin, from which we analyze 50 years of basin evolution under different model settings. The model results are compared with field data to determine their validity and to identify what combination of parameters most closely resembles the morphology of real-life tidal basins.

In **Chapter 5**, we investigate the factors controlling the sediment composition in the upper bed, using field data and numerical models. The findings that initially apply to the Wadden Sea have also been tested with a general theoretical approach and an idealized model, making them widely applicable to other sand-mud systems.

Lastly, **Chapter 6** presents conclusions which are further synthesized into general findings and suggestions for future research.

Photograph of the Wadden Sea - by Kevin Krautgartner

2

THE DEPOSITIONAL RECORD

Abstract
Human interventions and climate change can heavily influence the large-scale morphological development of tidal basins. This has implications on sediment management strategies, as well as ecological and recreational purposes. Examples of heavily impacted tidal basins are those in the Western Dutch Wadden Sea. The closure of a large subbasin in 1932 triggered a shift in the sediment budgets of the remaining basins, leading to sediment infilling that is still ongoing. This chapter presents a quantitative analysis of the post-closure sediment volumes, differentiating between sand and mud. Analysis of historical sediment composition data combined with bathymetry data revealed that the intervention caused a redistribution of sand and mud sedimentation. The responses of both sediment types differ spatially and temporally. The total infilling of the basins over the last century was substantially caused by mud ($\sim$32%, which is much larger than the average mud content in the upper bed). Initially, large mud volumes accreted in abandoned channels. At present, mud sedimentation along the mainland coast is still ongoing with nearly constant sedimentation rates over the past century, while the net import of sand significantly decreased over time and has been fluctuating around 0 over the last two decades. This research shows the importance of distinguishing between the response of sandy and muddy sediments when analyzing the morphodynamic impact of an intervention, since they operate on different time and spatial scales. Sea level rise is currently a major threat for the existence of the Wadden Sea; its future fate will depend on whether the tidal flats are able to keep pace. Our results show that the supply of mud is sufficient to keep pace with the current sea level rise rates.

This chapter is largely based on the publication in *Marine Geology*:

Colina Alonso, A., van Maren, D. S., Elias, E. P. L., Holthuijsen, S. J., & Wang, Z. B. (2021). The contribution of sand and mud to infilling of tidal basins in response to a closure dam. *Marine Geology*, 439,106544. [Link]

2.1. INTRODUCTION

Coastal wetlands and tidal basins are unique ecosystems providing nature, navigation, recreation and flood safety services (Barbier et al., 2011). At present, many tidal basins are under pressure by climate change and increasing human activities, threatening their ecological value and role in protecting the hinterland (e.g., Syvitski et al., 2005; de Vriend et al., 2011; Yang et al., 2011; Wang et al., 2012; Monge-Ganuzas et al., 2013; Wang et al., 2015). While climate change is mostly a slow and continuous process (such as the gradual rise in sea level), anthropogenic interventions have caused many abrupt system transitions worldwide, some of which irreversibly influence the morphological development and the large-scale sediment budgets of tidal basins. Examples of such interventions are closures, land reclamations and coastal protection structures. Preservation of the multiple purposes of coastal wetlands and tidal basins requires thorough understanding of the morphodynamic impact of human interventions. An indicator reflecting the dynamics of tidal basins, and the impact of human interventions, is its sediment composition.

The sediment composition of the bed is an important characteristic of tidal environments: it governs sediment mobility, hence sediment transport and morphological evolution (Geleynse et al., 2011). In addition, the substrate influences its suitability for local biological activity, which in turn also influences bed level morphodynamics. Bed sediments in most tidal basins are a mix of sand (non-cohesive) and mud (cohesive). Sand and mud are typically differentially deposited and preserved in the bed stratigraphy, but their deposition also varies horizontally, which is usually referred to as *sand-mud segregation* (van Ledden, 2003). Sand-mud segregation is influenced by local hydrodynamics and sediment supply, but also by the interaction of sand and mud, greatly influencing sediment dynamics (van Ledden, 2003; Winterwerp & van Kesteren, 2004; Jacobs, 2011).

The Western Dutch Wadden Sea provides examples of tidal basins that have been heavily impacted by anthropogenic changes. The partial closure of the South Sea (*Zuiderzee*) in 1932 still influences the morphodynamics of the Wadden Sea basins (Elias et al., 2003; Elias et al., 2012; Wang et al., 2018), including the overall sediment budget. Previous studies on the sediment budget of the Wadden Sea did not differentiate between sand and mud fractions. However, understanding the contribution of both sediment types to the morphologic evolution is crucial for unravelling the processes responsible for the observed bathymetric changes. This is especially relevant if we want to predict future change, under the influence of climate change or local human interventions.

Previous studies elsewhere have demonstrated that the (partial) closure of tidal basins can result in large accumulation of fines (i.e., mud). Elias et al. (2016) showed that the closure of an estuary in the Dutch Southwest Delta, in combination with an extension of the nearby Port of Rotterdam, created a sheltered environment transforming a predominately sandy coast (Piekhaar & Kort, 1983; van Alphen, 1990; Hendriks et al., 2020) into a muddy area. Williams et al. (2014) showed that construction of the Yeongsan Estuarine Dam (South Korea) resulted in local distinctive scouring and a dramatic increase of sedimentation rates in the Yeongsan Estuary by at least an order of magnitude over average Holocene sedimentation rates. Construction of the Noksan Dam in the Nakdong Estu-

ary (also South Korea) significantly reduced flow velocities and caused a severe depletion of coarse grained sediment in the West Nakdong River, resulting in the accumulation of fine-grained sediments advected from the estuary and offshore (Williams et al., 2013). These examples show the impacts of a dam on estuary sedimentation and shifts in sediment composition, but a quantitative analysis of the post-closure sediment budgets in all these estuaries is still lacking.

The objective of this chapter is to better understand the contribution of sand and mud to the morphodynamic evolution of tidal basins in response to human interventions. The tidal basins of the Western Dutch Wadden Sea provide an ideal case study for this purpose, because of the long and well documented response period following the 1932 closure of the South Sea. Unique long-term data sets of bathymetry and bed sediment composition provide detailed information on the response of sand and mud over the past century. We use this information to understand the effect of human interventions on sand and mud transport and how this affects morphological response timescales and sediment budgets.

The structure of this chapter is as follows: In Section 2.2 we present the general setting of the Western Dutch Wadden Sea, its historical morphodynamic evolution and the current conditions. Subsequently, we present our bathymetric and sediment composition data sets in Section 2.3, and we introduce our method for the sediment volume analysis of the basins. In Section 2.4, we first analyze the long-term evolution of the bed composition, after which we combine this evolution with the bed level changes to derive the sediment volume changes of sand and mud. In addition, we present a sensitivity analysis to test the assumptions of the method. The implications of our findings for a general understanding of sand and mud responses to human interventions are discussed in Section 2.5. Concluding remarks are summarized in Section 2.6.

2.2. STUDY AREA

2.2.1. GENERAL SETTING

The Wadden Sea is the world's largest uninterrupted system of barrier islands and tidal flats, spanning over a distance of nearly 500 km along the North Sea coasts of the Netherlands, Germany and Denmark (Pedersen & Bartholdy, 2006; Elias et al., 2012; Benninghoff & Winter, 2019). The tidal basins of the Wadden Sea — which are separated from the North Sea by barrier islands — contain extensive systems of branching channels, sand- and mudflats, and salt marshes. They provide important habitats for numerous species of fish, mammals and birds. Therefore, in 2009 the Wadden Sea became a UNESCO world heritage site, requiring preservation of its characteristics.

Sea level rise (SLR) has been a primary driver in the formation of the current Wadden Sea morphology. In the early Holocence, the sea level was many 10s of meters below the current level and the Wadden Sea did not yet exist. However, the subsequent rapid rise of the sea level (Zagwijn, 1986; Beets & van der Spek, 2000), in combination with land subsidence, caused a gradual expansion of the North Sea. Consecutive cycles of marine ingression and subsequent basin sedimentation, and sufficient sediment supply to retain

or prograde the coastline, filled in the entire western part of the Dutch coastal plain. The sediment supply along the Wadden Sea was sufficient to retain the extensive systems of tidal flats and salt marshes over the past 7,000 years, but insufficient to fill in the basin completely (Wang et al., 2018).

Human interventions have been influencing the evolution of the system since the Middle Ages, partly fixing the basin dimensions with dike constructions, land reclamation, peat excavations and salt marsh accretion works. Later, the closures of the Middle Sea (*Middelzee*, 1600), the South Sea (*Zuiderzee*, 1932) and the Lauwers Sea (*Lauwerszee*, 1969) largely impacted the morphological evolution of the Wadden Sea (Oost, 1995; van der Spek, 1995; Elias et al., 2012).

2.2.2. MORPHODYNAMIC EVOLUTION OF THE WESTERN DUTCH WADDEN SEA

In this chapter we focus on the Western part of the Dutch Wadden Sea, consisting of the inlets: Texel inlet, Eijerlandse Gat inlet and Vlie inlet. Figure 2.1 provides an overview of the morphology before closure of the South Sea and of the present-day situation. This closure was motivated by a large flood in 1916 and the famine in 1918, which led to the construction of the 30 km closure dam 'Afsluitdijk' to protect the land along the former South Sea against flooding, and to create a fresh water lake and new polders with agricultural land. This resulted in a considerable reduction of the total basin area (from 4,000 km^2 to 712 km^2) and of the basin length (from 130 km to 30 km; Elias et al., 2003). The tidal range, however, increased nearly instantaneously with approximately 15% at Den Helder and almost 100% in front of the closure dam at Den Oever, leading to a 20% increase of the tidal prism.

The disturbance of morphological equilibrium led to morphological changes inside and outside the tidal basins. Large infilling rates have been observed in disconnected channels and along the basin shoreline, while ebb tidal deltas and adjacent coastlines eroded (Figure 2.1). Elias et al. (2012) show that the sedimentation of the basins has been primarily a response to the closure of the South Sea and not an adaptation to SLR. See Schoorl (1973, 1999, 2000a, 2000b, 2000c) and Elias and van der Spek (2006) for more detailed historical reconstructions of the morphodynamic evolution of the Wadden Sea.

2.2.3. PREVAILING CONDITIONS

The Wadden Sea is a mixed energy environment (Davis & Hayes, 1984), influenced by tides and waves. The tidal range at Den Helder (Texel inlet) is 1.4 m and increases in eastward direction. Offshore, the mean significant wave height is 1.3 m, with a corresponding mean wave period of 5 s and a WSW direction (Wijnberg, 1995; Elias et al., 2012). During storms, wind-waves can reach heights of over 6 m, accompanied by surges of over 2 m. Fresh water supply by rivers is limited, and dominated by discharges from Lake IJsselmeer (former South Sea) through drainage sluices in the closure dam (yearly average discharges of 450 m^3/s).

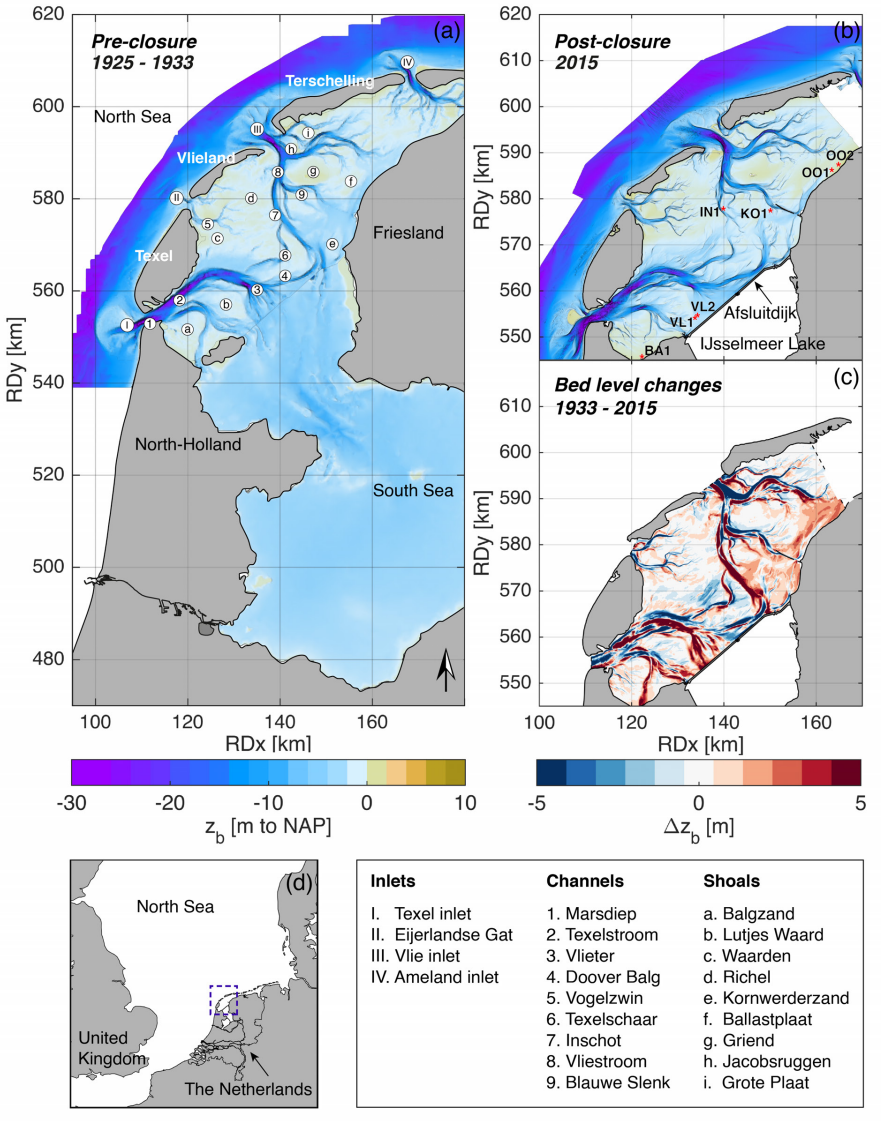

Figure 2.1: Location map of (a) the Western Dutch Wadden Sea, pre-closure and (b) post closure. Panel (c) shows the total bed level changes and panel (d) shows the location of the Wadden Sea. The names of the main inlets, channels and shoal are indicated in panel (a). In panel (b) we also show the locations of sediment cores (in red) analyzed in Figure 2.8. Bed levels are shown in meters relative to NAP (the Dutch Ordnance Level, equivalent to MSL).

The basins have relatively large channels and small intertidal areas, with a channel/shoal ratio of 0.3 and 0.4 at the basins of Texel and Vlie inlet (Oost, 1995). Many Wadden Sea basins are separated by tidal divides minimising the flow and sediment exchange between the basins. However, an important characteristic of the present-day Western Wadden Sea is that Texel and Vlie basins are not solitary closed systems, but share a connection on their landward side, allowing exchange between the two basins (Ridderinkhof, 1988; Elias & van der Spek, 2006; Duran-Matute et al., 2014; Duran-Matute et al., 2016).

2.3. METHODS

2.3.1. DATA SETS

Bathymetry

The bathymetry of the Western Dutch Wadden Sea has been monitored for over 400 years for nautical reasons (because of the presence of shipping lanes and harbors), with nautical maps dating back to the 16th century that indicate the main morphological features. Since 1925, the bathymetry has been monitored consistently and regularly, with a resolution and accuracy progressively increasing in time, by the Navy (Hydrografische Dienst) and the Dutch Ministry of Transport, Public Works and Water Management (the *Vaklodingen* data set). This data includes Wadden Sea bathymetry, currently measured on a six-year interval using single-beam echo sounders. Until 1987, the data was published as analogue maps, which were later digitized in 250 $\times$ 250 m resolution. More detailed measurements after 1987 have been interpolated to a 20 $\times$ 20 m grid (see de Kruif, 2001, for a detailed overview of the *Vaklodingen* data set).

The accuracy of the *Vaklodingen* data has been estimated to range between 0.11 m and 0.40 m (Wiegmann et al., 2005; Perluka et al., 2006). According to Marijs and Parée (2004), the total error of the data originates from three sources: stochastic errors due to individual data outliers, systematic errors introduced by the measuring instruments and variable systematic errors consisting of user errors in measuring and handling the data. To enable reliable estimates of sedimentation-erosion trends and volume budgets, we have inspected the data in detail manually. Maps showing unrealistic trends have been excluded from the analysis.

Bed sediments

We analyze the long-term evolution of the bed sediment composition (measured in summer) using four data sets that span over 125 years (Figure 2.2). The first synoptic map of the bed composition in the Wadden Sea was produced by Lely (1892), as part of impact studies for the closure of the South Sea and other potential land reclamations. Extensive measurement campaigns were set up in the summers of 1889 and 1890, in which cores were taken up to one meter depth in subtidal and intertidal zones of the Wadden Sea basins and the former South Sea. After removing organic matter and calcium carbonate, the grain size was determined and the samples were classified based on the sand content (4 sediment classes). We digitized the resulting map making use of ArcGIS Software.

In the 1950s, about 2,500 cores were taken at 0–25 cm depth, as part of an effort to better understand the mud dynamics in the Wadden Sea (de Glopper, 1967). Again, samples

were treated to extract organic matter and calcium carbonate (Hofstee, 1980) prior to gravimetric analysis. This work was later digitized (Zwarts, 2004).

Between 1989 and 1996, sediment samples were taken of the top layer of the sediment (up to 10 cm depth), with measurements at 500–1,000 m distance covering the whole Dutch Wadden Sea, as well as the ebb-tidal deltas and the coastal zone along the North Sea side of the barrier islands. These samples were analyzed with a *Malvern Laser Particle Size Analyzer* (without prior treatment) and complete grain size curves were stored in the publicly available *Sediment Atlas Wadden Sea* (Rijkswaterstaat, 1998).

The most recent and detailed set is the Synoptic Intertidal Benthic Survey (*SIBES*) data set, which contains samples from approximately 4,500 sites, taken at 500–1,000 m intervals every year since 2008. The samples are analyzed with a *Coulter LS 13 320* (optical module 'gray', grain sizes from 0.04 to 2,000 μm in 126 size classes), without prior treatment to extract organic matter and calcium carbonate. A detailed description of the measuring campaign and the sediment analysis method is given by Bijleveld et al. (2012) and Compton et al. (2013).

The data of the sediment composition is interpolated to the grid of the *Vaklodingen* bathymetric data using the Natural Neighbor Interpolation method by MATLAB. We have performed tests with other interpolation methods (Linear and Nearest Neighbor Interpolation), resulting in negligible differences between the results ($\leq 2\%$). Note that the interpolation method becomes more important for small-scale analysis (morphological features with dimensions smaller than 1,000 m), or for a similar analysis with a less detailed data set. In that case, a Co-Kriging approach correlating the sediment composition to the bed level is probably a better alternative (Leecaster, 2003; Meiliand et al., 2011; Park & Jang, 2014).

The Geological Survey of the Netherlands (TNO-NITG) provides borehole data (of several meters deep) which is stored in the database *DINO* and is publicly available. We make use of the lithostratigraphic data containing classified borehole information.

2.3.2. SEDIMENT VOLUME ANALYSIS

We separate the contributions of sand and mud to volume changes in the basins using the available data sets on bathymetry and sediment composition. Mud is herein defined as a mixture of clay and silt particles (with a particle size diameter $D \leq 63\mu m$), including organic and calcareous materials. The contributions of sand and mud are separated as follows: First, total sedimentation/erosion volumes (ΔV) are calculated based on the bathymetric data of the *Vaklodingen* data set (as presented in Figures 2.1 and 2.3). Next, these volumes are multiplied with the sand/mud content in volume fractions f_V (see Figure 2.2), to obtain the relative volumetric contribution of the two sediment fractions:

$$\Delta V_{sand} = \Delta V f_{sand,V}, \tag{2.1}$$

$$\Delta V_{mud} = \Delta V f_{mud,V}. \tag{2.2}$$

This approach requires a number of assumptions:

1. **Bed sediment data**: We use a single bed composition data set for separating the sand and mud contribution through time (rather than the various historic bed composition data) for the following reasons: (1) the spatial density of the various bed composition data sets varies, and (2) the methodologies applied to pre-treat and analyze the samples differ. With this, we implicitly assume that one sediment composition distribution is representative for the entire period of time, implying a vertical homogeneity of the sediment distribution. Closure of the South Sea caused an abrupt transition, but since then sedimentation/erosion trends of most individual morphological features are approximately constant. This is in line with Wang et al. (2014a) and Wang et al. (2014b), who show that bed sediment grain size changes much faster than the bed elevation, such that a new equilibrium distribution of bed sediment can be rapidly attained after interruptions. Besides, no large changes have been observed in the large-scale sand-mud patterns (see Section 2.4.1). Therefore, the use of a single data set is the most accurate approach for analyses on basin scale.

   We use the data of the *Sediment Atlas Wadden Sea*, since this has the largest spatial extent and was collected halfway the majority of our bathymetric observations. The *SIBES* data is collected at identical locations for consecutive years since 2015, allowing a sensitivity analysis (minimum, maximum and mean values of each data point). Quantitative use of data before the 1990s (1890, 1950) is not possible because of poor spatial coverage.

2. **Dry density of sand-mud mixtures**: The *Sediment Atlas Wadden Sea* provides data on the mass fractions which need to be converted into in situ volume fractions, requiring the use of density relations of sand-mud mixtures. Both Mulder (1995) and van Rijn and Barth (2019) derived equations relating the dry density to the sediment composition. Equation 2.3 by Mulder (1995) is based on unconsolidated sediment in the Ems Estuary (East of the Dutch Wadden Sea) while Equation 2.4 by van Rijn and Barth (2019) uses dry density data from the Wadden Sea subjected to a primary consolidation period (Migniot, 1968, 1989). These equations are:

$$\rho_{dry} = 450 + 4.5 p_{sand} + 0.063 p_{sand}^2, \tag{2.3}$$

   where p_{sand} is the sand content in weight-percentages, and

$$\rho_{dry} = (1 - \frac{p_{org}}{100})[400(\frac{p_{clay}}{100}) + 800(\frac{p_{silt}}{100}) + 1600(\frac{p_{sand}}{100})] \tag{2.4}$$

   where p_{org} is the organic content, p_{clay} the clay content and p_{silt} the silt content, all in weight-percentages. van Rijn et al. (2018) show that this relation also well predicts the dry density of Wadden Sea sediments when ignoring the contribution of organic matter.

   We use the relation derived by van Rijn and Barth (2019) with p_{org} = 0 since this equation was derived for Wadden Sea sediments, best resembling our conditions.

We estimate the sensitivity of the computed sediment volumes to the density formulation by comparing the results with those using the relation of Mulder (1995).

To convert the sediment mass percentages into sediment volume fractions, we use the following relations:

$$p_{mud,V} = 100 - (p_{sand}\frac{\rho_{dry}}{\rho_{dry,sand}}), \tag{2.5}$$

$$f_{mud,V} = \frac{p_{mud,V}}{100}, \tag{2.6}$$

$$f_{sand,V} = 1 - f_{mud,V}. \tag{2.7}$$

3. **Negligible contribution of small mud contents**: Not all fines that settle on top of the bed contribute to the long-term sediment volume increase, since mud can be reworked into the pores between sand grains by bioturbation and mixing. According to Winterwerp and van Kesteren (2004), the sand skeleton is not affected by mud particles up to 15% mud. On the other hand, field measurements show that the density of pure sand is higher than that of sand-mud mixtures (Mulder, 1995; van Rijn & Barth, 2019). This is in contrast with the findings of Winterwerp and van Kesteren (2004), which would result in the highest densities for sand-mud mixtures. Therefore we assume that mud always contributes to the sediment volume, even when the mud weight percentage is below 15%. However, we evaluate the effect of this assumption by also executing our analysis without the contribution of mud to the total volume when the local mud content is below 15%.

Based on the assumptions above, we define a *best estimate* setting to compute the sand and mud volumes (see Table 2.1 for an overview). Alternatives to these primary settings are evaluated as part of a sensitivity analysis to evaluate the robustness of this method. The results are subsequently validated through a comparison with additional sediment cores from the DINO database.

Table 2.1: Overview of the assumptions included in the volume balance. The assumptions included in the *best estimate* are marked in bold. The gray options are used to determine the sensitivity of the results.

Bed sediment data	**Dry density formulation**	**Correction V_{mud}<15%**
Sediment Atlas		
SIBES, mean	**van Rijn, 2019**	**no**
SIBES, max		
SIBES, min	Mulder, 1995	yes

2.4. RESULTS

First, we briefly summarize the morphodynamic evolution of the Western Dutch Wadden Sea and the changes in sediment composition in response to the closure of the South Sea. We refer to Figure 2.1 for the names of the channels and shoals. This is followed by a quantitative analysis of sand and mud deposition rates over time (for both the study area as a whole, and for subsections), validation of the results, and a sensitivity analysis.

2.4.1. LONG-TERM CHANGES IN THE BED SEDIMENT COMPOSITION

In order to qualitatively compare the different sediment composition maps, the various data sets need to be converted to the same classification scheme. Lely's (1892) data is already classified, providing ranges of sand content rather than absolute numbers. As it is impossible to extract the exact sand content from these classified ranges, all data points have been classified using Lely's (1892) scheme (Figure 2.2). Blue dots indicate sandy sediments with either very little mud ($p_{mud} < 10\%$, dark blue) or 10%–20% of mud (light blue). The yellow dots show the sites that are around the transition between non-cohesive/cohesive behavior ($p_{mud} = 30\%$ according to van Ledden et al., 2004a). Fully cohesive, muddy areas ($p_{mud} > 40\%$) are marked in red.

The overall sediment distribution in the Western Dutch Wadden Sea is characterized by a strong sand-mud segregation, which has also been observed and described in various earlier studies (e.g., Postma, 1954; van Straaten & Kuenen, 1957; de Glopper, 1967; van Ledden, 2003; Zwarts, 2004). The central parts of the basins mainly consist of sandy channels with low mud content ($< 10\%$). The mud content sharply increases to more than 40% near the mainland coastlines. In addition to this pattern, many local patches with high mud content are observed in areas with otherwise relatively low mud content.

Despite significant bathymetric changes in the Wadden Sea basins (see Elias et al., 2012; Wang et al., 2018; and also Figure 2.1c), the bed sediment composition has remained relatively stable over the last century. Only three areas show large-scale changes: 1) the sheltered embayment of Balgzand, 2) abandoned channels at the seaward side of the closure dam, and 3) the tidal divide behind Terschelling Island.

Prior to the closure, Balgzand area was a sandy tidal flat, surrounded by Texel inlet and access channels to the South Sea. Only a few local mud patches could be distinguished. Since the closure, the bed has become more muddy, with increasing mud content closer to land. The sudden accumulation of fines here is explained by the sheltered environment that was created by the closure and the land reclamation. The flow velocities in the channel connecting this area to the South Sea abruptly decreased. This channel filled in and the surrounding shoal accreted. Because of its location, this area is relatively sheltered from offshore waves entering the basin, allowing fine-grained sediments to deposit.

The former access channels to the South Sea — which were previously in equilibrium (Elias, 2006) — used to be predominantly sandy, but became muddy after closure. The tidal divide behind Terschelling seems to have become more sandy over the past century. The mud content exceeded 20% along the entire tidal divide in the early 20th century, but

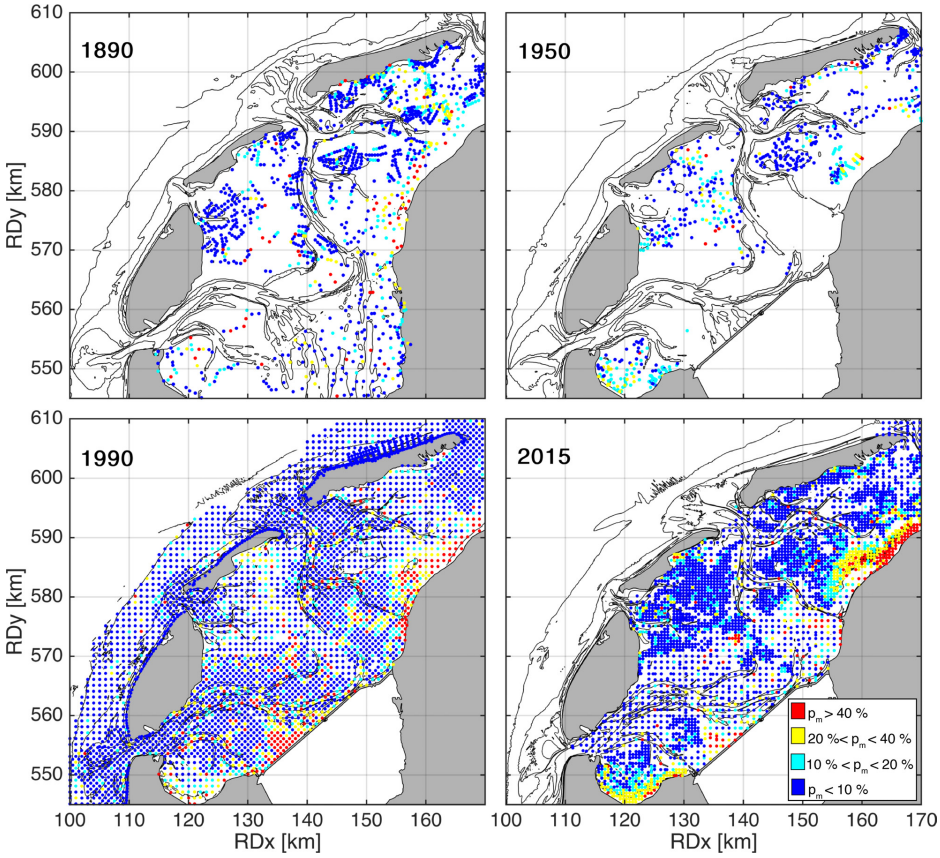

Figure 2.2: Bed sediment composition of the upper layer plotted against the depth contours of the Western Wadden Sea. The colored dots indicate the mud content p_m in percentages, based on Lely's classification.

all observations after closure of the South Sea reveal a mud content over most parts of the tidal divide below 20%. The reason for this could be the alterations in the tidal regime after the closure.

2.4.2. MORPHOLOGICAL CHANGES: THE CONTRIBUTION OF SAND AND MUD

The bed composition data is combined with historic bathymetric charts (Figure 2.3) to separate the contributions of sand and mud to the long-term morphodynamic development, following the methodology described in Section 2.3.2. Pronounced sedimentation/erosion patterns of sand (Figure 2.4a) are observed in the main channels of the Texel and Vlie inlets, resulting from lateral channel migration. Sedimentation rates are large in the terminal parts of the channels that connected the Texel and Vlie basins to the South Sea. Here, the tidal currents reduced to almost zero, which led to rapid accretion (Elias et al., 2003). Whereas the main channel connecting the Vlie basin to the South Sea (*In-*

schot) filled in with sand, the access channels of Texel basin (such as *Vlieter*) largely filled in with mud (Figure 2.4b). This infilling was a rapid response to the closure and mostly occurred before 1971, after which the sedimentation rates in the channels significantly decreased. The mudflat and salt marsh area along the mainland coast of Friesland has been another notable mud sink. Historical data shows no clear trend breaks in the bed composition, since this was a muddy environment already before closure. However, this area has been, and still is, rapidly accreting and expanding, providing a large mud sink.

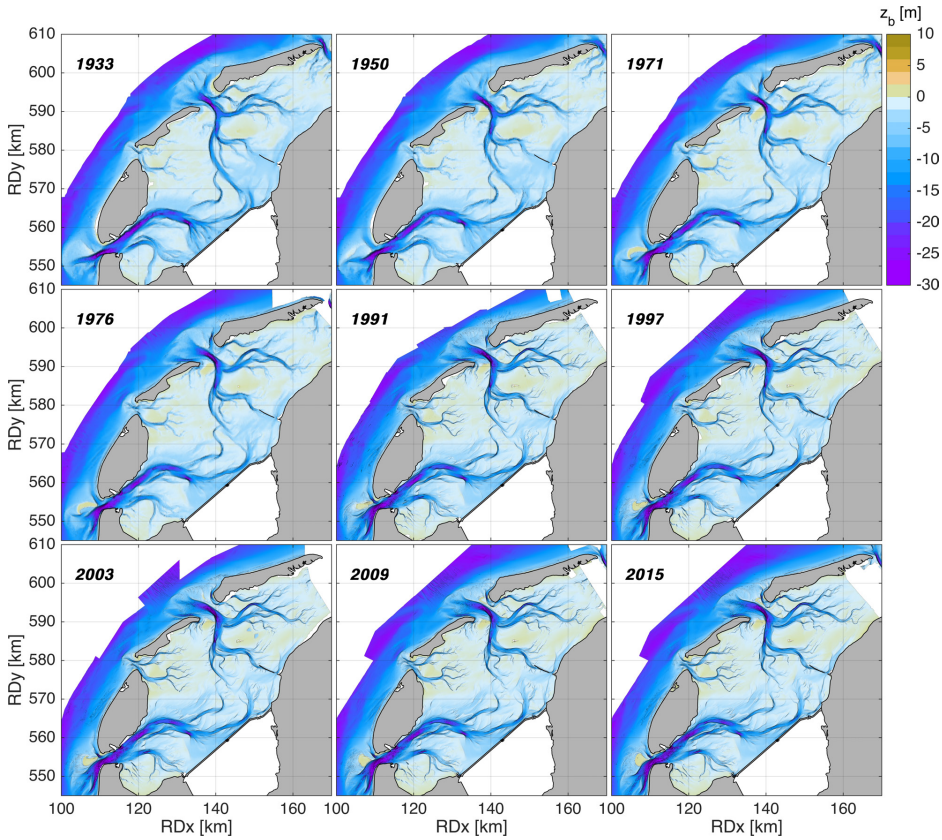

Figure 2.3: Overview of available bathymetric charts of the Western Wadden Sea used in this chapter. Bed levels are shown in meters relative to NAP (the Dutch Ordnance Level, equivalent to MSL).

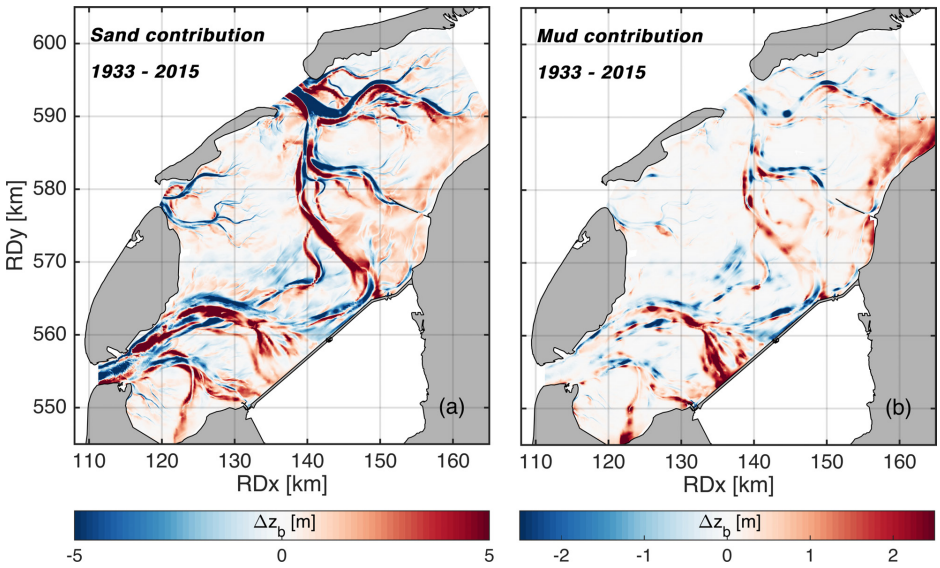

Figure 2.4: The contribution of sand (left panel) and mud (right panel) to the bed level changes of 1933–2015 inside the basins of the Western Dutch Wadden Sea.

2.4.3. SEDIMENT VOLUME CHANGES

Figure 2.5a shows the net volume changes (the sum of the total sedimentation and erosion) in the basins for the period 1933–2015. The blue line provides the total volumetric changes and is based on topographic data only. We first discuss the volume changes by sand (red line) and mud (yellow) resulting from the *best estimate* procedure (see Section 2.3.2) indicated with the solid lines. The total volume changes reveal a rapid initial response of the basins after closure but slowed down after 1971, as also observed earlier by e.g., Wang et al. (2018). The contribution of mud to the net infilling is large (over 30%), and its relative contribution is also increasing in time. The sensitivity of these computed net volume changes is evaluated by also computing volume changes using alternative assumptions (related to the density formulation or grain size distribution data set). These results (shown with the scatter points in Figure 2.5) reveal that the assumptions do not influence the observed trend, but only (and fairly limitedly) the relative contribution of sand and mud. The sensitivity of the results to original assumptions of the method is discussed in more detail in Section 2.4.6.

The contribution of mud to the total net volume changes is 21%–42% (32% for the *best estimate*), which is significantly larger than the current mud content in the upper bed of the Western Wadden Sea (11.8% on average, but with a median mud content of only 3.6% resulting from sand-mud segregation). The much larger contribution of mud to the total infilling results from preferential settling of mud in areas where net sedimentation prevails.

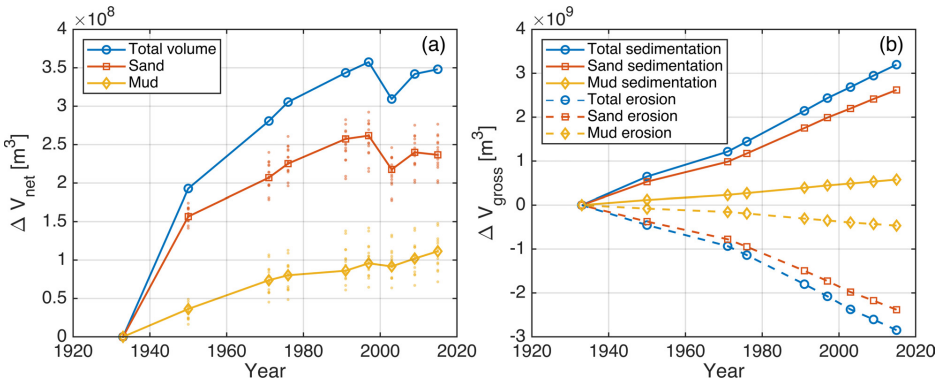

Figure 2.5: Volume changes by sand (red) and mud (yellow) to the bed level changes: (a) Net volume changes for 1933–2015. Lines show the results following the *best estimate* procedure, based on the assumptions of Section 2.3.2. The scattered dots show the range of the results for different assumptions. (b) Gross volume changes consisting of a separate analysis of the sedimentation and erosion patterns.

The total accretion rates of sand started decreasing after 1950, and even reverted to erosion after 1997. Mud accretion, on the other hand, slowed down two decades later, and continues to date. Examining the mud volume changes in more detail reveals that infilling was approximately linear until 1971 and after 1991, but sedimentation stagnated in between these periods. However, this observation may also be a data-artefact, becoming prominent as a result of the low frequency of observations. However, the decreasing rate of net volume changes is not the result of a reduction in bed level dynamics. Figure 2.5b shows the gross sediment volume changes, consisting of the cumulative sedimentation and erosion volumes. While the net volume change rate clearly decreases in time, the gross volume changes have increased since 1971. This increase — both for sand and for mud — is observed in both the sedimentation and the erosion volumes, although it is more pronounced in the latter. Apparently, bed level changes without a residual component (i.e., lateral migration of channels) become more pronounced relative to net changes (e.g., net infilling), suggesting the morphology is gradually adapting to the closure of the South Sea.

The relative contribution of sand and mud to the volume changes in the basins has not been constant over the evaluated period, as is evident from the normalized contribution of sand and mud (Figure 2.6a). The cumulative contribution of mud to infilling volumes has increased from 19% to 32% since the closure of the South Sea (with present-day mud sedimentation volumes exceeding sand deposition volumes, see Figure 2.5a). The reason for this relative increase in mud deposition is that initially, net bed level changes were primarily a response to closure of the South Sea (impacting both sand and mud). In later stages, net sedimentation continued on the tidal flats, which are very muddy.

The more depositional character of mud is also evident from the ratio between the sedimentation and the erosion volumes (Figure 2.6b). A ratio larger than 1 represents sed-

iment import and a ratio smaller than 1 export (with a ratio equal to 1 representing a closed sediment system without external sediment exchange). The ratio of sand has a median value of 1.1 and a relatively low spread (between 0.97 and 1.25, depending on assumptions required for separating sand and mud). The ratio for mud however, has a larger median (1.3, showing the more depositional behavior within the basin) but also a greater spread, with minimum values around 0.82 and maximum realistic values up to 2.3.

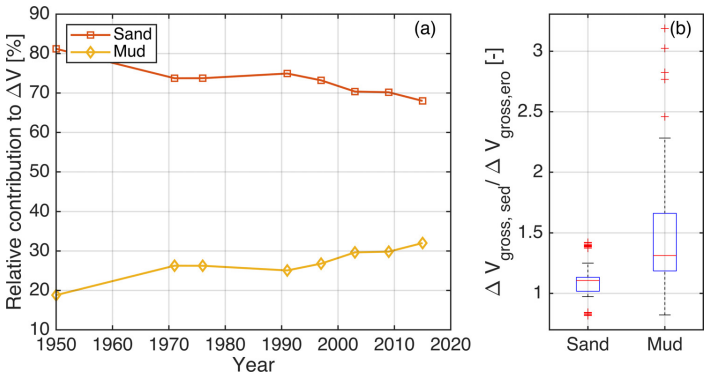

Figure 2.6: (a) Relative cumulative contribution of sand and mud to the net volume changes. (b) Boxplots showing the sedimentation/erosion ratio for sand and mud based on the gross volume changes of all years, calculated for all possible combinations of methodologies to separate the sand and mud contribution.

2.4.4. LOCAL ANALYSES OF NET ACCUMULATION AREAS

To examine the response of fines to the closure of the South Sea in more detail, the evolution of five main areas that have acted as pronounced sediment sinks is further analyzed. To compare these sites, we compute an average accretion per site by dividing their volume change by their area (Figure 2.7). For comparison, we have added the SLR since 1933 (same unit as the normalized volume changes), allowing direct assessment of to what extent the areas can keep pace with SLR.

Both in the Balgzand embayment and in the abandoned Vlieter Channel we observe a gradual decrease in sedimentation rates for both sediment fractions. These volume changes reveal that the local response was fastest in the Balgzand area, where maximum sedimentation rates occurred in the first 20 years. In the abandoned Vlieter, net sedimentation rates increased until 1971. This difference could be related to the distance to the main inlet, which is less for Balgzand since it is closer to the sediment source. However, more accommodation space was created at Vlieter Channel: Note that the presented response of the Balgzand polygon is determined by the infilling of a former channel (small compared to Vlieter Channel) and the heightening of the Balgzand flats (see also Figure 2.1). The larger accommodation space explains the larger sedimentation rate at Vlieter Channel.

In Kornwerderzand, sand infilling continued until 1990, after which net infilling was primarily with mud. However, on the adjacent tidal flat area of Oostbierum we still observe an almost linear accretion of both sand and mud. Infilling rates are higher here for both sediment types, with averaged mud accretion rates twice those in Kornwerderzand. Inschot Channel on the other hand, shows a preferential infilling with sand, and although sedimentation rates of sand have decreased over time, they exceed sand sedimentation rates in the other areas. Mud sedimentation rates in Inschot Channel are similar to those in Balgzand area, already sufficient to keep up with SLR.

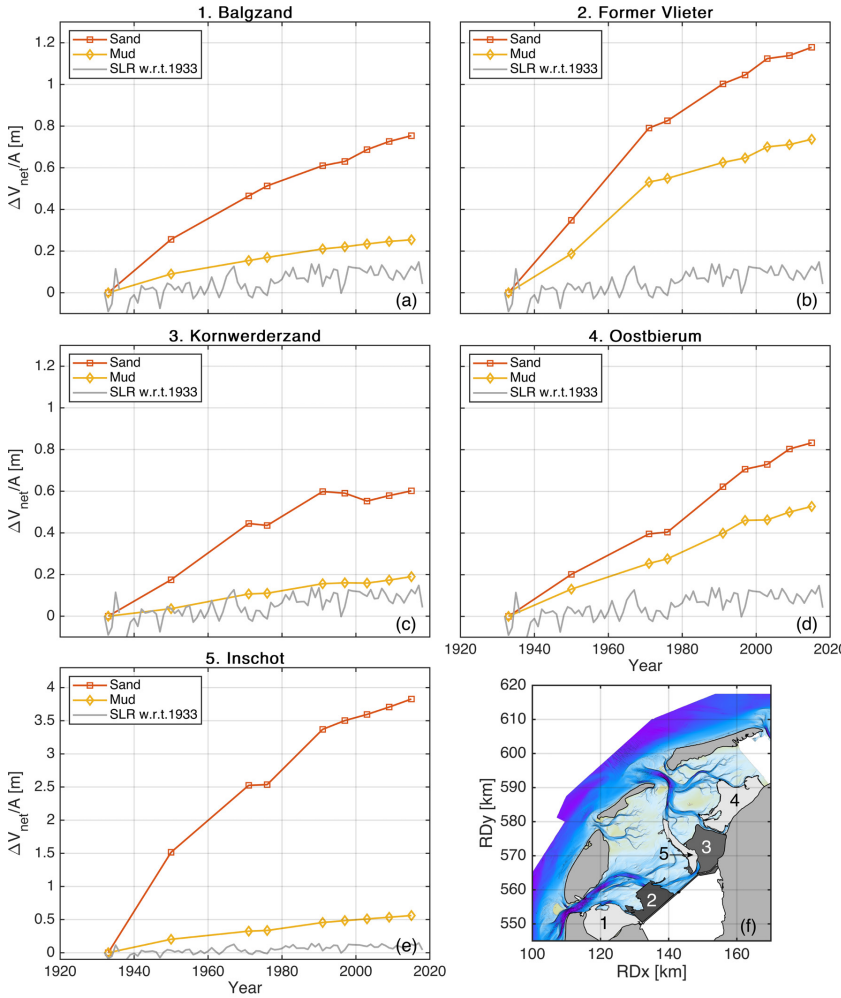

Figure 2.7: Volume changes of distinct net accumulation areas, plotted as net volume changes divided by area (m^3/m^2) to enable a comparison between the study areas. The local SLR with respect to the mean sea level in 1933 (measured at Texel inlet) is plotted in gray. Note the different y-axis in panel (e). Panel (f) shows the polygons of the analyzed sub-areas.

2.4.5. VALIDATION

To verify our methodology, we compare the calculated accretion volumes and sediment type to the sediment classes derived from sediment cores (see Figure 2.8). At the location of core BA1, the bathymetric charts suggest a sedimentation of 1.85 m in the period 1933–1951, consisting of mostly muddy sediment. Core BA1 (taken in 1946) supports our assumption that the sediment composition depositing in response to closure was constant in time. We analyze two cores taken at the former Vlieter channel. At the location of VL1 we calculated about 1.5 m net accretion in the period 1933–1951, with a mud contribution of about 50%. Since we know this site used to be sandy previous to the closure (see Figure 2.2), we can derive from the core that 1.6 m of predominantly fine sediment accreted since the closure until 1946. At the location of VL2 (at a distance of 150 m from VL1) we calculated higher accretion rates, consisting of 2.5 m in total of which 60% mud. The core taken at this location shows that mud was found up to a depth of 3.5 m. We assume that large volumes of mud already deposited before 1933, in the four years between closure (1929) and the bed level observations (1933), and in the years prior to the closure in which construction of the side works had already started. Calculated sedimentation rates over a shoal in Kornwerderzand area also match the findings from core KO1. This area only has a few spots where mud had a large contribution to the sedimentation, which is also reflected in Figure 2.4. Cores OO1 and OO2 reveal that mud was already present in the tidal flat area of Oostbierum before the closure (in line with Lely's observations). Core IN1 shows that indeed, Inschot Channel has been filling in with mostly sand (medium fine to fine). Summarizing, the accumulated sediments shown by the deep cores match well with the calculated sedimentation of sand and mud. There are no indications that the long-term deposits significantly differ from the short-term deposits regarding the sediment composition.

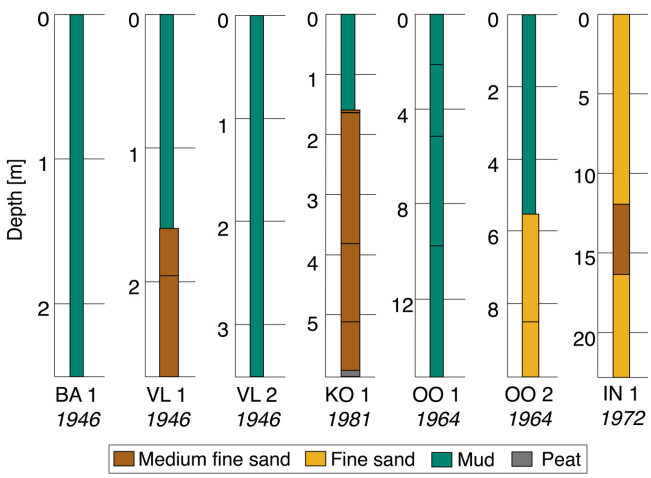

Figure 2.8: Lithology of sediment cores, retrieved from *www.dinoloket.nl*. The locations where the cores were taken are indicated in Figure 2.1. Below each core it is indicated when it was taken.

2.4.6. SENSITIVITY ANALYSIS

As already briefly discussed, the calculated total contribution of mud may vary between 21% and 42%, depending on the used data set, density formulation, and definition of the contribution of fines. In this section, we determine the sensitivity of the computed volumes to these assumptions in more detail. Figure 2.9 shows the contribution of each individual assumption to the mean volume evolution of mud in the basin. An important observation is that our assumptions do not influence the temporal patterns in mud and sand volume changes. The greatest uncertainty is introduced by the sediment composition data. Depending on the choice of the data set, the computed net mud sedimentation volumes range between 90 and 131 million m³, corresponding to a mud contribution of 26%–38% to the total sedimentation. Computing volume changes with data of the *Sediment Atlas* is comparable to using the mean value of *SIBES* data, except for the period 1980–2000, when using *Mean SIBES* data would lead to an overestimation of the mud accretion volumes. Collecting more frequent data will not improve this, since mud contents in the upper bed show a large variability, even in the short term (Yang et al., 2008; van der Wal et al., 2010a; Herman et al., 2018; Hendriks et al., 2020). This shows that the absolute values of our findings should be interpreted carefully. The effect of the dry bed density formulation is much smaller. The formulation by van Rijn and Barth (2019) predicts higher bed densities compared to the formulation by Mulder (1995), resulting in smaller net mud volumes. The effect of the correction factor for small mud contents is minor compared to the other assumptions. Excluding the contribution of small mud fractions on bed level changes results in a small decrease of the mud volume results (less than 10%).

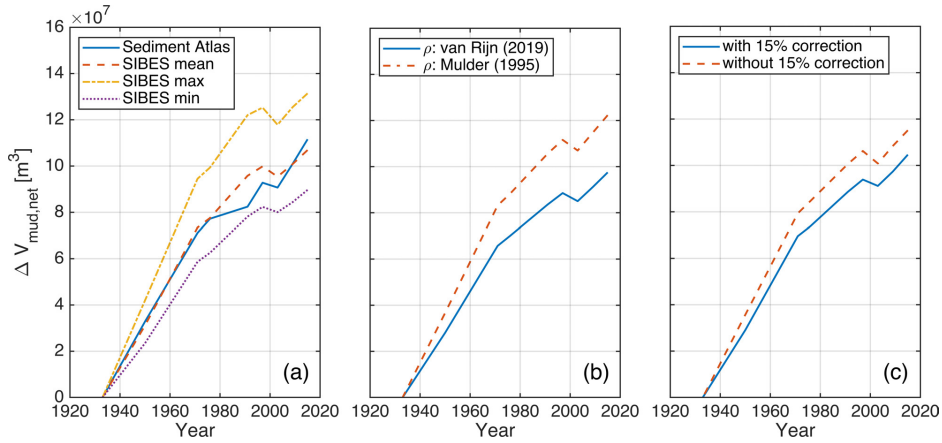

Figure 2.9: Sensitivity analysis showing the mean evolution of mud volumes in the basin, calculated for each assumption of (a) sediment composition data, (b) dry bed density formulation and (c) correction factor for the contribution of small mud contents.

2.5. DISCUSSION

2.5.1. RELATION TO LONG-TERM HYDRODYNAMIC CHANGES

The evaluated morphodynamic evolution results from local human interventions and changing hydrodynamic conditions, such as SLR. Local measurements of the mean sea level during the past century reveal a fairly constant SLR rate of 2 mm/year along the Dutch coast and 1.2–1.4 mm/year in the Dutch Wadden Sea (Deltacommissie, 1960; Baart et al., 2012; Vermeersen et al., 2018). Figure 2.10b shows the yearly averaged sea level at the tidal gauge of Den Helder, located at Texel inlet. To determine which part of the morphodynamic evolution in the Western Wadden Sea may be attributed to SLR, we have calculated the required sediment volumes to keep pace with the sea level changes (by multiplying the total area with the sea level changes, see the right axis of Figure 2.10b). The total observed volume gain in the basins (350 million m^3) is more than the volume required to compensate for SLR (around 150 million m^3).

Figure 2.5b shows a distinct increase in gross volume changes between 1970 and 1980 (both sedimentation and erosion rates suddenly increased). This sudden increase in sedimentation corresponds to an increase in tidal range observed during this period, which originates from an increase in M2 amplitudes (Figure 2.10c–d). In five tidal stations in the Western Dutch Wadden Sea the M2 amplitude increased 3%–8% between 1970 and 1980. The reason for this increase in tidal range still remains unknown (Hollebrandse, 2005), but it extends into the adjacent North Sea (i.e., it is not caused by changes in the Wadden Sea). A larger tidal range influences sediment transport in two ways: First, the sediment transport capacity increases, leading to larger erosion and deposition rates. This is reflected in the increase of the gross volumes of especially sand (e.g., increased channel migration), without necessarily leading to a change in the net sediment volume. Secondly, larger tidal amplitudes increase the tidal accommodation space for sediment to deposit. This increase in accommodation space is especially illustrated with High Water (HW) levels which increased approximately 20 cm, especially between 1960 and 1990 (see Figure 2.10e–i). This increase in HW substantially enlarges the intertidal area where fine-grained sediments may deposit.

2.5.2. BALANCE BETWEEN ACCOMMODATION SPACE AND SEDIMENT SUPPLY

The rate at which a coastal system evolves is controlled by sediment supply (the rate at which sediment can be transported toward a certain location) and accommodation space (the space available for sediment to deposit; Beets et al., 1992). Here, we interpret the post-closure large-scale evolution of the Dutch Wadden Sea in terms of both controls. In short basins a closure would result in a smaller tidal prism, corresponding to reduced relative channel cross-sectional areas (e.g., Eysink & Biegel, 1992; Yu et al., 2014), resulting in lower flow velocities and therefore channel infilling. However, the pre-closure Western Dutch Wadden Sea was a long basin, where the tidal prism did not decrease, but even slightly increased after closure (Elias et al., 2003). Still, the closure caused sediment deficits, which has driven sediment import into the basins.

Sediment supply is determined by the sediment availability and the transport capacity (Beets & van der Spek, 2000). Sediment availability is primarily regulated by sediment

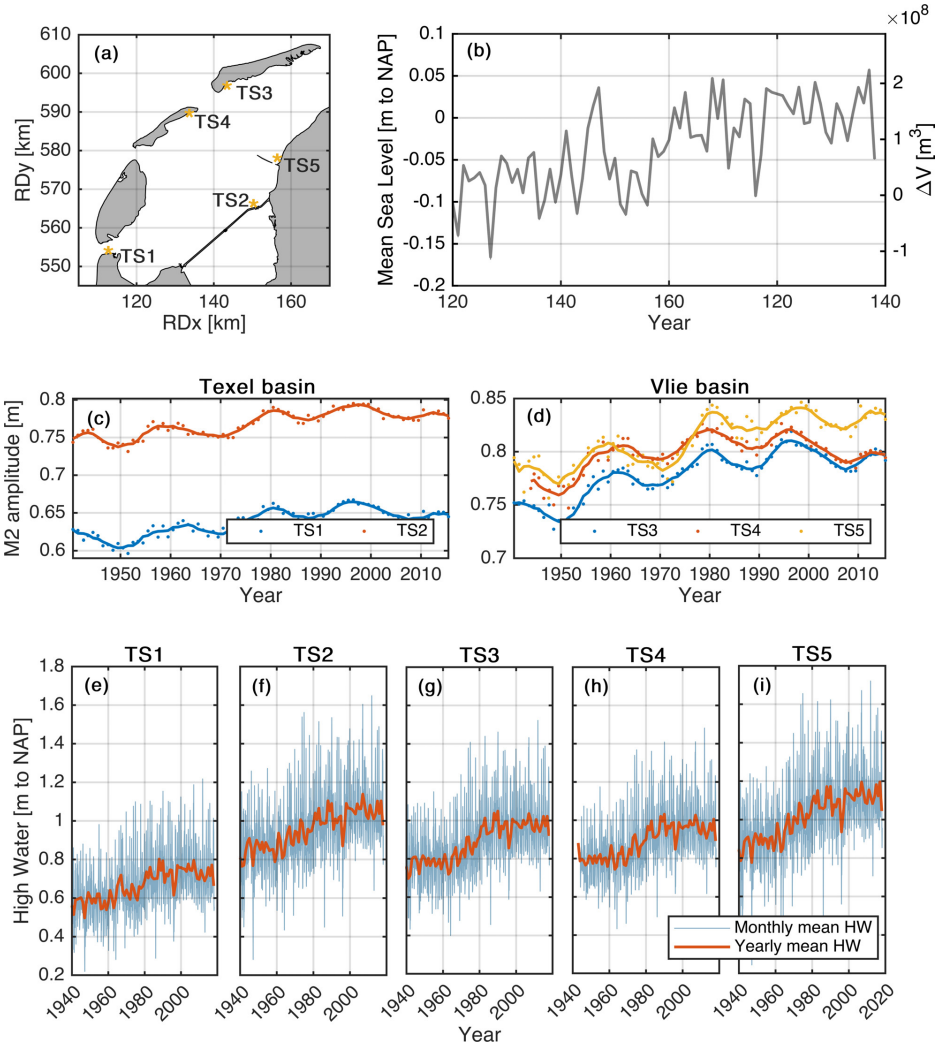

Figure 2.10: Long-term hydrodynamic changes in the Western Dutch Wadden Sea. (a) Locations of the Tidal Stations (TS). (b) Tide-gauge observations of the local mean sea level at Den Helder (station TS1). The right axis shows the sediment volume required to directly compensate for SLR. In panels (c) and (d) we present a tidal analysis of the M2 component, after Nederhoff et al. (2017), showing the 18.6-year lunar nodal cycle and an additional increase between 1970 and 1980. Panels (e–i) show the evolution of the HW levels (monthly and yearly average).

sources, being the adjacent coastlines and ebb-tidal deltas for sand and the North Sea for mud. Elias et al. (2012) analyzed all major ebb-tidal delta systems in the Dutch Wadden Sea, revealing a landward retreat of the outer rim of the deltas and rapidly decreasing volumes since closure of the South Sea. Our results show that also large amounts of mud deposited after closure. Along the Dutch Coastal Zone fines are transported in a residual

north-easterly direction, with a yearly flux estimated at ∼12 million ton/year (see Chapter 3). These suspended sediments originate from sources south of the Dutch Coastal Zone (Hendriks et al., 2020). This coastal mud flux is transported eastward along the Wadden Sea islands, some of which enters the tidal basins through their inlets. Gross exchange rates between the North Sea and each of the tidal basins are in the order of 50 million ton/year (Herman et al., 2018).

Construction of the closure dam created accommodation space in abandoned channels, in addition to the existing accommodation space provided by the intertidal areas along the Frisian mainland coast. In absence of accumulation potential (i.e., when conditions for accumulation are not favorable) no fines permanently deposit (Hendriks et al., 2020). The closure changed the local conditions, probably creating calm areas thereby affecting the accumulation potential, which facilitated permanent deposition of fines. It is unlikely that the present-day deposition rates are natural, i.e., pre-dating closure, because that would have resulted in fairly rapid infilling of the Wadden Sea. However, an alternative explanation for the large deposition rates is related to supply. Before closure, the South Sea provided a large sink for fine sediments to deposit. This sink disappeared after closure, resulting in a greater availability of fine sediment in the remaining basins, and therefore an increase in suspended sediments and deposition elsewhere (van Maren et al., 2016).

In addition, accommodation space has been created by relative SLR, consisting of rising sea levels (see Figure 2.10) and land subsidence. Natural subsidence over the past century, mainly caused by postglacial isostasy and tectonics, has been estimated around 0.564–0.611 mm/year for the Western Dutch Wadden Sea (Hijma & Kooi, 2018a, 2018b). This component is included in the SLR measurements of Figure 2.10. Human induced land subsidence, because of gas and salt mining, takes place on local scale and is estimated around 0.001–0.026 mm/year in the Western Dutch Wadden Sea. In total, land subsidence should have caused an extra 89 million m^3 increase in water volume in the basins over the past century, of which 1.9 million m^3 caused by mining activities (Hijma & Kooi, 2018a). However, no indications of subsidence of the seabed have been observed, which suggests that this increase in accommodation space in the basins has quickly been filled in with sediment (Wang et al., 2018). By multiplying the additional volume created by subsidence with the mean sand and mud content in the basins, we can estimate how much of this has been filled in with sand and mud, as shown by the dashed lines in Figure 2.11. The bandwidth shows the uncertainty range, as calculated by Hijma and Kooi (2018a). To determine the total sediment infilling, these contributions must be added to the observed volume changes, as shown by the red and yellow lines of Figure 2.11.

Our results show that the infilling of accommodation space by sand and mud differs spatially: while some abandoned channels mainly filled in with mud (e.g., Vlieter channel) others have filled in with sand (e.g., Inschot channel). This shows the complexity of the morphodynamic response when differentiating between the two sediment classes. Using only the conceptual framework where sedimentation is a balance between accommodation space and sediment supply, it is difficult to predict where sand and mud will deposit. Moreover, we have shown that the contribution of mud to net infilling is much larger than the average mud content in the top layer of the bed. Therefore, the bed composition

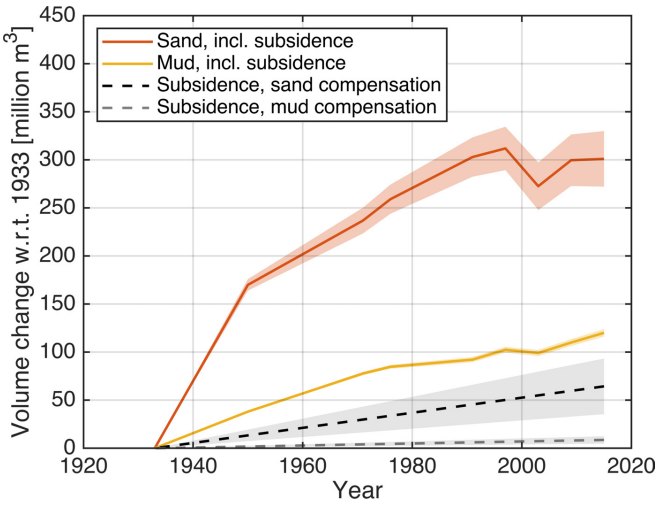

Figure 2.11: Calculated volume changes of sand and mud in the Western Dutch Wadden Sea basins including corrections for land subsidence (following Hijma & Kooi, 2018a, 2018b). The bandwidth shows the uncertainty range of the land subsidence component.

before or after an intervention is not necessarily a good indicator for the contribution of the different sediment types to the net morphological changes.

2.5.3. RESPONSE TIMESCALES

The responses of sand and mud do not only vary spatially, but also the involved timescales are different. Since the closure of the South Sea, the availability of both sand and mud has been sufficient to adapt the Wadden Sea morphology. However, the transport capacity of sand and mud (and therefore response timescales) is markedly different. Both Elias et al. (2012) and Wang et al. (2018) state that the response of the Wadden Sea is limited by the transport capacity, even though sediment sources and accommodation space can be abundant. Therefore, the sandy system will be able to compensate for the intervention over longer timescales. Sediment concentrations of mud, on the other hand, may be up to 10s of kg/m^3 (Colosimo et al., 2020). This implies mud is not transport-limited, and as long as a sediment source and accommodation space where mud can settle are available, the response will be fast.

Dastgheib (2012) simulated 2100 years of evolution of the Wadden Sea after closure of the South Sea, and showed that the sediment import of the basins would mainly take place during the first 300 years after the intervention, with a maximum sand infilling rate through Texel Inlet of about 3 million m^3/year in the first 40 years. However, he based these calculations on sand transport only, without accounting for the contribution of mud in the infilling. Our results show average sand infilling rates that are two times higher (6.2 million m^3/year, including corrections for subsidence) during the first 40 years for the entire Western Dutch Wadden Sea, and an additional mud deposition of 2 million

m^3/year. Therefore, we expect the total response timescale to be shorter than Dastgheib's estimates.

Although sand and mud have different response timescales, their contribution to the total response time of the system cannot be considered separately. Mud sedimentation on the tidal flats, for example, reduces the tidal prism, which may subsequently promote infilling of sand-dominated tidal channels. On a smaller scale, interaction of sand and mud influence their mutual erosion rate (van Ledden et al., 2004a). This interdependency of the morphodynamic response by both sediment types makes it very difficult, if not impossible, to strictly separate the sandy and muddy response of the system. Yet, we have shown that for sand-mud systems, it is crucial to study the response of both sediment types simultaneously and mutually when addressing large-scale morphological changes. Therefore, we advocate collection of detailed sediment distribution data in the vicinity of large scale past or future interventions, and use of this data in combination with available historic topographic data.

2.5.4. SEA LEVEL RISE

SLR is one of the major future threats for the preservation of the Wadden Sea. Keeping pace with SLR requires two things: first, sufficient sediment supply, and second (especially for fine sediment) low-energetic accommodation space. The previously discussed limitation in sand transport capacity may become limiting for morphological adaption to SLR if SLR is faster than a critical rate. Over time, this would result in an eventual disappearance of the intertidal morphology (Wang et al., 2018). On the other hand, our results show that the current supply of mud is sufficient to keep pace with the current SLR rates, and there are no indications showing that future concentrations of suspended matter will significantly decrease. Therefore, we hypothesise that for a critical increase of the sea level the system can only keep up by means of predominant mud sedimentation. This could trigger a shift from a sand-dominated system toward a mud-dominated system.

However, mud deposition requires low-energetic accommodation space. Therefore only low-energy shoals (intertidal and upper subtidal) are presently muddy, and it seems unlikely that the energetic central channels will become muddy as well. When sand import becomes a limiting factor, the channels will not be able to keep pace with the rising sea levels while the muddy shoals can keep up with SLR. This would result in an overall steepening of the coastal profile. Steepening leads to higher wave energy over the flats, and thereby a reduction of mud deposition. This steepening therefore provides a mechanism leading to the shoals no longer being able to keep up with SLR.

2.6. CONCLUSIONS

Closure of the South Sea in 1932 largely changed the morphology of the remaining tidal basins in the Western Dutch Wadden Sea, including the bed composition: it induced local transitions in bed sediments, although the rest of the basins show little large-scale variation on timescales of decades to centuries. The closure triggered an infilling of the basins that is still partly ongoing. By differentiating between the contribution of sand and

mud in this infilling, we have shown that the response was substantially caused by mud (21%–42%, with a best estimate of 32%). This contribution of mud is much larger than the average mud content in the upper bed. The responses of sand and mud to the intervention have been very different in time and in space. During the initial response of the basins, large sand and mud volumes accreted in abandoned channels. At present, mud sedimentation along the mainland coast is still ongoing with fairly constant import rates, while the net import of sand significantly decreased over time and has been fluctuating around 0 in the past two decades. Although we can differentiate between the total contribution of sand and mud to the import volumes, it is not possible to derive independent response timescales for the sandy and the muddy response, since their morphological development is interdependent.

In the future, SLR will be a major threat for the existence of the Wadden Sea; tidal flats may drown depending on their ability to keep pace. We have argued that for slow, gradual changes, both sand and mud sediments are likely to be able to keep pace. Yet, for rapid changes (such as increased SLR rates) only the transport capacity of mud will be sufficient to compensate directly, as long as the sediment source remains sufficient.

This study shows the importance of differentiating between sand and mud in sediment budget studies. We have shown that both human interventions and natural hydrodynamic changes can induce major changes in the bed sediment composition of tidal basins, having implications for sediment management strategies, and affecting ecological and recreational values.

Photograph of the Wadden Sea - by Kevin Krautgartner

3

A SYSTEM-WIDE MUD BUDGET

Abstract
The world's coasts and deltas are progressively threatened by climate change and human activities. The degree at which coastlines can adapt to these changes, especially sea level rise (SLR), strongly depends on the availability of sediments. But despite its importance for coastal adaptation, the availability of muddy sediments is poorly known. This chapter aims at developing the first mud budget for the world's largest uninterrupted system of barrier islands and tidal flats: the Wadden Sea. The resulting mud balance is nearly closed: ∼12 million (M) ton/year enters the system on its western end, ∼1.5 M ton/year is added by local rivers, while we estimate ∼12 M ton annually deposits or is extracted by anthropogenic activities. Our data suggests that a mud deficit already exists in the downdrift areas, which will only become more pronounced with increased SLR rates. Mud is thus a finite resource similar to sand, and should be treated as such in sediment management strategies. Resolving future challenges related to climate change therefore requires a cross-border perspective on sediment management.

This chapter has been accepted for publication at *Communications Earth & Environment* as:

Colina Alonso, A., van Maren, D. S., Oost, A. P., Esselink, P., Hagen, R., Kösters, F., Bartholdy, J., Bijleveld, A. I., & Wang, Z. B. (conditionally accepted). A mud budget of the Wadden Sea and its implications for sediment management.

3.1. INTRODUCTION

The world's coasts and deltas are increasingly influenced by human interventions. Deltas are subsiding at alarming rates (Syvitski et al., 2009; Brown & Nicholls, 2015; Minderhoud et al., 2018), the influx of fluvial sediments is reduced because of upstream dams (Vörösmarty et al., 2003; Syvitski et al., 2005) or sand mining (Eslami et al., 2019; Jordan et al., 2019), and the alongshore drift is interrupted by coastal structures (Luijendijk et al., 2018; Mentaschi et al., 2018). Superimposed on these local interventions are global climate change effects, with sea level rise (SLR) progressively threatening coastlines worldwide (Nicholls & Cazenave, 2010; Bilskie et al., 2014; Vousdoukas et al., 2020). In the coming century, both human interventions and climate change will put the livelihoods of millions of people at risk (IPCC, 2022). Deltas and coastal environments are dynamic systems in which erosion, transport, and deposition of sediments provide a delicate balance. The degree at which coastlines will be able to adapt to future changes, especially in view of SLR, strongly depends on modifications to coastal sediment budgets.

Coastal systems display a wide variety of types, ranging from exposed high-energy beaches to estuaries and back-barrier lagoons. Sediment budgets along sandy open-coast beaches are strongly driven by the wave climate, and adapt relatively quickly to SLR or human interventions (Nordstrom & Jackson, 2012; Toimil et al., 2023). Using empirical formulations (Fredsoe & Deigaard, 1992; van Rijn, 2007a, 2007b), the sediment fluxes along sandy beaches are relatively well known, and their adaptation to SLR can be reasonably predicted when assuming the coastal profile to remain constant (Vousdoukas et al., 2020) — although such a simplification is debated (Cooper et al., 2020). Sediment transport in estuaries, tidal basins and lagoon systems is primarily driven by tidal transport of both mud and sand. Adaptation of such relatively sheltered systems to SLR requires enhanced sediment trapping. Predicting this enhanced trapping introduces two challenges: one is related to the delicate balance in erosional and depositional processes within the basins, the other to the availability of sediments (Coco et al., 2013; Ranasinghe et al., 2013). In many of such basins the availability of sand will be a limiting factor, but this may be (partly) compensated with fine-grained sediments (i.e., mud; Wang et al., 2018; Braat et al., 2019; Elmilady et al., 2022; Boechat Albernaz et al., 2023). In contrast to sand-dominated systems, the alongshore fluxes of fine-grained sediments are poorly known. We aim to develop such a fine-grained sediment flux and highlight the importance of knowing it for the world's largest uninterrupted system of barrier islands and tidal flats — the Wadden Sea.

The Wadden Sea spans over a distance of nearly 500 km along the coastlines of the Netherlands, Germany and Denmark in the Northwestern European shelf (Figure 3.1). As a protected UNESCO world heritage site, it provides crucial habitats for numerous species of fish, mammals and birds. It also plays an important role as sink for CO_2, in particular by blue carbon storage in its sediments, seagrass and salt marshes (UNESCO, 2020). Water motion in the Wadden Sea basins is influenced by tides (with tidal ranges from about 1.5 to over 4 meters), offshore waves generated in the North Sea that penetrate through the inlets, and smaller locally-generated wind waves (Figure 3.1d). Besides, wind-driven currents play a significant role in the shallow parts of the basins (Colosimo et al., 2020; van

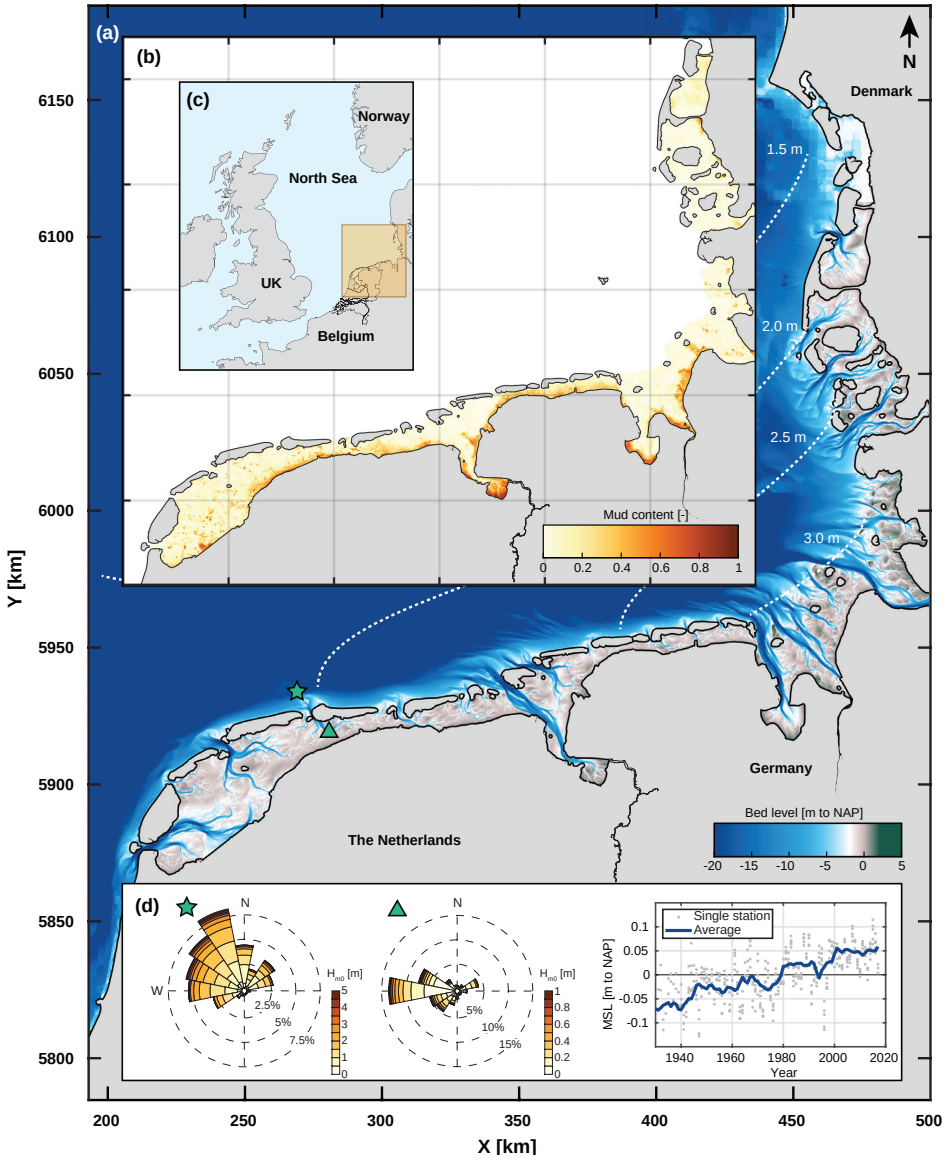

Figure 3.1: Overview map of the Wadden Sea. (a) Current bathymetry (combined maps of 2015–2021 in m to NAP, Netherlands Ordnance Datum). The white dotted lines indicate the tidal range (Wehrmann, 2016). (b) Bed sediment composition plotted as the mud content in the upper bed (top 4–10 cm). The Danish part of the Wadden Sea is not included in the plot, because there is no data available of this area. (c) Location of the Wadden Sea. (d) Example of a wave climate on an ebb-tidal delta and in a Wadden Sea basin (both calculated over the period 2015–2018), and average yearly mean sea level (MSL) from tide gauge records in the Dutch basins over the past century.

Weerdenburg et al., 2021). The main fresh water sources enter the Wadden Sea through the IJssel Lake sluices (average yearly discharge of ∼450 m^3/s; Duran-Matute et al., 2014), and the Ems (∼100 m^3/s; Gräwe et al., 2016), Weser (∼300 m^3/s; Herrling et al., 2021) and Elbe (∼750 m^3/s; Gräwe et al., 2016) estuaries. SLR has so far been limited, with rates of 1.2–2.3 mm/year in the past century (Figure 3.1d; Wahl et al., 2013). Accelerated SLR and subsidence however threaten the Wadden Sea's existence: if the sediment import cannot keep up with increased relative SLR rates, this will result in partial loss or even disappearance of the ecologically valuable intertidal areas (Timmerman et al., 2021; Huismans et al., 2022).

The sediment bed of the Wadden Sea, as that of many other coasts and deltas (e.g., Yangtze Delta, Mekong Delta, Nakdong Estuary, San Francisco Bay), consists of sand and mud. Despite decades of scientific attention to sandy alongshore sediment budgets (Bowen & Inman, 1966; Komar, 1996; Rosati, 2005) and sand-mud budgets of fluvial systems (Milliman & Meade, 1983; Milliman & Syvitski, 1992; Walling & Webb, 1996), marine mud budgets remain largely unknown. This is probably related to the inherent difficulties with obtaining such a budget. Transport of mud cannot be predicted with empirical formulae because its transport is supply-limited, and therefore needs to be based on observed bathymetric changes or detailed measurements of hydrodynamics and sediment concentrations. The Wadden Sea provides herein a globally unique case, with detailed observations of bathymetric changes and grain size distribution (Rijkswaterstaat, 1998; Bijleveld et al., 2012; Compton et al., 2013; Bundesanstalt Für Wasserbau, 2020; Sievers et al., 2021; Folmer et al., 2023; Rijkswaterstaat, 2023). Such observations can be used to quantify the contribution of sand and mud to infilling (Chapter 2; Colina Alonso et al., 2021), thereby providing a sediment budget.

In this chapter we expand on previous work by developing the first complete mud budget of the entire Wadden Sea by carefully quantifying sources and sinks. We synthesize earlier studies to obtain a best estimate for the sources while we compute sinks using extensive bathymetric and grain size distribution data. By demonstrating that this mud budget is nearly closed, we show that mud is in fact a commodity that may become a limiting factor under conditions of accelerated SLR.

3.2. METHODS

3.2.1. MUD SOURCES OVERVIEW

North Sea

The biggest source of mud transported into the Wadden Sea is the North Sea, where mud transport follows the long-year residual current patterns. The North Sea Continental Flow (NSCF, sometimes referred to as Continental Coastal Water) is the most relevant path to the Wadden Sea's mud import. We reconstruct an estimate of its magnitude, based on data and model results reported in literature as explained below.

The mud flux transported by the NSCF originates from the Dover Strait, where a net inflow of water and suspended particulate matter is transported into the North Sea (Prandle et al., 1993; Gerritsen et al., 2001). The magnitude of the mud flux has been widely researched, but the results show a large variety originating from the high temporal and

spatial variability of mud fluxes in combination with the methodologies that have been used (Fettweis et al., 2007). An extensive recent study, where the net flux was calculated based on satellite images as well as on numerical model simulations, indicates a mud flux through the Dover Strait of 22.26–31.74 million (M) ton/year (Fettweis et al., 2007). Approximately 60% of this flux enters the NSCF, whereas the remaining 40% is transported in the East Anglia Plume (EAP; Fettweis et al., 2007).

As the NSCF travels North, it transports mud along the French and Belgian coasts towards the Netherlands. Transport from France to Belgium is estimated at 15.5 M ton/year, and further on to the SW Netherlands at 12.8–14.5 M ton/year (Fettweis & van den Eynde, 2003). North of the Netherlands-Belgian border, but before reaching the Wadden Sea, the NSCF encounters mud sinks in the Eastern Scheldt and around the Port of Rotterdam, as well as a fluvial source from the Rhine river. Together, this results in a net sink of 0.1 M ton/year (de Kok, 2004), resulting in 12.7–14.4 M ton/year of mud reaching the coastal zone just South of the Wadden Sea. Other research (van Alphen, 1990) reports slightly lower values of around 10 M ton/year. We therefore assume a range between 10 and 14.4 M ton/year of mud reaching the Wadden Sea.

The EAP is another North Sea current that transports suspended matter from the Dover Strait, the Thames estuary and cliff erosion to the North East along the southern English coast (Fettweis et al., 2007; Pietrzak et al., 2011). So far, the amount of suspended matter travelling with the EAP that can reach the Wadden Sea coast seems limited (van Raaphorst et al., 1998; de Kok, 2004; Pietrzak et al., 2011). Instead, observations and modelling studies indicate that it is transported via the Oyster Grounds directly to the Skagerrak and the Norwegian Channel (Sundermann, 1993; van Raaphorst et al., 1998).

Main fluvial sources

Similar to the marine mud sources, we have collected data from literature to estimate the average magnitude of the main fluvial sources. These are the fresh water input from Lake IJssel (via the sluices den Oever and Kornwerderzand) and the Ems, Weser and Elbe estuaries. Their magnitudes are shown in Table 3.1.

Table 3.1: Main fresh water sources of mud in the Wadden Sea. The basin numbers refer to Figure 3.1. The magnitude of the sources are derived from literature.

Source	Basin nr	Magnitude [M ton/year]
Lake IJssel	1	0.4 (de Kok, 2004)
Ems	10	0.03 (Puls et al., 1997)
Weser	19	0.4 (Grabemann & Krause, 1998; Grabemann & Krause, 2001)
Elbe	22	0.66 (Ackermann & Schubert, 2007)

Atmospheric deposition

We base our estimate of the atmospheric contribution to the mud budget on previously published data. Studies in the North Sea yielded average atmospheric deposition rates

of 1.6–2.2 ton/km²/year (McCave, 1973). Applied to the total area of the Wadden Sea (11,400 km²), this results in a contribution of 0.018–0.025 M ton/year. This contribution is orders of magnitude smaller than that of the marine and fluvial sources, for which we will consider it to be negligible.

3.2.2. MUD SINKS CALCULATIONS

Tidal basins

To calculate the average deposited mud mass in the basins, we follow a previously developed approach that makes use of bathymetry change data in combination with sediment composition data to calculate the contribution of mud to the observed morphodynamic evolution (see Chapter 2; Colina Alonso et al., 2021).

Net sedimentation and erosion volumes (ΔV) are calculated by subtracting measured bathymetries. Next, these volumes are multiplied with the volumetric mud fraction in the upper bed (top 4–10 cm) to obtain the volumetric contribution of mud (ΔV_{mud}). Our sediment composition data provides information about the mass fraction of the sediment, for which we use a density relation for sand-mud mixtures in the Wadden Sea (Mulder, 1995) to derive the volumetric mud fraction. We subsequently transform the calculated volumetric mud sinks into a mud mass by assuming that pure mud in the tidal basins has an average density of 700 kg/m³, while in the estuaries it is slightly lower (500 kg/m³).

We use Dutch bathymetry data of the *Vaklodingen* data set (resolution of 20 × 20 m; Rijkswaterstaat, 2023) and German data collected within the *EASY-GSH* project (resolution of 10 × 10 m; Bundesanstalt Für Wasserbau, 2020; Sievers et al., 2021). Sediment composition information is based on the *Sediment Atlas* (sediment samples taken in the 1990s in Netherlands parts of the Wadden Sea, resolution of 500 × 500 m in the channels, and 1,000 × 1,000 m on the intertidal flats; Rijkswaterstaat, 1998), *SIBES* (sediment samples taken in 2008–2018 in the Netherlands parts of the Wadden Sea, based on 50,000 surface sediment samples of approximately 7,400 locations, with a resolution of 1,000 × 1,000 m in the channels, and 500 × 500 m on the intertidal flats; Bijleveld et al., 2012; Compton et al., 2013) and *EASY-GSH* data sets (German parts of the Wadden Sea, based on 45,000 surface sediment samples which are interpolated on a 10 × 10 m grid; Sievers et al., 2021).

Calculations are performed for the period 1996–2015 (based on data availability) on a computational grid with a resolution of 250 × 250 m. We determine an uncertainty band by assuming that the calculated volumes might vary 40% (20% higher and 20% lower) because of variations in the sediment density of sand-mud mixtures and of sediment composition changes within the observed period (i.e., between *Sediment Atlas* data and *SIBES* data; Colina Alonso et al., 2021) . No detailed bathymetric evolution or sediment composition data of the Danish basins is available, for which we have based the results of these mud sinks on existing literature (Pedersen & Bartholdy, 2006).

Salt marshes

Similarly, we make use of bed composition data in combination with accretion rates (Esselink et al., 2017) to calculate the mud sinks on the salt marshes. The size of salt marshes in the study area was derived from literature (also Esselink et al., 2017), and is based

on surveys carried out between 2004 and 2014. For sedimentation, we follow the terminology for sedimentation where this is expressed as the amount of sediment that is deposited in the marsh per unit area and time, i.e., kg/m²/year (Nolte et al., 2013). No adjustments were made for organic matter, since Wadden Sea salt marshes are generally minerogenic and thereby low in organic matter. Salt marsh vegetation does contribute to an enrichment of organic matter in the upper sediment layers of the marsh bed, but this organic matter appears to be lost at greater depth when it is buried by new sediment layers (Mueller et al., 2019). Similar to the calculations of the basin sinks, we account for an uncertainty range of 40% total in the salt marsh sinks calculations, originating from variations in the sediment density and in the sediment composition.

3.3. RESULTS

3.3.1. MUD SOURCES AND SINKS

To establish the mud budget, we determine the magnitude of the main sources and sinks focusing on inorganic particulate matter. The largest mud source is the marine North Sea Continental Flow (NSCF). This flow transports mud from the Dover Strait (in between France and the United Kingdom) along the French, Belgian and Netherlands coasts. Its magnitude at the most western end of the Wadden Sea is on average approximately 10–14.4 M ton/year (see Section 3.2.1). The sediment plume first deflects to the East, after which it turns northward again in the German Bight, while interacting with the various tidal basins (Figure 3.2a). Although these basins primarily act as sediment sinks, several rivers (from Lake IJssel and the Ems, Weser and Elbe estuaries) constitute an additional sediment source, adding a total amount of mud of 1.5 M ton/year into the Wadden Sea.

The main mud sinks throughout the Wadden Sea can be divided into four categories: deposition in the basins (7.95 M ton/year) and on the salt marshes (1.84 M ton/year), offshore deposition (0.56 M ton/year), and anthropogenic extraction (1.98 M ton/year, see Figure 3.2b). Most basin deposition presently takes place in the intertidal areas, especially along the mainland coast, although abandoned channels also acted as major mud sinks in the past (Chapter 2; Colina Alonso et al., 2021; van Maren et al., 2023). The average mud deposition in the basins and on the salt marshes largely varies per basin (see also Tables A.1–A.2 and Figures A.1–A.2 in Appendix A). The main offshore sink is the area around Helgoland, where continuous deposition rates of about 1.6 mm/year (Hebbeln et al., 2003) amount to a sink of approximately 0.5 M ton/year. Anthropogenic sediment extraction provides the second biggest sink, even surpassing salt marsh deposition. With this we refer to the removal of sediments by dredging without disposing the sediment within the Wadden Sea or in its vicinity in the North Sea. Although most dredged sediment is redistributed within the Wadden Sea, some of the sediment dredged from the lower Ems (Vroom et al., 2022; Pierik et al., 2023), Weser (BIOCONSULT & Coastal Defence and Nature Conservation Agency (NLWKN), 2012; BIOCONSULT et al., 2018), and Elbe estuaries (Netzband et al., 2002; HPA & WSA, 2011; Weilbeer & Uliczka, 2019) is disposed on land (either on disposal sites for contaminated sediments, or as coastal protection reinforcement).

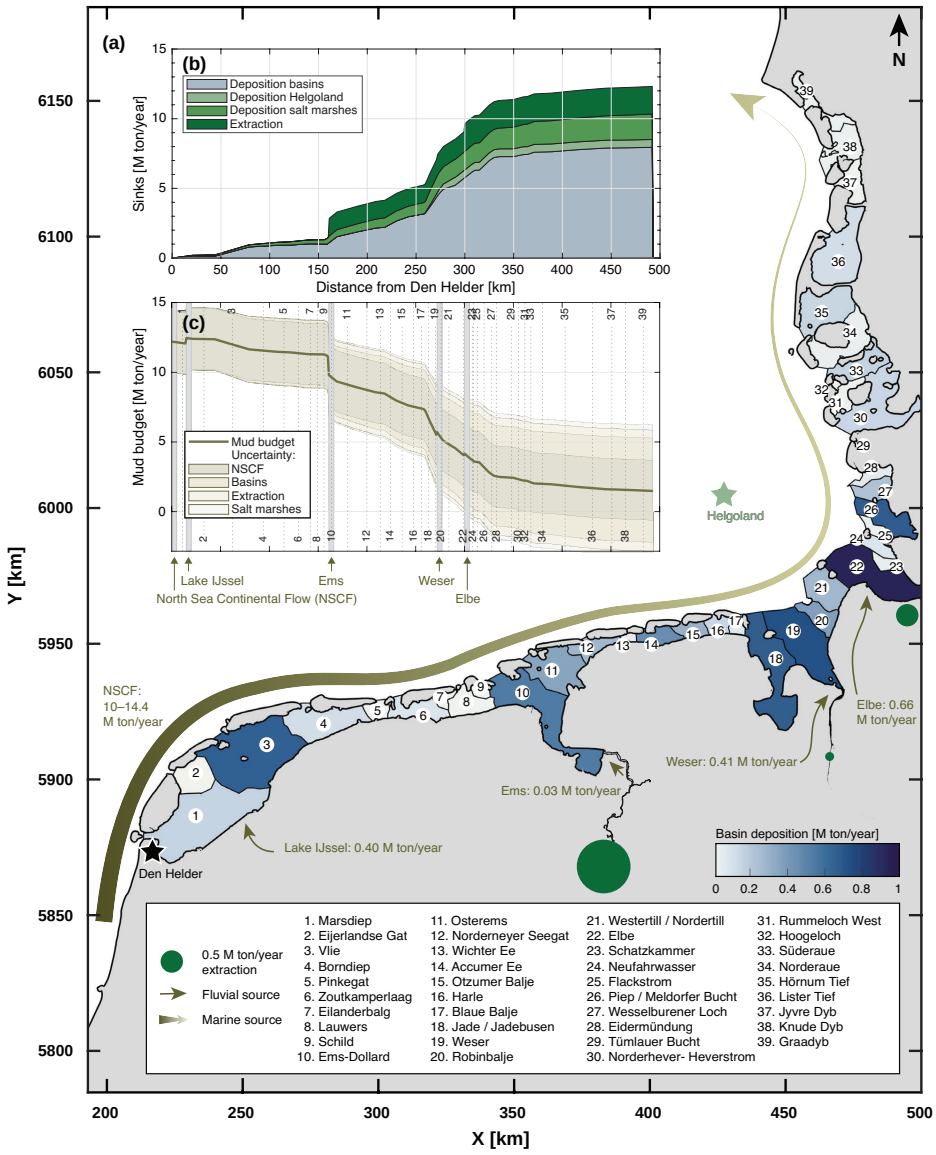

Figure 3.2: Mud budget of the Wadden Sea. (a) The blue colors show the basin-average mud deposition, calculated for 1996–2015. The brown arrows indicate the main mud sources and the green dots the average mud extraction from the Ems, Weser, and Elbe estuaries (in which we assume an uncertainty range of 20% originating from a variation in sediment composition of the dredged material). (b) Cumulative alongshore sediment sinks per type. (c) Estimated alongshore mud budget and its uncertainty as a function of distance from Den Helder. The uncertainty is initially resulting from the NSCF flux (10–14.4 M ton/year, darkest brown band) but becomes progressively more influenced by sedimentation in the basins, on salt marshes and through extraction (lighter brown bands). The vertical grey bars indicate the location of sources, the numbered dotted lines the location of individual basins.

3.3.2. THE MUD BUDGET IS NEARLY CLOSED

The various sediment sources and sinks have been converted into a sediment pathway (Figure 3.2c). Starting West (at Den Helder) where the NSCF enters the Wadden Sea, it follows the anti-clockwise rotation of the flow along the barrier islands, until the most northern end. With increasing distance from Den Helder, the magnitude of the cumulative sinks increases far beyond the sources along its pathway. With our best estimate for the initial sediment supply and various sources and sinks, there is only about 1.5 M ton/year unaccounted for in the northern end. This can be considered a small amount given the wide range in apparent uncertainties and the possible loss of mud to the offshore areas along its pathway.

The largest uncertainty in our estimate is the magnitude of the flux in the NSCF, followed by the basin deposition, mud extraction and salt marsh sedimentation. The uncertainty in these latter three includes the variability in the mud density and sediment composition over time (see Section 3.2). The lower end of the cumulative error band is considered to be unrealistic, since this would imply that there is no mud left after the Elbe estuary (basin 22), while mud sedimentation has been observed in the basins and on the marshes to its North. The observation that the mud budget is nearly closed is only limitedly affected by uncertainties in the fluvial sources: even if those would vary by a factor of 2 (which does not seem to be the case when comparing our data to other estimates; Milliman & Farnsworth, 2011), the total sources would still only be slightly larger than the sinks.

The spatial variability of the mud sinks is large throughout the entire domain (see Figure 3.3a). To compensate for the basin size, we determine the basin deposition per km², revealing a distinctive trend (Figure 3.3b): mud deposition largely increases with increasing distance from Den Helder until km 224 (basin 14, in East Frisia), after which it sharply drops (especially after the Elbe estuary, km 300). Salt marshes are efficient mud traps. Here, sedimentation rates are up to an order of magnitude larger than in the basins (although their total area is much smaller), and follow the same spatial trend. Most sediment deposits on the foreland marshes, while a smaller amount accretes on the island- and hallig marshes (Figure A.2 in Appendix A). The decline of sedimentation rates in the last 200 km of the Wadden Sea is even more pronounced in these foreland marshes (Figure 3.3d). These spatial trends in the basin and marsh sedimentation suggest that there could be a mud shortage in this downdrift part of the Wadden Sea (Maan et al., 2018; Willemsen et al., 2022).

Another indicator for the potential mud shortage in the northern German and Danish parts of the Wadden Sea is the upper bed sediment composition in the basins. Whereas the mean mud content ranges between 5%–25% in the first 300 km without showing a distinctive spatial trend between the basins, it drops abruptly below 10% afterwards (Figure 3.3e). Even more pronounced is the trend in the bimodality of the mud content (Figure 3.3f). The mud content in the Wadden Sea tends to be bimodally distributed (Chapter 5; Colina Alonso et al., 2022), with the sediment bed being either relatively sandy (mode 1) or relatively muddy (mode 2). This bimodality may disappear if suspended mud concentrations become low (only mode 1 remains) or high (only mode 2 remains). Figure 3.3f shows that bimodality disappears after km 300, suggesting that sus-

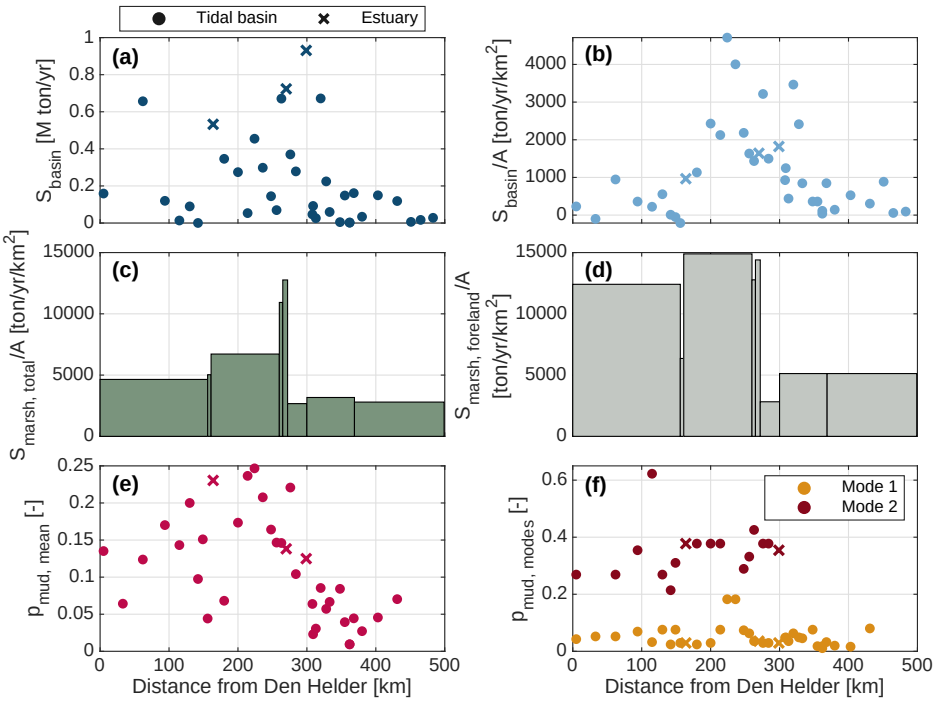

Figure 3.3: Spatial variation of sinks and indicators of a decreasing mud availability. (a–b) Scatter plot of the total mud sinks in the basins. Tidal basins are indicated by a dot, estuaries by a cross. Basin sinks per km^2 show a clear spatial trend along the Wadden Sea coast. (c) Histogram of the average salt marsh sinks per km^2. (d) Histogram of the salt marsh sinks in foreland salt marshes. This type of marshes has the largest contribution to the total marsh sinks (see also Figure A.2 in Appendix A). (e) Average mud content ($p_{mud,mean}$) in the upper sediment bed of the basins. (f) Modes of the probability density function (pdf) of the mud content in the sediment bed ($p_{mud,modes}$, plotted per basin), representing the equilibrium mud content in the bed (see Chapter 5; Colina Alonso et al., 2022). Bimodality is detected up to km 300 (Elbe estuary).

pended mud concentrations are lower here, and therefore also indicating a potential mud shortage compared to the other Wadden Sea basins. Thus, both the sedimentation rates and the bimodality of the bed sediments indicate that mud sedimentation in the northern parts of the Wadden Sea might be supply limited, which matches the observation that the cumulative mud budget in these areas is largely reduced. Note however that a potential higher energy exposure in these areas could also be a contributing factor to this. The western parts of the Wadden Sea appear to be accommodation space limited (i.e., sediment deposition rates are restricted by available space to deposit and not by the supply of sediments). This also explains the high suspended sediment concentrations observed in many parts of the Western Wadden Sea, exceeding many g/l even on the exposed tidal flats (Colosimo et al., 2020).

3.4. DISCUSSION

3.4.1. FINE SEDIMENTS AS A RESOURCE

Intertidal areas comprise nearly half of the surface of the Wadden Sea (de Jonge et al., 1993) and provide important functions related to safety, ecology and economy. In combination with salt marshes, the intertidal areas protect the mainland coast (Temmerman et al., 2013; Zhu et al., 2020). Intertidal areas also provide habitat for benthic communities and higher trophic levels, acting as e.g., fish nurseries (Elliott et al., 2007) and feeding ground for birds (van Roomen et al., 2012). Their disappearance would lead to large-scale loss in biodiversity (Laursen et al., 2023). Their economic importance is also evidenced by other ecosystem services such as fisheries (de Jonge et al., 1993; Lotze, 2007).

These intertidal systems are composed of sand and mud. Mud plays a crucial role creating specific habitats for benthic species (Ysebaert et al., 2002; Compton et al., 2013; Singer et al., 2023), and contributing to the current morphological evolution of the intertidal areas (Chapter 2; Colina Alonso et al., 2021) as well as their ability to keep pace with relative SLR (Wang & van der Spek, 2015). The rate at which sand is transported towards the intertidal areas is namely largely depending on the transport capacity (Wang et al., 2018), and will become a limiting factor under conditions of accelerated SLR (Dissanayake et al., 2012; Lodder et al., 2019; Huismans et al., 2022). The decline in sand supply will increase with increasing distance from the inlet, resulting in partial drowning of the intertidal areas if the sediment deficit is not compensated by mud. Deposition of fine-grained sediments is supply- or accommodation space limited and hardly depending on transport capacity.

The accretion rates on some of the tidal flats presently outpaces SLR (Benninghoff & Winter, 2018; Wang et al., 2018; Benninghoff & Winter, 2019; Colina Alonso et al., 2021), but this may change in the future for two reasons: First, it is expected that SLR will accelerate in the coming centuries. The global sea level has risen 2.1 mm/year since 1970, but this speed is accelerating (Dangendorf et al., 2019; IPCC, 2019). The region-mean SLR in the Wadden Sea has been slower — 1.77 mm/year since 1958, most likely due to regional geological, glacio-isostatic and meteorological effects — but projections of SLR rates range from 2.2 to 18.3 mm/year for the year 2100 (Vermeersen et al., 2018). Secondly, the current accretion rates of the tidal flats do not necessarily represent their ability to keep up with SLR. The present-day development of the Wadden Sea is largely influenced by human interventions, of which the response timescales are long. The observed sedimentation rates are partly a response to these interventions, and given the exponential decay of such a response (van Maren et al., 2023) it is likely that sedimentation rates will slow down in the future. Accretion rates will largely depend on the sediment availability in combination with sediment management strategies.

3.4.2. IMPLICATIONS FOR FUTURE SEDIMENT MANAGEMENT

Our findings are important for future sediment management of the Wadden Sea specifically (Lodder & Slinger, 2022), but also in general for muddy environments where fine-grained sediments are often assumed to be abundantly available. Our work illustrates that mud is a finite resource, and therefore circularity is key. Mud is abundantly available

in the Western Wadden Sea, leading to regular maintenance dredging. Here, even without interventions, SLR will probably lead to higher sedimentation rates over the supra- and intertidal areas because of the increase in accommodation space. But even more, a likely future sediment management strategy will be to progressively trap fine-grained sediments in anticipation of accelerated SLR. SLR, especially when combined with modified sediment management strategies, will then lead to a downdrift reduction of available fine-grained sediments. With the Wadden Sea spanning three different countries, such dependencies illustrate the importance of cross-border sediment management policies.

With mud being a finite resource and SLR in time inducing shortages, some of the policies related to extraction of mud should potentially be revisited. In the past, sediments were primarily extracted for the construction of flood safety infrastructure (e.g., dikes, dwelling mounds) and roads (Vollmer et al., 2001). Nowadays, the main motivation for extraction is the deepening of navigation channels (and the costs associated with disposal). Although the total extracted mud mass has decreased over time (BIOCONSULT & Coastal Defence and Nature Conservation Agency (NLWKN), 2012; van Maren et al., 2016), it still amounts to 12%–17% of the total mud budget. Sediment extraction may provide a relatively cost-effective methodology of dredging, and may also lower the suspended sediment concentrations locally (van Maren et al., 2016). However, the negative impact of sediment extraction over longer timescales and larger spatial scales in the context of climate change is at present not considered in policy frameworks. Given the expected future demand for sediments in order to keep pace with SLR, these long-term large-scale impacts should be accounted for when planning sediment extraction. Such planning would also need to account for a delayed response resulting from on the system's previous buffer capacity (Luan et al., 2016; Wang et al., 2018; Raff et al., 2023).

Consequently, we stress the need for cross-border sediment management strategies fuelled by our findings that not only sand but also mud is often a finite resource. The accuracy of tools to predict a coastal system's response to SLR is limited, posing a challenge for scientists, coastal engineers, and decision makers. While numerical models may capture short-term up to decadal morphodynamic evolution — especially after large-scale distortion of the system (Luijendijk et al., 2017) — their ability to predict (natural) long-term development remains limited (Lesser, 2009). Moreover, the absence of calibration and validation data of a system's response to future SLR conditions introduces major uncertainties. We believe that understanding this response should start with a sediment budget on a system scale, i.e., crossing international borders and national policy frameworks.

Photograph of the Wadden Sea - by Kevin Krautgartner

4

SAND-MUD INTERACTION

Abstract
The morphology of tide-dominated systems is progressively influenced by human activities and climate change. Quantitative approaches aiming at understanding or forecasting the effects of interventions and climate change are often aggregated, thereby simplifying or schematizing the investigated area. In this work, we advance on the knowledge of sediment transport processes shaping tidal systems and on methodologies translating schematized model output into physically realistic variables. In terms of improved physics, we systematically evaluate the influence of sand-mud interaction processes. Most tidal systems are shaped by a mixture of sand and mud. Morphological models typically compute transport of sand and mud independently, despite studies clearly demonstrating that their physical behavior is mutually dependent. We investigate the effects of two interaction mechanisms (erosion interaction and roughness interaction, applied with varying mud erodibility) with a schematized process-based morphodynamic model. We convert model output into metrics that describe the macro-scale configuration of the modeled systems, allowing a quantitative comparison of scenarios. Modeled patterns and intertidal flat shape, size and composition widely vary with mud erodibility settings, but equally depend on the evaluated sand-mud interaction mechanisms (with erosion interaction having a larger effect than roughness interaction). Sand-mud interaction thus needs to be accounted for from a physical point of view, but also to improve predictions of tidal basin evolution models, particularly the (bimodally distributed) sediment composition of intertidal flats.

This chapter has been published in *Journal of Geophysical Research: Earth Surface* as:

Colina Alonso, A., van Maren, D. S., van Weerdenburg, R. J. A., Huismans, Y. & Wang, Z. B. (2023). Morphodynamic modeling of tidal basins: The role of sand-mud interaction. *Journal of Geophysical Research: Earth Surface, 128*, e2023JF007391. [Link]

4.1. INTRODUCTION

Worldwide, deltas are under pressure from climate change and increasing human activities, undergoing transitions in their abiotic and biotic systems (e.g., Syvitski et al., 2009). Anthropogenic interferences in estuaries and tidal basins can irreversibly influence their morphological development and threaten their existence (Wang et al., 2015; Dijkstra et al., 2019). In addition, climate change introduces a new spectrum of coastal challenges, such as coping with sea level rise (SLR), increased storminess and saltwater intrusion (IPCC, 2022). To face these existential threats and protect our deltas, we must gain a thorough understanding of the effects of climate change, as well as of the effectiveness and potential side-effects of mitigating measures such as coastal interventions.

Morphodynamic effects of climate change and human interventions play a role on decadal to centennial timescales. Forecasting the morphological impact requires numerical tools that can handle such long timescales. However, model complexity and simulation periods are coupled. Long forecasting periods require simplified model configurations because of error propagation (Hajek et al., 2012), the associated computational time, and the requirement of morphodynamic equilibrium (Hoitink et al., 2020). In the context of climate change, especially this latter requirement is very relevant because morphological adjustment to SLR introduces subtle variations in sediment transport. When the timescale related to the investigated changes (T_c) is smaller than the time required for the model to attain morphodynamic equilibrium (T_e) the model is still spinning up, overwhelming the small variations introduced by for example, SLR.

A solution to use complex numerical models while satisfying $T_c > T_e$ is to use highly schematized configurations in which the topography and the forcing are largely simplified. Moreover, simplified schematizations are more suitable to study morphodynamic mechanisms in isolation, compared to models with realistic but also inherently complex geometries and boundary conditions. Such simplified models have advanced our understanding of the macro-scale coastal evolution of deltas on large timescales. Initially, these studies focused on the dynamics of sandy coasts only (e.g., Hibma et al., 2003; Marciano et al., 2005; van der Wegen & Roelvink, 2008; Dissanayake et al., 2009; Guo et al., 2015). However, real tidal systems are often shaped by a mixture of sand and mud. A number of follow-up studies were extended with mud-sized sediment to improve the prediction of large-scale delta evolution (Edmonds & Slingerland, 2010; Geleynse et al., 2011; Caldwell & Edmonds, 2014) and of intertidal flat formation (e.g., Braat et al., 2017; Elmilady et al., 2020, 2022). These existing studies so far largely treated sand and mud as independent fractions, despite overwhelming evidence that erosion of sand and mud is mutually coupled (Torfs, 1995; van Ledden, 2003; Jacobs, 2011; van Rijn, 2020). Besides, the substrate introduces complex feedback mechanisms related to hydraulic roughness — which can be lower in muddy beds, thereby promoting deposition of mud (Soulsby & Clarke, 2005) — and to biologic activity. An example of the latter is that intertidal benthic algae prefer a muddy substrate, and once in place facilitate more net mud deposition (see e.g., van der Wal et al., 2010b; Grabowski et al., 2011; Brückner et al., 2021). Although some of these complexities have been addressed in numerical models (van Ledden et al., 2004b; Le Hir et al., 2011; Brückner et al., 2021), their inclusion in long-term prediction

models remains limited. As a result, despite advances in our understanding of small-scale sand-mud interaction processes, their large-scale morphological implications still remain poorly understood.

In this chapter we aim at a better understanding of the effects of including small-scale sand-mud interaction on modeled large-scale morphodynamics of tidal basins. We focus on abiotic interactions, since the increasing complexity arising from biotic effects (Herman et al., 2001; Grabowski et al., 2011; Brückner et al., 2021; Chen et al., 2021b) may obscure the abiotic interactions which are already complex themselves. We study long-term tidal basin evolution with a schematized model inspired by the tidal basins in the Dutch Wadden Sea, in which two sand-mud interactions have been implemented. An important drawback of such schematized configurations is that it is difficult to correlate simplified model layouts with real world issues. A key challenge is how to capture the fundamental aspects of real-world systems in low complexity models, and how to quantitatively validate the schematized model performance. We therefore introduce metrics to correlate the range of model realizations resulting from sand-mud interaction mechanisms with the real world.

The structure of this chapter is as follows: We first introduce the theory of the two studied sand-mud interaction mechanisms in Section 4.2. In Section 4.3, we present our modeling methodology and the implementation of the sand-mud interaction mechanisms. The model results in which we analyze 50 years of basin evolution under different model settings are presented in Section 4.4. Here, we also compare them with field data from the Wadden Sea. In Section 4.5 we discuss our results, focusing on the large-sale impact of sand-mud interaction and on the opportunities it provides to improve morphodynamic modeling. Lastly, conclusions are given in Section 4.6.

4.2. THEORY ON ABIOTIC SAND-MUD INTERACTION MECHANISMS

4.2.1. INTERDEPENDENT EROSION

Sand-mud mixtures can be non-cohesive or cohesive, depending on the small-scale structure of the sediment bed (two regimes, see Figure 4.1a). When clay contents are below a critical amount ($p_{clay,crit}$), the internal structure is determined by the inter-particle locking of sand grains and the mixture can be treated as non-cohesive sediment. At $p_{clay,crit}$, sand grains lose contact and they become part of a mud matrix in which clay cohesion determines the structure (Torfs, 1995; van Ledden et al., 2004a; Jacobs et al., 2011). This critical clay content is a function of the sand grain size, the type of cohesive material, the water content and the organic content. The transition between the two regimes takes place at $p_{clay,crit}$ of 5%–10% (van Ledden et al., 2004a). Assuming a constant clay/silt ratio, which is a reasonable assumption for cohesive sediments in the considered tidal and estuarine systems (van Ledden et al., 2004a; Colina Alonso et al., 2022, Chapter 5), a critical mud content ($p_{mud,crit}$) can be determined at which the transition takes place ($p_{mud,crit} \approx 0.3$ for the considered systems). Herein, mud is defined as all sediment with a grain size smaller than 63 μm (i.e., silt and clay).

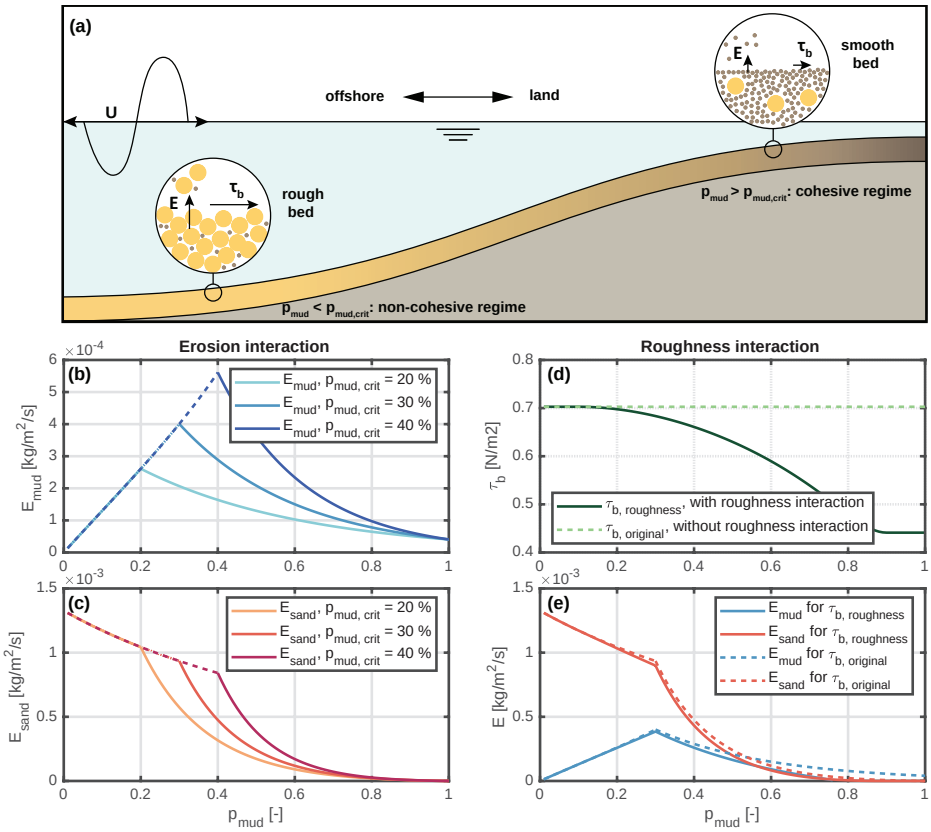

Figure 4.1: (a) Sketch illustrating sediment erosion and bed roughness for different sand-mud content. (b–c) Erodibility feedback: Relation between the erosion rate of mud and sand and the mud content, based on van Ledden (2003) for several values of $p_{mud,crit}$. (d–e) Roughness feedback: Bed shear stresses decrease with increasing mud content, hence decreasing erosion rates. $\tau_{b,original}$ refers to the bed shear stresses calculated without accounted for roughness interaction. Panels (b–e) are calculated for the conditions: U = 0.75 m/s, h = 5 m, $\tau_{e,mud}$ = 0.5 Pa, M_e = 10^{-4} m/s, $D_{50,sand}$ = 150 μm. A gradual transition is imposed between rough beds ($k_s = k_{s,sand}$) and smooth beds ($k_s = k_{s,silt}$) at 0.1 $< p_{mud} <$ 0.9.

The erosion behavior of sand-mud mixtures has been the topic of experimental studies (e.g., Mitchener & Torfs, 1996; Jacobs, 2011; van Rijn, 2020) and has been numerically parameterized (e.g., van Ledden, 2003; Le Hir et al., 2011). From experimental and theoretical studies it follows that the erosion fluxes of sand and mud are proportionally coupled with erosion of both sand and mud depending on the erosion properties of the non-cohesive or cohesive mixture (Mitchener & Torfs, 1996; van Ledden et al., 2004a; Winterwerp & van Kesteren, 2004; Jacobs et al., 2011; Le Hir et al., 2011; Chen et al., 2021a). Non-cohesive erosion can thus be parameterized with sand transport formulations such as van Rijn (1993); cohesive erosion with a Partheniades-type equation. Following this parametrization, we illustrate the erosion rates as a function of mud content (computed with van Ledden's, 2003, model, which we use in Section 4.3.2) in Figure 4.1b and 4.1c.

4.2.2. HYDRAULIC ROUGHNESS OF THE BED

The sediment composition also affects the hydraulic roughness of the bed, which can largely impact effective bed shear stresses and erosion rates. The hydraulic roughness consists of a form drag component (resulting from bedforms) and a skin friction component (resulting from the grain size of the bed). Water-bed exchange processes are determined by a thin layer near the bed depending on skin friction rather than form drag, whereas the large-scale flows depend on the form drag (Winterwerp et al., 2021). The hydraulic roughness (skin friction) of mud beds is lower than that of sand beds, because larger sand grains generate more near-bed turbulence. Since the bed shear stress increases with the hydraulic roughness, and assuming the depth-averaged flow is not or only limitedly influenced by the small-scale skin roughness, lower bed shear stresses will be exerted on muddy beds (Yao et al., 2018). An increase in the mud content of the bed therefore weakens the erosion forces.

Assuming that the hydrodynamic roughness influencing water-bed exchange of sediment is primarily influenced by skin friction (as above), the effect of the mud content on the bed shear stress can be computed using the method of Soulsby and Clarke (2005; see Figure 4.1d for the bed shear stress with this effect in dark green and without this effect in dashed light green). The reduction of the bed shear stress has a notable effect on the sand and mud erosion fluxes, as illustrated in the example of see Figure 4.1e (which is calculated using the formulations of van Ledden, 2003, with $p_{mud,crit} = 0.3$): The erosion fluxes are lower for higher mud contents, which already follows from van Ledden (2003), but this is substantially strengthened when accounting for bed roughness effect, especially in the cohesive domain. In the example of Figure 4.1, the mud erosion fluxes are even reduced to 0 for very muddy sediments ($p_{mud} > 0.7$) for the considered hydrodynamic conditions.

4.3. METHODS

4.3.1. NUMERICAL MODEL SET-UP

We explore the effects of erodibility interaction and roughness interaction (as defined in Section 4.2) on tidal basin evolution using a depth-averaged (2DH) Delft3D morphodynamic model (version 6.03.00.59659, see also Lesser et al., 2004). We have developed a schematized model of a tidal basin instead of a realistic case, because such a schematized basin is minimally restricted by initial topography or bed sediment — which would otherwise strongly influence the model outcome (see e.g., Dastgheib et al., 2008; Rahdarian et al., 2022).

The schematized configuration of the tidal basin is based on the tidal basins of the Wadden Sea. The model domain consists of a tidal inlet in between two islands and a back-barrier basin with dimensions of 15×10 km. The computational grid is regular with a resolution of 100×100 m. We work with a stratified bed consisting of an active transport top layer with a thickness of 0.1 m and 20 Eulerian bed layers with a thickness of 1 m underneath. Starting from a sloping bathymetry and a uniform sediment composition ($p_{sand} = 0.95$, $p_{mud} = 0.05$), basin evolution is simulated for a period of 50 years. Within this period, its morphological and sedimentological state converges to a dynamic equi-

Table 4.1: Model parameter settings

Parameter	Value	Description
a	1.5	Tidal amplitude [m]
$k_{s,hydro}$	2e-2	Bedform-related roughness height for hydrodynamic calculations [m]
$k_{s,sand}$	6e-4	Nikuradse roughness height (skin friction) for pure sand [m]
$k_{s,silt}$	3e-5	Nikuradse roughness height (skin friction) for pure mud [m]
MorFac	50	Morphological scale factor [-]
D_{50}	250	Median grain diameter of sand [μm]
w_s	2.5e-4	Settling velocity of mud [m/s]
τ_e	0.125–2	Critical bed shear stress for erosion of mud [N/m^2]
M	1e-4	Erosion parameter [m/s]
$p_{mud,crit}$	0.3	Critical mud content for cohesive behavior [-]
β_m	1	Bed packing coefficient [-]
$c_{mud,bound}$	5	Suspended mud concentration at the boundary [mg/l]

librium. The model is forced by a semi-diurnal tide with an amplitude of 1.5 m (S2+S4) entering from the (only) open boundary at the North (located 15 km from the inlet), and a wave-climate created by locally generated wind-waves of varying strength (with wind speeds of 4–8 m/s) and direction (SW-NW). Flow and wave calculations are coupled online during the simulation, such that there is a two-way wave-current interaction. In the sediment transport module, the bed shear stresses under combined currents and waves are computed according to Soulsby and Clarke (2005) while we assume the hydrodynamics to be driven by a form roughness independent of the sediment type. The mud concentration at the offshore (northern) open boundary is set to 5 mg/l, which is representative for offshore concentrations in the North Sea.

Simulations are carried out with one medium fine sand fraction ($D_{50} = 250\ \mu m$) and one mud fraction. The form roughness height driving hydrodynamics is set at $k_{s,hydro}$ = 0.02 m (typical for bedforms in sandy systems, see e.g., van Rijn, 1993), and is independent of the sediment type (see Section 4.2.2). The type of mud differs between scenarios, ranging from mud that is easily eroded (τ_e= 0.125 Pa) to consolidated mud (τ_e= 2.0 Pa). For simulations not accounting for sand-mud erosion interaction, sand transport is calculated with the van Rijn (1993) transport formulations, and mud transport with the Partheniades (1965) erosion formulation and a gross deposition flux depending on the suspended mud concentrations and settling velocity (Sanford & Halka, 1993; Winterwerp, 2007). Details on the implementation of sand-mud interaction are provided in Section 4.3.2. Computational times were not affected when including sand-mud interaction in the model simulations. Basic model settings are summarized in Table 4.1; model scenarios to explore the effect of sand-mud interaction in Table 4.2. For additional information on the model set-up, we refer to Appendix B.

Table 4.2: Model scenarios, executed with τ_e = 2 Pa, τ_e = 1 Pa, τ_e = 0.5 Pa, τ_e = 0.25 Pa and τ_e = 0.125 Pa. No erosion interaction means that erosion of sand and mud are calculated independently following the van Rijn (1993) and Partheniades (1965) formulations respectively. When erosion interaction is included, sand and mud erosion are calculated following van Ledden (2003). When accounting for roughness interaction, the roughness height used to calculate the skin friction (thus also the erosion bed shear stress) depends on the mud content in the bed. Otherwise, this value is independent of the sediment composition (see also Section 4.3.2).

τ_e	Erosion interaction	Roughness interaction
x	no	no
x	yes	no
x	no	yes
x	yes	yes

4.3.2. IMPLEMENTATION OF SAND-MUD INTERACTION MECHANISMS

Erosion interaction

We follow the sand-mud erosion formulations by van Ledden (2003), using $p_{mud,crit} = 0.3$ (see also van Ledden et al., 2004b, 2006, and Section 4.2.1). In the non-cohesive regime ($p_{mud} < p_{mud,crit}$), sand erosion (E_{sand}) is calculated using the sand entrainment formulation of van Rijn (1993). Although the sediment mixture is non-cohesive, the presence of small amounts of mud does slightly influence the critical bed shear stress for erosion. This is accounted for as follows:

$$\tau_{e,nc}/\tau_{cr} = (1 + p_{mud})^{\beta_m}, \tag{4.1}$$

in which $\tau_{e,nc}$ is the critical shear stress for non-cohesive mixtures, τ_{cr} is the critical shear stress for pure sand, p_{mud} is the mud content at the bed surface and β_m is an empirical coefficient (ranging from 0.75 to 1.25) which depends on the packing of the bed (van Ledden, 2003). Sand erosion fluxes (E_{sand}) are calculated following:

$$E_{sand} = \frac{\alpha_{b1}}{3} \frac{\sqrt{\Delta g D_{50}}}{D_*^{0.9}} T_{nc}^{\alpha_{b2}-0.9}, \tag{4.2}$$

in which α_{b1} and α_{b2} are coefficients depending on the transport parameter T_{nc} (α_{b1}=0.053, α_{b2}=2.1 for $T < 3$ and α_{b1} =0.1, α_{b2}=1.5 for $T \geq 3$), Δ is the specific gravity of sand, g is the gravitational acceleration, D_{50} is the median sand grain size and D_* is the dimensionless grain size. T_{nc} includes the bed shear stress for non-cohesive mixtures (see also Equation 4.1) and is defined as:

$$T_{nc} = \frac{\tau_b}{\tau_{e,nc}} - 1 = \frac{\tau_b}{\tau_{cr}(1 + p_{mud})^{\beta_m}} - 1, \tag{4.3}$$

in which τ_b is the bed shear stress.

Mud erosion fluxes (E_{mud}) are proportional to the calculated sand erosion fluxes following:

$$\frac{E_{mud}}{E_{sand}} = \frac{p_{mud}}{p_{sand}} = \frac{p_{mud}}{1 - p_{mud}}. \tag{4.4}$$

Therefore, they follow the following relation in the non-cohesive regime:

$$E_{mud} = \frac{p_{mud}}{1 - p_{mud}} \frac{\alpha_{b1}}{3} \frac{\sqrt{\Delta g D_{50}}}{D_*^{0.9}} T_{nc}^{\alpha_{b2} - 0.9}. \tag{4.5}$$

The reader is referred to van Ledden (2003) for the derivation of Equations 4.2–4.5.

In the cohesive regime ($p_{mud} \geq p_{mud,crit}$), E_{sand} and E_{mud} are both computed with a Partheniades-type of equation, stating that above a certain critical bed shear stress the cohesive bed starts to erode with an erosion rate M_c. Following van Ledden (2003), the erosion formulations for both sediment types are as follows:

$$E_{sand} = (1 - p_{mud}) M_c (\frac{\tau_b}{\tau_{e,c}} - 1) H(\frac{\tau_b}{\tau_{e,c}} - 1), \tag{4.6}$$

$$E_{mud} = p_{mud} M_c (\frac{\tau_b}{\tau_{e,c}} - 1) H(\frac{\tau_b}{\tau_{e,c}} - 1), \tag{4.7}$$

in which $H(\frac{\tau_b}{\tau_{e,c}} - 1)$ is a Heaviside function that equals 1 when the argument is larger than 0 and equals 0 when the argument is less than or equal to 0. $\tau_{e,c}$ is the critical erosion shear stress for cohesive sand-mud mixtures, and is linearly interpolated between $\tau_{e,nc}$ (the critical bed shear stress for the non-cohesive regime) and τ_e (the critical bed shear stress for a pure mud bed):

$$\tau_{e,c} = \frac{\tau_{cr}(1 + p_{m,cr})^{\beta} - \tau_e}{1 - p_{m,cr}} (1 - p_m) + \tau_e. \tag{4.8}$$

The expression for the cohesive erosion coefficient reads:

$$log(M_c) = \frac{log(\frac{M_{nc}}{1 - p_{mud,crit}}) - log(M)}{1 - p_{mud,crit}} (1 - p_{mud}) + log(M), \tag{4.9}$$

in which M is the erosion coefficient for a pure mud bed, which in reality can range from 10^{-5} to 10^{-3} kg/m²/s (Winterwerp & van Kesteren, 2004). M_{nc} is the erosion coefficient for non-cohesive mixtures, defined as:

$$M_{nc} = \frac{\alpha_{\beta 1}}{3} \frac{\sqrt{\Delta g D_{50}}}{D_*^{0.9}}. \tag{4.10}$$

The drawback in this approach is that for multiple sand and mud fractions it becomes mathematically complex, since each fraction may have its own value for M_c and M_{nc}. Even though our model simulations only contain one mud and one sand fraction, we apply the more generic modification of van Kessel et al. (2012), in which the erosion rate

itself is interpolated instead of $\tau_{e,c}$ and M_c separately (but which results in very similar E_{mud} values). The erosion flux then reads:

$$E_{mud,i} = E_{f,mud,i}\left(\frac{E_{s,mud,i}}{E_{f,mud,i}}\right)^{\frac{1-p_{mud}}{1-p_{mud,crit}}}, \tag{4.11}$$

where $E_{mud,i}$ is the erosion velocity of mud within the cohesive mixture for fraction i, $E_{f,mud,i}$ is the erosion velocity of pure mud for mud fraction i, and $E_{s,mud,i}$ is the erosion velocity for mud fraction i in the non-cohesive regime (based on Equation 4.5).

Roughness interaction

We calculate the effect of the mud content on the hydraulic roughness close to the bed, and consequently on the bed shear stress driving sediment erosion, using the method of Soulsby and Clarke (2005). Here we focus on the aspects of their methodology that relate to the sediment composition, but we refer to Soulsby and Clarke (2005) for a complete overview of their method.

In case of hydrodynamically rough turbulent flows, the bed roughness (z_0) depends on the surface texture of the sediment bed. Following Soulsby and Clarke (2005), a representative grain size (D_{50}) of the sediment is used as a measure for the surface texture such that:

$$z_0 = D_{50}/12. \tag{4.12}$$

Herein, they assume that

$$k_s = 2.5D_{50}. \tag{4.13}$$

The dependency of the bed roughness on the grain size implies that the bed roughness is adjusted for changes in sediment composition, such that the bed roughness decreases with an increasing mud fraction (and vice versa). Since the characteristic grain size diameter D_{50} is not a dependent variable in the Delft3D modeling suite, a slightly different alternative to Equation 4.12 has been implemented. Following Equations 4.12 and 4.13, z_0 is determined as:

$$z_0 = k_s/30. \tag{4.14}$$

We define $k_{s,silt}$ as the roughness height (in [m]) for a mud-dominated sediment bed and $k_{s,sand}$ as the roughness height (in [m]) for a sand-dominated sediment bed. k_s is thus implemented as a Nikuradse roughness height depending on the sediment grain size (Equation 4.13) and it switches between $k_{s,silt}$ (0.03 mm) and $k_{s,sand}$ (0.6 mm) depending on the mud content (see Figure 4.1d and Table 4.1). We have introduced a gradual transition in between to better represent actual physical conditions and avoid numerical instabilities.

4.4. RESULTS

4.4.1. PHENOMENOLOGICAL DESCRIPTION

We first evaluate the model results by comparing the morphodynamic evolution in terms of bed morphology and spatial mud distribution (Figure 4.2). All model scenarios generate an intricate pattern of tidal channels and flats, where in general the mud content in-

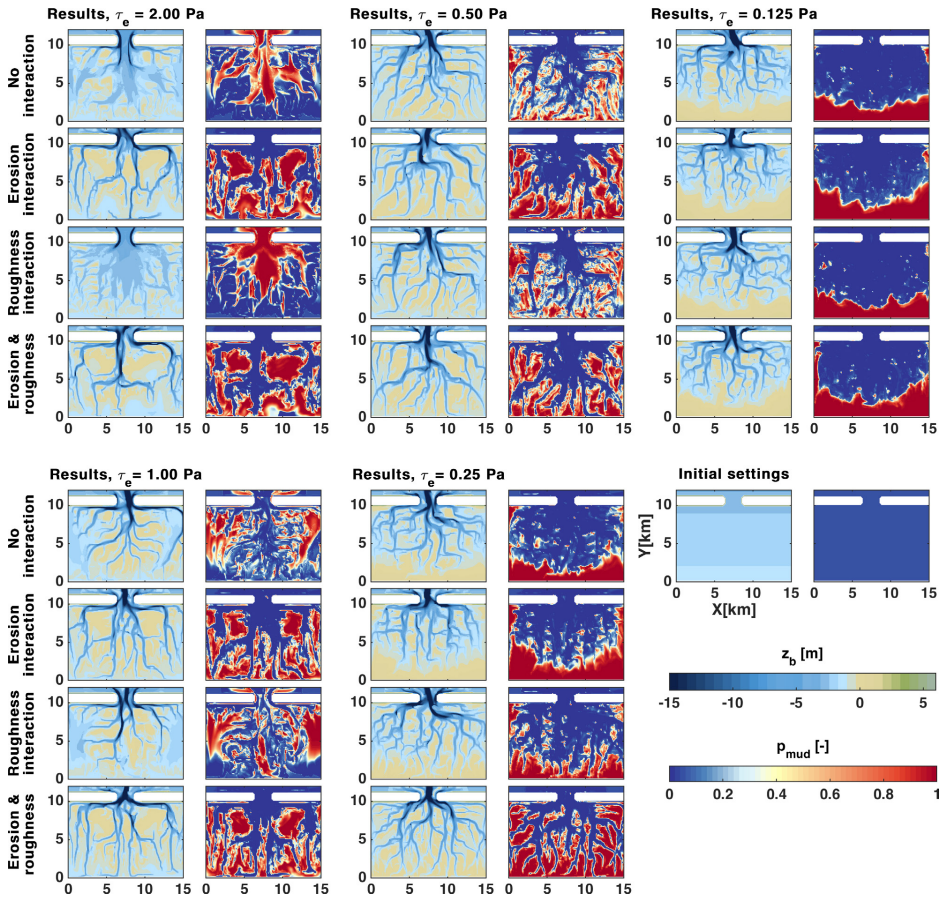

Figure 4.2: Modeled morphological evolution (50 years) of a synthetic tidal basin for a range of erosion settings, showing computed bed levels (z_b, left panel per model realization) and sediment composition (mud content, p_{mud}) of the upper bed (0.1 m, right panel).

creases in landward direction. Yet, both the bathymetry and the bed composition largely vary depending on the mud erosion settings and the interaction mechanisms.

Erosion interaction most strongly influences morphology for simulations with poorly erodible mud ($\tau_e = 1.00$ Pa, $\tau_e = 2.00$ Pa, see Figure 4.2). Without this interaction mechanism, mud is too immobile to be eroded from the channels, resulting in a morphology with large, shallow, muddy subtidal areas and few intertidal flats. These model results are quite unrealistic compared to real-world tidal systems such as the Wadden Sea or the Western Scheldt, where channels are predominantly sandy and both sand- and mudflats exist. In the remainder of this chapter, we will put limited focus on these unrealistic scenarios. Erosion interaction allows mobilization of poorly erodible mud, especially around the threshold between the non-cohesive and cohesive regime. This leads to an increased E_{mud} with p_{mud} for mixtures with $p_{mud} \approx p_{mud,crit}$ (see also Figure 4.1b),

whereas for higher p_{mud} the erodibility decreases. This allows transport of mud toward tidal flats, such that they become progressively more difficult to erode (as sedimentation of mud continues), enabling (large) mudflat formation and stabilization.

Simulations with high $\tau_{e,mud}$ and only roughness interaction do not develop a realistic morphology because the mud is not sufficiently mobile (as explained above). However, roughness interaction can promote mudflat growth when combined with more mobile mud. This effect is strongest for $\tau_e = 0.25$ Pa (as will also follow later from Figure 4.6c), where more and larger mudflats develop in the central parts of the basin when accounting for this effect (and even more when combined with erosion interaction). The physical explanation hereof is that when the bed shear stress is close to the critical bed shear stress for erosion, roughness interaction lowers the bed shear stress below the critical value. This reduction in erosion rates leads to increased net mud deposition, thereby further lowering the bed shear stress — a positive feedback mechanism leading to progressive mud deposition.

Not only the interaction method, but also the type of mud (in terms of erodibility) largely influences the morphodynamic evolution. In general we observe that large intertidal shoals are formed in the central parts of the basin when applying a high τ_e (1 or 2 Pa) in combination with erosion interaction. Herein we define intertidal shoals as intertidal flats that are surrounded by channels. Intertidal flats adjacent to the outer contours of the basin are referred to as fringing flats. With medium high τ_e (0.5 Pa), muddy shoal formation occurs at all scenarios. For more easily erodible mud ($\tau_e = 0.25$ Pa), especially fringing mudflats develop while the shoal size decreases. With $\tau_e = 0.125$ Pa, only fringing mudflats can develop.

In the following sections, we will evaluate the numerical model results in a more quantitative and aggregated way by computing tidal basin hypsometry, the size and type of intertidal area, and characteristics of the subtidal areas.

4.4.2. HYPSOMETRY

Figures 4.3 and 4.4 show the computed hypsometric curves after 50 years of evolution, organized per τ_e and per interaction type respectively. These hypsometric curves are interpreted in terms of changes in intertidal area (between high and low water) and subtidal area (with the space between low water and –5 m representing the higher subtidal, and deeper water the lower subtidal).

Low mud erodibility without erosion interaction largely increases the subtidal area, at the expense of the lower/mid intertidal area (up to $z_b = 0.5$ m; Figures 4.3a–b and 4.4a–d). With erosion interaction, the intertidal area is similarly large for all models regardless of the choice for τ_e (Figure 4.4f). However, the spatial patterns do differ strongly (e.g., less but larger intertidal flats for high τ_e, see Figure 4.2). Conversely, without erosion interaction (Figure 4.4a–d), the hypsometry strongly depends on τ_e. Our idealized tidal basin only developed higher intertidal area ($z_b > 0.5$ m) for very low τ_e. The limited development of the higher intertidal area is probably a result of the sheltered environment with limited waves along the borders of the basin, the absence of extreme storms and

surges and the oversimplification of the tidal signal (de Vet et al., 2018; Galiforni-Silva et al., 2020; Schrijvershof et al., 2023).

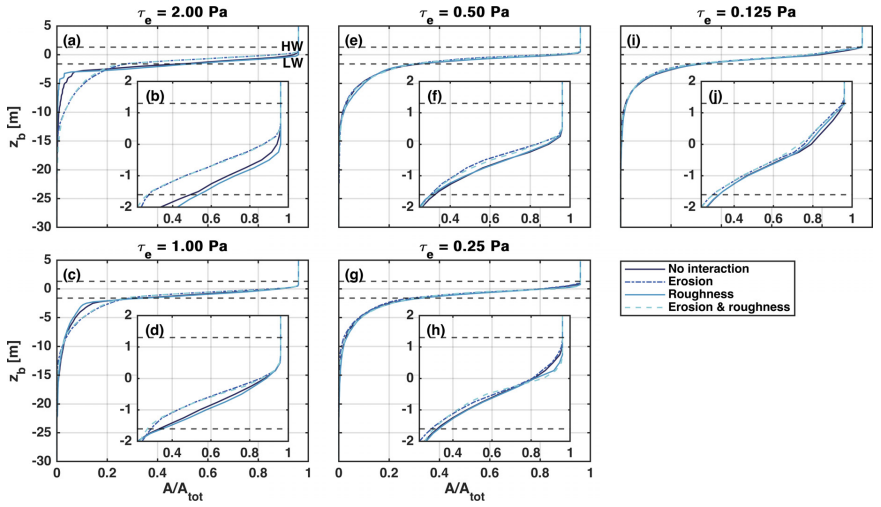

Figure 4.3: Hypsometric curves showing the cumulative area (A) per bed level (z_b), organized per τ_e. The black dashed lines mark the low water (LW) and high water (HW) lines. Inset plots zoom in on the intertidal areas.

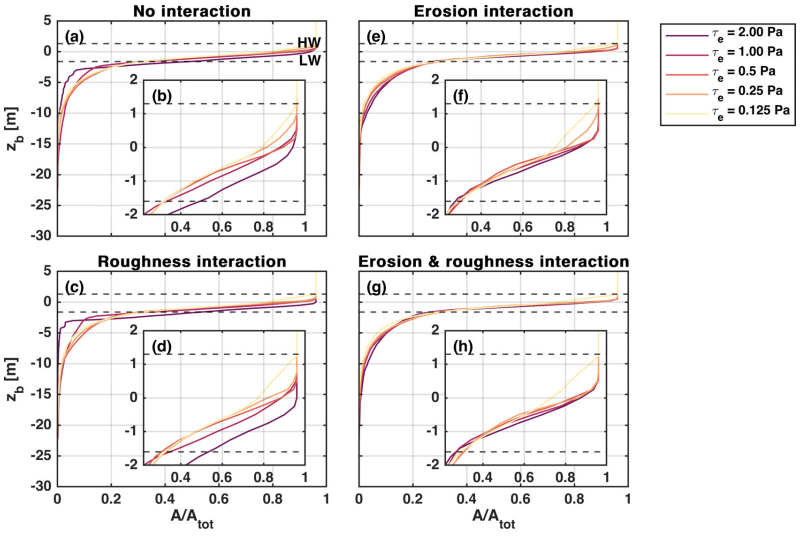

Figure 4.4: Hypsometric curves showing the cumulative area (A) per bed level (z_b), organized per interaction type. The black dashed lines mark the LW and HW lines. Inset plots zoom in on the intertidal areas.

The individual hypsometries are aggregated by averaging per model scenario (see Figure 4.5), showing that in general, erosion interaction leads to expansion of the intertidal area at the cost of the higher subtidal areas becoming deeper. The more mobile the mud, the higher the intertidal bed levels. However, the total size of the intertidal area remains approximately the same, except for the extreme case of τ_e = 2 Pa.

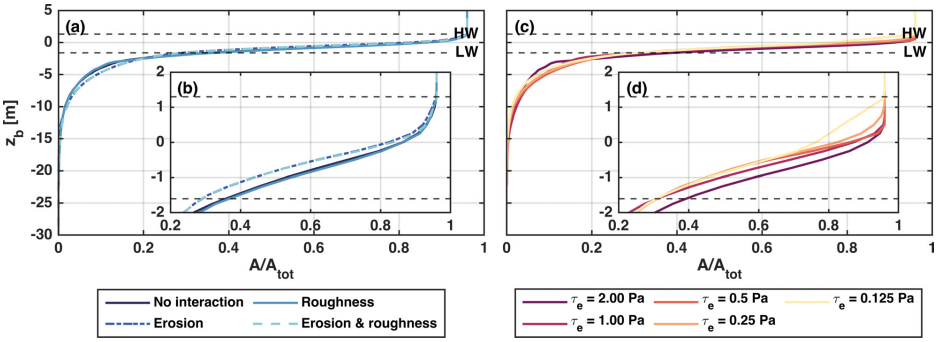

Figure 4.5: Combined hypsometric curves of averaged results. The black dashed lines mark the LW and HW lines. Inset plots zoom in on the intertidal areas.

4.4.3. DEVELOPMENT OF INTERTIDAL AREAS

Total intertidal area

The hypsometric curves after 50 years are subsequently aggregated into areas of sandy, muddy and total intertidal area (Figure 4.6). The total intertidal area A_i reveals that within the range 0.125 Pa $\leq$ τ_e $\leq$ 0.5 Pa, A_i depends little on the type of sand-mud interaction, and varies between 63% and 67% (95–100 km²). For τ_e $>$ 0.5 Pa, erosion interaction leads to an increase of the intertidal area of up to 5% compared to scenarios with $\tau_e \leq$ 0.5 Pa. The rapid decrease in A_i at higher τ_e when not accounting for this type of interaction is considered unrealistic (as discussed earlier).

Sediment composition

We further analyze intertidal flat dynamics by defining non-cohesive beds ($p_{mud} < 0.3$, Figure 4.6b) as sandy intertidal areas ($A_{i,sand}$) and cohesive beds ($p_{mud} \geq 0.3$, Figure 4.6c) as muddy intertidal areas ($A_{i,mud}$). Scenarios with erosion interaction strongly differ from simulations without erosion interaction, whereas simulations with roughness interaction only slightly deviate from simulations without it. In general we observe a decreasing trend of $A_{i,sand}$ and an increasing trend of $A_{i,mud}$ with increasing τ_e for simulations with erosion interaction.

Without sand-mud interaction, $A_{i,mud}$ is highest (and $A_{i,sand}$ lowest) at τ_e = 0.5 Pa. Mud with high τ_e is too immobile to reach the flats and remains in the channels, which results in unrealistic results. With erosion interaction, in the non-cohesive regime mud erosion increases with increasing p_{mud} (see also Figure 4.1b) until $p_{mud,crit}$, after which it decreases. This allows for mud to be eroded from the (sandy) channels (regardless of the

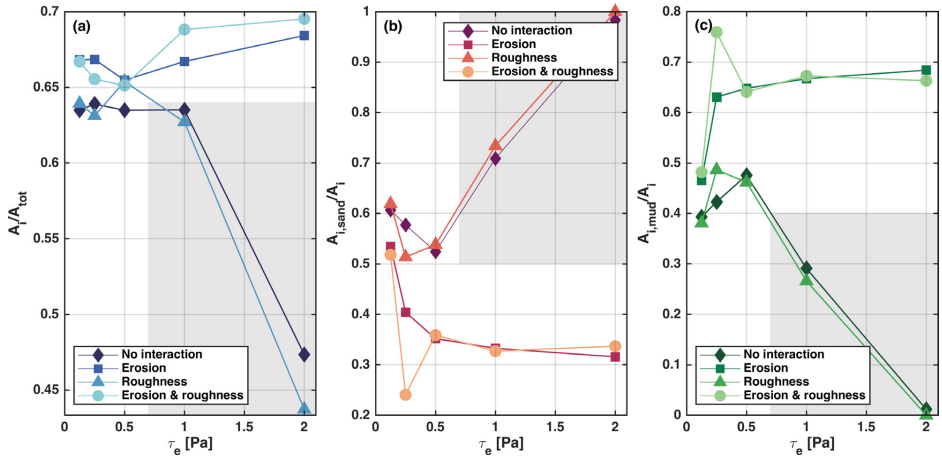

Figure 4.6: Development of intertidal areas. (a) Total intertidal area relative to the total basin area (150 km^2), A_i/A_{tot}. (b) Relative sandy intertidal area $A_{i,sand}/A_i$. $A_{i,sand}$ is defined as the intertidal area with a non-cohesive sediment composition (i.e., $p_{mud} < 0.3$). (c) Relative muddy intertidal area $A_{i,mud}/A_i$. $A_{i,mud}$ is defined as the intertidal area with a cohesive sediment composition (i.e., $p_{mud} \geq 0.3$). The gray boxes represent a model parameter space yielding unrealistic results which are excluded from further analysis.

very high τ_e) and be transported toward the flats, where mud accumulates and therefore erosion rates decrease again. This mechanism thus enables modeling of large mudflat formation during low-energy tide-dominated conditions as well as stabilization, allowing the flats to survive episodic storms. The effect of roughness interaction on morphology is much more subtle than that of erosion interaction. Roughness interaction enhances mudflat formation for relatively mobile mud ($\tau_e = 0.25$ Pa), which was already indicated by Figure 4.2.

Interestingly, the absolute maximum predicted values for $A_{i,sand}$ and $A_{i,mud}$ are fairly similar (around 60–70 km^2), but require very different model settings. Moreover, the variability of $A_{i,sand}$ and $A_{i,mud}$ over the various scenarios is much larger than the variability of the total intertidal area A_i. The sediment composition is thus much more sensitive to the model settings related to sand-mud interaction than the total intertidal flat area. Despite a fairly constant total intertidal area, the size of individual shoals does strongly differ among the various scenarios, as will be explored hereafter.

Intertidal flat size

The analyzed model parameter space results in a striking variation in flat size. We analyze the flat size by calculating the exceedance probability of the distance from the subtidal areas of all grid cells with $z_b >$ LW (i.e., the intertidal areas, see Figure 4.7). This is similar to Edmonds et al.'s (2011) calculation of the nearest-edge distance of shoals in river deltas. An overall large probability reflects small intertidal flats and vice versa. To prevent confusion, we have left out the unrealistic results of the models with $\tau_e \geq 1.0$ Pa and without erosion interaction.

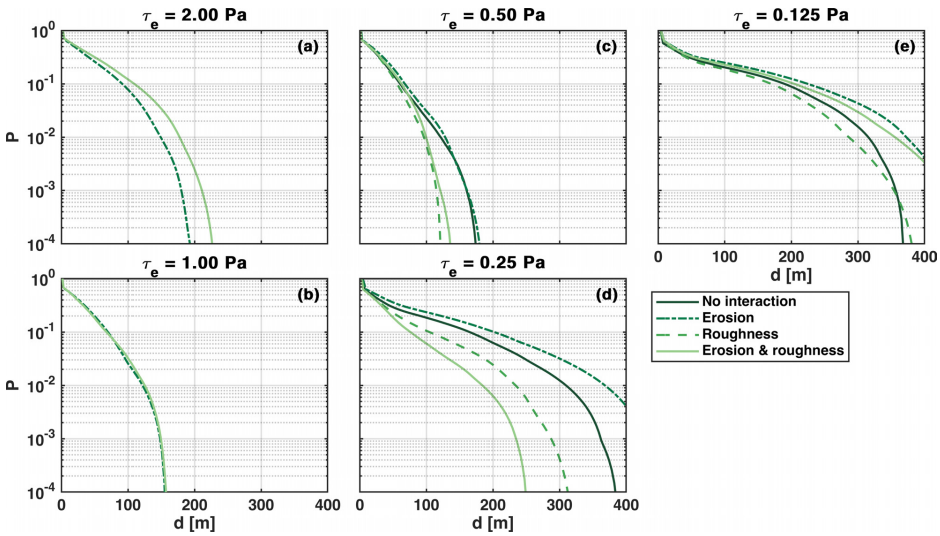

Figure 4.7: Probability of exceedance (P) of minimum distance to channel (d).

The remaining simulations with $\tau_e \geq 1.0$ Pa result in the formation of relatively large shoals (see also Figure 4.2). The shoal size is smallest for $\tau_e = 0.5$ Pa (comparing Figures 4.7a–4.7c) but it increases again at lower τ_e (Figures 4.7d and 4.7e). This increase at low τ_e is caused by progressive growth of fringing flats bordering the basin boundaries with large distances to the channels, outpacing the decline of shoals in the central basin. The size of these fringing flats increases with decreasing τ_e. In general we observe the largest distances from the flats to the channels for erosion interaction only; roughness interaction reduces the development of fringing flats.

4.4.4. DEVELOPMENT OF SUBTIDAL AREAS

Areas and volumes

To quantify the effect of sand-mud interaction and model parameter settings on the development of subtidal areas, we have determined the total relative subtidal area (A_s/A_{tot}) and absolute volume (V_s) for the deep subtidal (depth $d > 5$ m, $A_{s,deep}$, $V_{s,deep}$) and for the shallow subtidal ($d \leq 5$ m, $A_{s,shallow}$, $V_{s,shallow}$, see Figure 4.8). Again, we have marked unrealistic scenarios (yielding the largest variation) with gray boxes and exclude them from our analyses. A_s (Figure 4.8a) is relatively stable regardless of τ_e and shows a variability of $< 5\%$ resulting from the type of sand-mud interaction. On the other hand, V_s (Figure 4.8d) shows a larger variability (35%), mainly because of the variation of τ_e and much less depending on the sand-mud interaction method.

$A_{s,shallow}$ decreases with increasing τ_e (Figure 4.8c) whereas $A_{s,deep}$ (Figure 4.8b) increases with increasing τ_e. The trend in $A_{s,shallow}$ corresponds to that of the total subtidal area A_s because about 70% of the subtidal area is shallow. Despite of its limited contribution to the area, the deep subtidal contributes to 60%–80% of the total channel

volume and therefore the trends of $V_{s,deep}$ largely follow the trends of $V_{s,total}$. Here, we observe that an increase in τ_e leads to an increase in $V_{s,deep}$ and a decrease in $V_{s,shallow}$ (within the considered range of τ_e).

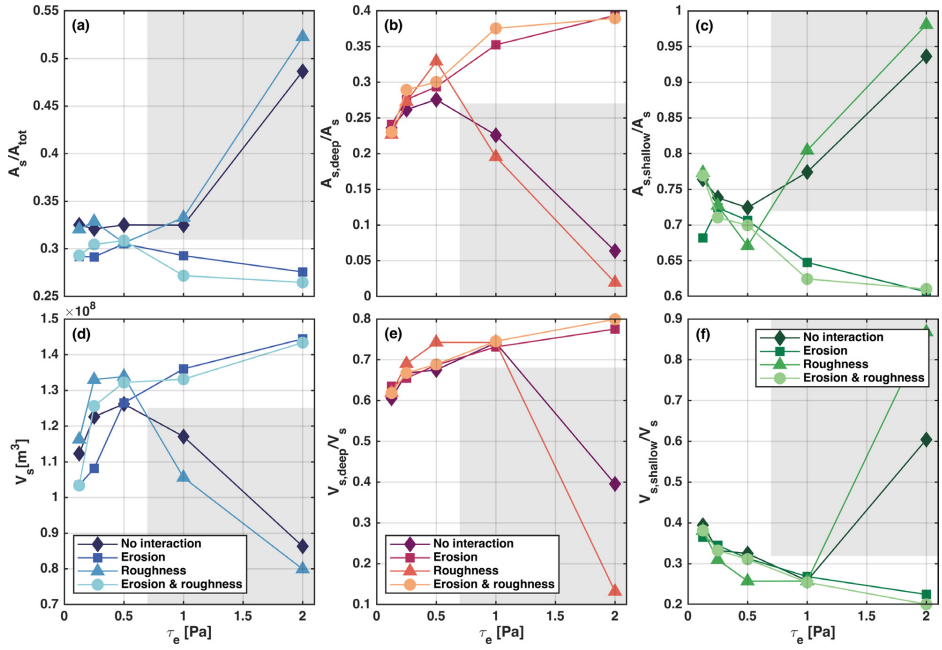

Figure 4.8: Development of subtidal area and volumes. (a) Total subtidal area A_s relative to the total basin area (A_{tot}, 150 km^2). (b) Relative deep subtidal area $A_{s,deep}/A_s$, defined as the subtidal areas below –5 m. (c) Relative shallow subtidal area $A_{s,shallow}/A_s$, defined as the subtidal area between LW and –5 m. (d–f) Subtidal volumes $V_{s,total}$, $V_{s,deep}$, $V_{s,shallow}$. The gray boxes represent a model parameter space yielding unrealistic results which are excluded from further analysis.

Channel depth

The channel depth is further analyzed by visualizing the distribution of the bed level occurrence in the deeper subtidal (Figure 4.9). The maximum channel depth varies between 17.5 and 23 m, whereas the median depth (white dots) is very stable (around 7 m). The mean depth, marked with the black lines, is slightly larger (around 8 m). These values are not directly correlated with τ_e nor with the types of sand-mud interaction.

Scenarios with a higher τ_e do not necessarily lead to more overall erosion or deeper channels: for all model scenarios the median bed level of the deeper subtidal areas varies between –7 m and –8 m only. Since channels are, both in our models and in reality, predominantly sandy, erosion rates will mainly be determined by sand characteristics. This explains the small differences between the various model scenarios and the minor dependence on the investigated parameter settings. Factors that are more likely to affect channel depths are hydrodynamic forcing and sand grain size.

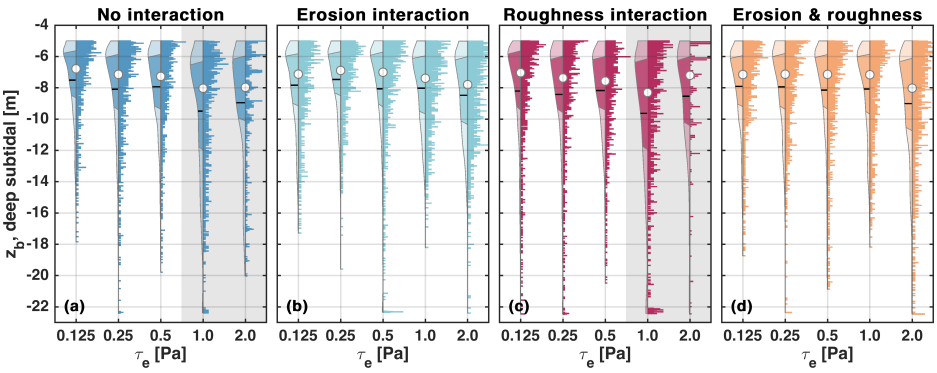

Figure 4.9: Channel depth variation: violin plots (including histograms right of the violin plot) show the bed level (z_b) occurrence in the deeper subtidal areas. Violin plots are a combination of a kernel density plot and a box plot, providing the distribution of the data as well as a summary of its statistics. The white dots show the median values, the black bars indicate the mean values. The interquartile range (between 25% and 75%) is displayed with a shadow. The histograms right of the plots show the distribution over the depths at a greater detail. The gray boxes represent a model parameter space yielding unrealistic results which are excluded from further analysis.

4

Channel length and complexity

To further analyze the channel patterns, we make use of Chirol et al.'s (2018) creek parametrization algorithm by extracting the channel data below low water. This enables a morphometric analysis of the dimensions and complexity, including the reverse Strahler order. The Strahler order is a numerical measure of the branching complexity. In the Strahler method, all links without any tributaries are assigned an order of 1 and are referred to as first order. When channels of the same order intersect, the order increases. Intersection of two channels of different orders does not result in an increase in order. Following Chirol et al. (2018, 2022), we convert the Strahler order to a reverse Strahler order (see Figure 4.10). The benefit of using reverse Strahler ordering compared to traditional Strahler ordering is that reverse Strahler ordering ensures that the entry channel at the basin inlet is always classified as the first order.

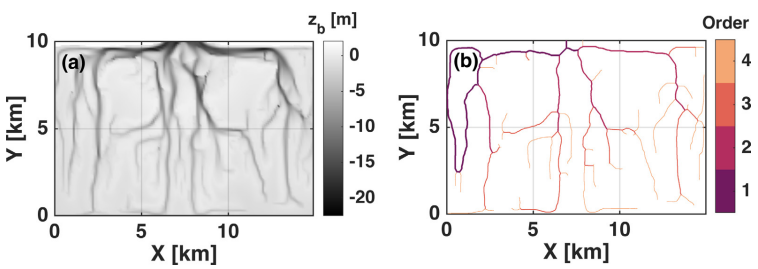

Figure 4.10: (a) Digital elevation model (bed levels z_b), derived from Delft3D output. (b) Extracted channel structure and computed reverse Strahler order.

The total channel length in the basin (L_{tot}) is obtained by summation of the length of all individual channels (Figure 4.11a). A high L_{tot} may result from for example, many short channels (complex system), less but longer channels (less complex system), or a high sinuosity. For all model scenarios L_{tot} increases with τ_e up to $\tau_e = 0.5$ Pa, because channels penetrate deeper into the basin at cost of the fringing flat development. Less channels develop for $\tau_e > 0.5$ Pa, and L_{tot} decreases with increasing τ_e.

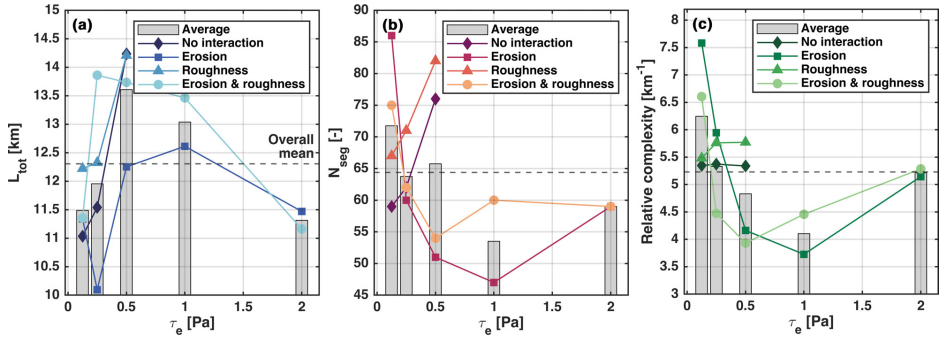

Figure 4.11: (a) Total channel length (sum of all channels in the model, L_{tot}) depending on τ_e and the interaction type. Scattered lines show the model results for all models except for scenarios 1, 3, 5, 7 (unrealistic). Histograms show the average per τ_e choice. Dashed line shows the overall mean value. (b) Total number of channel segments (N_{seg}) depending on τ_e and the interaction type. (c) Relative complexity, defined as the number of segments divided by the total channel length (N_{seg}/L_{tot}), depending on τ_e and the interaction type.

The complexity of the channel patterns (Figure 4.11c) is defined as the number of channel segments (Figure 4.11b) divided by the total channel length (Figure 4.11a). A segment is defined as a channel part in between a bifurcation or confluence. With erosion interaction, both the number of segments and the relative complexity generally increase with decreasing τ_e. Without erosion interaction the number of segments decreases with decreasing τ_e and the relative complexity is independent of τ_e.

Channel complexity can be further analyzed by determining the reverse Strahler order of the channels (see also Figure 4.10). Figure 4.12 shows the occurrence of the number of segments, mean channel depth, mean channel length and total channel length of all model scenarios. Herein, we have first calculated the average values of these parameters per reverse Strahler order of each model scenario, such that Figure 4.12 shows the variability between model scenarios. As expected, the number of segments increase with reverse order increase, whereas the mean channel depth and length decrease. More interesting is that channel complexity (in terms of number of segments) is especially depending on scenarios for inverse Strahler order 3 and 4, while depth and length are more depending at lower inverse Strahler number. The total channel length is not clearly correlated with the Strahler number because it is influenced by both the number of segments and the segment length.

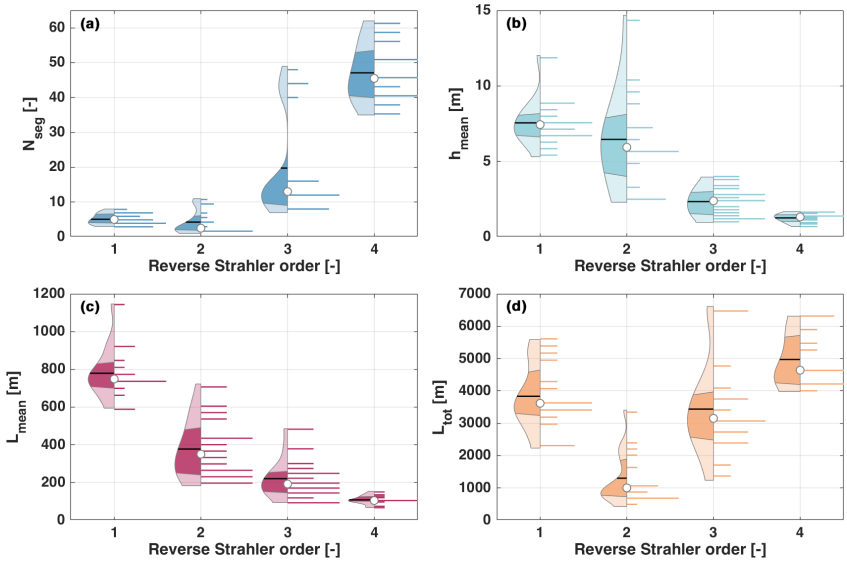

Figure 4.12: Violin plots including histograms showing the channel properties per reverse Strahler order. Values are based on the mean properties per scenario, showing the (a) variance of the average number of segments N_{seg}, (b) mean channel depth h_{mean}, (c) mean channel length L_{mean} and (d) total channel length L_{tot} per reverse Strahler order.

4.4.5. COMPARISON WITH FIELD DATA

To determine the validity of our model results and identify what combination of parameters most closely resembles the morphology of actual tidal basins such as those in the Wadden Sea, we compare our model output to field data. Herein, we focus on those aspects and metrics that are most influenced by the investigated sand-mud interaction mechanisms, being the morphological evolution (Figure 4.2), the hypsometry, channel patterns, and intertidal area development (within the latter especially the sediment composition). We make use of recent bathymetry data from the *Vaklodingen* and *EasyGSH* data sets and sediment composition data from *Sediment Atlas Wadden Sea*, *SIBES* and *EasyGSH*.

Figures 4.13a–4.13e show the bathymetries of five basins within the Dutch and the German Wadden Sea. We observe a relatively large morphological variation in terms of bed levels and channel patterns, which may at least partly be explained by the variation in basin size and shape. Figure 4.13f shows the range of hypsometries of all Dutch and German Wadden Sea basins (excluding the Ems, Weser and Elbe estuaries). This range is much larger than the variability that was obtained by varying sand-mud interaction settings and/or mud erodibility settings in our model (see the blue lines and also Figures 4.3 and 4.4). Cleveringa and Oost (1999) showed that the Wadden Sea basins contain similar characteristics as three- to four-times branching channel networks, with logarithmically decreasing branch lengths and increasing number of channels with increasing channel order. This is in line with our schematized model results (Figure 4.12). However, they also

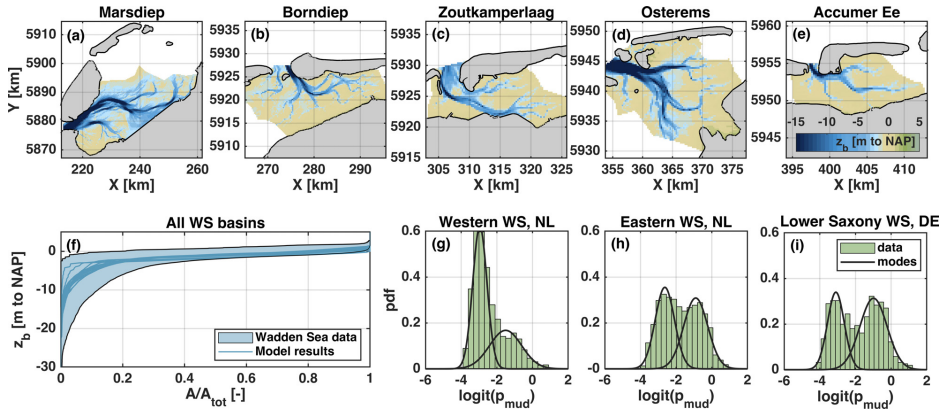

Figure 4.13: Morphology of the Wadden Sea (WS) basins. (a–e) bed levels of five basins in the Dutch (*Vaklodingen* data) and German WS (*EasyGSH* data), plotted in m to NAP (Dutch Ordnance Datum). (f) Envelope of the hypsometric curves of all Dutch and German basins, excluding the estuaries, compared to the modeled hypsometries. (g–i) Bimodal distribution p_{mud} of the upper sediment bed on the intertidal areas of the WS basins, based on Colina Alonso et al. (2022), see also Chapter 5.

show that the total channel length largely varies per basin, showing a much greater variation than our model results. This large natural variability in channel patterns and bed levels, resulting from among others the tidal basin shape, makes it difficult to state whether including sand-mud interaction improves the model performance regarding hypsometry and channel type.

The sediment composition of the Wadden Sea flats varies both on the large-scale (e.g., the Eastern Dutch Wadden Sea is more muddy than the Western Dutch Wadden Sea) and on the small-scale (e.g., large changes in the mud content over several 100s of meters and the occurrence of isolated mud patches in sand dominated environments; de Glopper, 1967; Oost, 1995; Colina Alonso et al., 2021). The overall sediment composition of the intertidal flats can vary strongly depending on among others the geometry of the basin, the hydrodynamic forcing and the suspended sediment concentration. Figure 4.14 shows the intertidal area in the Wadden Sea basins A_i (relative to the total area of the basins) and the contribution of non-cohesive sandy flats and cohesive mudflats to A_i. This is plotted against the basins' distance from Den Helder, following the coastline from West to East, such that the first data point is the Marsdiep tidal basin in the Netherlands and the last data point represents Lister Tief basin bordered by the German island Sylt and the Danish island Rømø. Danish basins are not included in this analysis, because of insufficient availability of bathymetry and sediment composition field data. Comparing the field data of the Wadden Sea (Figure 4.14) with our model results (Figure 4.6) shows that our predicted total intertidal area is within the observed range (which is again much wider), although the predicted contribution of sandy flats compared to mudflats is generally on the low side and best resembles the East-Frisian Wadden Sea (basins 12–20, km 200–275).

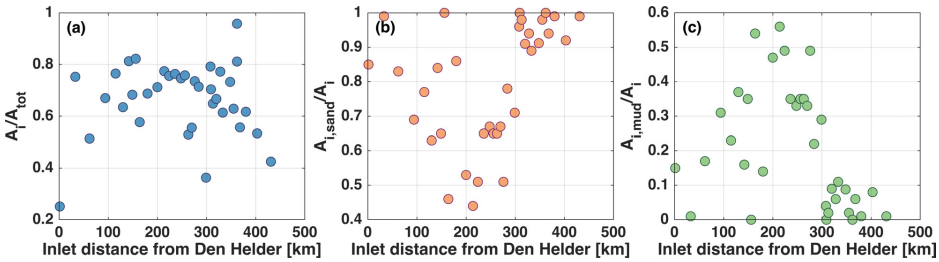

Figure 4.14: Intertidal areas in the Wadden Sea basins plotted against the distance of the basin inlet to Den Helder (starting West with the Marsdiep basin and moving East and North up to Lister Tief basin). (a) Total intertidal area relative to the total basin area, A_i/A_{tot}. (b) Relative sandy intertidal area $A_{i,sand}/A_i$ (c) Relative muddy intertidal area $A_{i,mud}/A_i$. $A_{i,sand}$ and $A_{i,mud}$ are defined as in Figure 4.6.

4

An important characteristic of the mud content in the Wadden Sea (and probably also in other tidal basins) is its bimodal distribution: the bed tends to be relatively sandy or relatively muddy, with fewer observations in between (see Chapter 5). This bimodality is most clearly visible after logit-transformation and is most pronounced on the intertidal areas (Figure 4.13g–i). Although bimodality is observed in the entire Wadden Sea, the location of the second mode (showing how muddy the mudflats are) varies within the system, with for example, a larger mud content in the Eastern Wadden Sea compared to the Western Wadden sea. Figure 4.15 shows the distribution of the mud content in the intertidal areas of our schematized model output. All models without sand-mud interaction fail to reproduce this bimodality (marked in gray), either because the distribution is unimodal or because a bimodality is predicted with a second mode at $p_{mud} \approx 99\%$, which is unrealistically high in these systems. Models with erosion interaction and $\tau_e \geq$ 0.5 Pa do reproduce the bimodality, even though they slightly underestimate the mud content in the sandy areas ($p_{mud,mode1} \approx 0.01$ whereas in reality this is approximately 0.04) and overestimate the mud content in the muddy areas ($p_{mud,mode4} \approx 0.50$ while in the Frisian Wadden Sea this is typically 0.35–0.40). In terms of the mud content within the bed, erosion interaction is therefore an important improvement.

4.5. DISCUSSION

4.5.1. USING SCHEMATIZED MODELS

Schematized model environments are an essential tool to improve our knowledge on morphodynamics. However, when the model conditions are strongly idealized, it becomes difficult to correlate such model findings with processes that take place in reality. The main aim of this chapter was to better understand the effects of small-scale sand-mud interaction on the (modeled) morphodynamics of tidal basins. In order to reduce complexity and restrict the degrees of freedom (and thus number of simulations) we strongly schematized tidal basin geometry and boundary conditions. We have quantified the effects of sand-mud interaction by defining a number of morphological metrics, but we also observe that some of these metrics vary even more in reality due to for instance the large-scale variability in tidal prism, storminess or suspended mud concentrations (Zhou et al.,

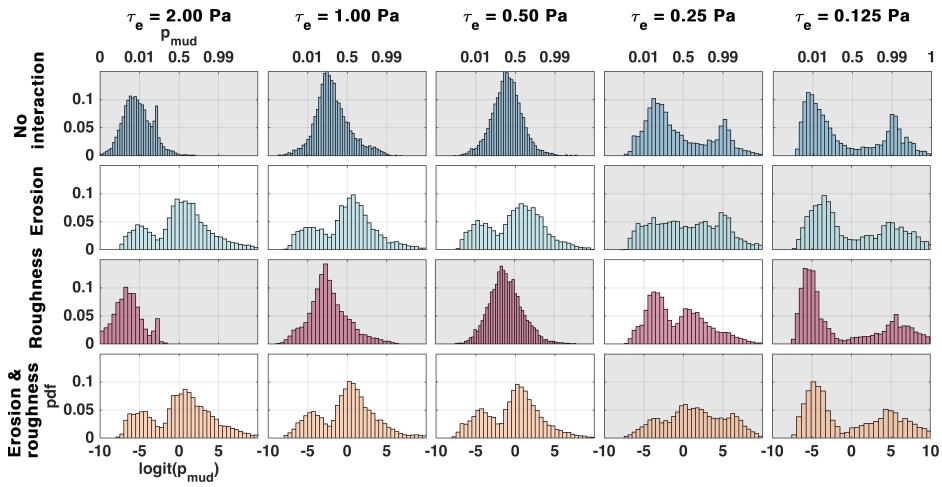

Figure 4.15: Distribution of the mud content, after logit-transformation, in the upper sediment bed of the numerical models. The upper y-axes show the corresponding p_{mud} values. The gray panels indicate the models that do not reproduce a realistic distribution, either because it is unimodal or because the second mode has a value ≥ 0.99.

2021, 2022) and the basin geometry on a smaller scale (e.g., comparing adjacent Wadden Sea basins; Cleveringa & Oost, 1999; Ridderinkhof et al., 2014). And even though our model simulations fit within the range of morphological metrics that describe the basins in the Wadden Sea, they are most useful to analyze in comparison with each other.

4.5.2. EFFECTS OF SAND-MUD INTERACTION ON MORPHODYNAMIC EVOLUTION

Including sand-mud interaction in modeling studies provides a better representation of underlying physical processes. Our model results show that sand-mud interactions impact long-term basin evolution: the patterns and intertidal flat shape, size and composition vary with mud erodibility settings, but equally with the considered sand-mud interaction method. We have demonstrated that sand-mud interactions steer large-scale morphodynamic evolution by enhancing intertidal flat formation, with erosion interaction having a much larger effect than roughness interaction — which is strongest for scenarios with poorly erodible mud ($\tau_e > 1$ Pa). Roughness interaction also enhances mudflat formation, but for a narrower range of conditions: our results show that this interaction type is mainly effective when mud is still relatively mobile ($\tau_e = 0.25$ Pa). We believe that this condition may however be different in other systems with different forcing, since we expect roughness interaction to have the largest effect when the bed shear stresses are close to the critical bed shear stress for erosion.

Yet, most effects of including sand-mud interaction on the morphological metrics are more subtle than the observed natural variability in the field. An exception is the bimodal distribution of the mud content, which is observed in the Wadden Sea basins, but cannot be reproduced by our numerical models when omitting sand-mud interaction. But

even though sand-mud interaction mechanisms improve the morphodynamic simulations, the underlying formulations still need to be more vigorously validated. Sand-mud erosion formulations, such as those by van Ledden (2003) but also others (e.g., Jacobs et al., 2011; Le Hir et al., 2011; Bi & Toorman, 2015; Mengual et al., 2017; van Rijn, 2020; Chen et al., 2021a), have only been verified for a limited range of conditions. Erosion rates predicted by these formulations should be compared to more extensive laboratory experiments in controlled environments. We especially recommend to execute more erosion experiments of sand-mud mixtures under combined forcing of currents and waves, which are only limitedly available at this moment, to improve our understanding of sand-mud dynamics.

Additional advances related to the physical behavior of sand-mud beds that should preferably be incorporated in sand-mud models are the dynamic behavior of bedforms and the role of biology in flocculation. Baas et al. (2021) have presented a new bedform phase diagram of current- and wave-generated bedforms in mixed sand-mud tidal environments. The presence of small amounts of clay can significantly reduce the bedform size (Baas et al., 2013), but also the steepness (Schindler et al., 2015). We have performed a first assessment of the effects of the imposed total drag because of different bedform sizes (see Appendix B). Here, we have compared the models with a total drag corresponding to bedforms in sandy systems ($k_{s,hydro}$ = 0.02 m, see Table 4.1), to models with (bedform-related) roughness heights that are 5 and 10 times smaller. The results show that, even though the bedform-related roughness does influence the hydrodynamics, its effect on the morphodynamic development remains limited in comparison with the investigated sand-mud interaction mechanisms (see Figures B.2 and B.3). Note that herein, we do not account for varying bedform dimensions depending on the bed sediment composition, which can introduce second order effects. Manning et al. (2011) showed that because of the greater binding effect of biology, sand particles can also flocculate with mud. This flocculation interaction may therefore result in joint transport of sand and mud. Spearman et al. (2011) demonstrated that including flocculation interaction into sand-mud models improves reproduction of the observed sediment dynamics. We recommend to include these additional sand-mud interaction mechanisms and evaluate their impact on long-term morphodynamic predictions by developing model scenarios that become progressively more complex, starting from simulations without sand-mud interaction mechanisms.

4.5.3. MODELING GUIDELINES FOR A PHENOMENOLOGICAL OPTIMIZATION

Relating sand-mud interaction mechanisms to aggregated morphological metrics, such as the intertidal area or the channel pattern complexity, leads to an improved process understanding of the morphological consequences of these mechanisms. Consequently, it also allows a phenomenological optimization of morphodynamic models on a high aggregation level. Since we have identified how channels and shoal patterns vary with sand-mud parameters, these parameters can be used to optimize schematized models toward real-life systems. We may therefore translate our sensitivity analysis on sand-mud processes and settings into a methodology to improve morphological model metrics, resulting in the following guidelines:

- **Intertidal area**: The overall intertidal area slightly increases by including erosion interaction. Promoting the development of higher intertidal areas requires inclusion of a mud fraction with low erodibility.
- **Shoal size**: Large (non-fringing) muddy intertidal shoals develop when sediment is poorly erodible (i.e., applying a high critical shear stress for mud) combined with erosion interaction. Large fringing flats and smaller intertidal shoals develop when the critical bed shear stress is lower.
- **Shoal composition**: Including erosion interaction generally leads to a higher mud content in the intertidal areas. The impact of erosion interaction on mud content becomes larger with increasing critical bed shear stress for mud erosion. In order to model large mudflat formation within our parameter settings, we thus advise to include erosion interaction and poorly erodible mud (a τ_e of 1–2 Pa). When combined with erosion interaction, including roughness interaction generally leads to an additional increase in mud content (given that $\tau_e < 2$ Pa). Note however, that other parameter choices (e.g., suspended mud concentrations) will also affect the simulated shoal composition.
- **Subtidal area development:** The value of the critical bed shear stress has a stronger influence on the development of subtidal areas and volumes than the type of sand-mud interaction mechanism included in the model. The total deep ($z_b <$ -5 m) subtidal area and its total volume increases with increasing τ_e (within the considered range). Shallow intertidal areas (-5 m $< z_b \leq$ LW) show an opposite trend.
- **Channel pattern complexity:** Channel complexity — defined as the number of channels corrected for the total channel length — increases for lower critical bed shear stress for mud erosion. This will however only have an effect on model results when erosion interaction is included in the model, since simulations without erosion interaction show very little variation in the complexity (regardless of the value of τ_e).

Using the method of Soulsby and Clarke (2005) to calculate bed shear stresses under flow and wave forcing in morphological models has an important additional benefit, next to those obtained by including roughness interaction. Hydrodynamic models are commonly calibrated by modifying the bed roughness parameter (e.g., including spatially varying roughness fields, reflecting bedforms or subgrid bathymetric effects). The resulting bed roughness is subsequently also used for sediment transport computations through its impact on the bed shear stress. This may result in realistic hydrodynamic results, but introduces inconsistencies when modeling morphodynamics. Preferentially, the bed roughness used for morphological modeling should therefore differ from the one used for calibrating the hydrodynamics. The formulations by Soulsby and Clarke (2005) provide such a decoupled bed roughness methodology.

4.5.4. PARAMETRIZATION OF MODEL RESULTS FOR COMPARISON WITH REAL-LIFE SYSTEMS

As explained in the introduction, schematized models are often used in studies related to the long-term morphodynamic behavior of deltas, for example, to determine their re-

sponse to SLR. An important drawback of such schematized configurations is that the model results are difficult to compare with real-world systems. To improve the applicability of schematized models for real-life predictions, we therefore advocate the use of model validation metrics. Computing such metrics for both real-world systems and for the outcomes of highly schematized models allows a quantitative comparison of the model with real systems on a higher aggregation level.

We have synthesized our model results in a number of parameters that represent the shoal and channel properties in terms of geometry and topography, including the sediment composition. These metrics mainly focus on the aggregated macro-scale configuration of the system. For a more exhaustive real-life comparison, we recommend an extension of this parametrization with metrics that represent the large-scale configuration, such as those presented by Edmonds et al. (2011) and Broaddus et al. (2022), and by metrics that further analyze a system's complexity and dynamics, such as those presented by Tejedor et al. (2015). The latter introduce several parameters to determine delta's complexity in terms of topology (imposed by the network connectivity) and dynamics (introduced by the flux partitioning in the system). Their results reveal an inverse relationship between the vulnerability of a system and its complexity, showing the importance of the ability to simulate systems with similar complexity as real systems when analyzing their resilience to for example, large-scale human interventions and SLR.

4.6. CONCLUSIONS

We have studied long-term tidal basin evolution including two physical sand-mud interaction mechanisms, namely erosion interaction and roughness interaction. Erosion interaction implies that sand and mud interact in the sediment matrix of the sediment bed, and hence their erosion is coupled. Depending on the sediment composition, a sand-mud mixture can be non-cohesive, in which erosion is defined by the sand skeleton, or cohesive, in which the mud matrix determines the erosive behavior of the mixture. Roughness interaction implies that the sediment composition affects the hydraulic roughness of the sediment bed and therefore also the near-bed turbulence and thus the bed shear stresses. Consequently, an increase in the mud content of the bed lowers the bed shear stresses and thus weakens erosion forces.

Our results show that sand-mud interaction impacts tidal basin evolution, with erosion interaction having a much larger effect than roughness interaction. Especially the intertidal flat shape, size and composition widely vary with mud erodibility settings, but equally with the considered sand-mud interactions. Both interactions can enhance mudflat formation, though under very different circumstances: erosion interaction has a stronger effect in scenarios with poorly erodible mud ($\tau_e > 1$ Pa), whereas roughness interaction shows this effect in scenarios with high mud erodibility ($\tau_e = 0.25$ Pa). On the other hand, the effects of including sand-mud interaction on the overall hypsometry and channel depths remain limited, despite the very different erosion formulations applied.

Including sand-mud interaction in morphodynamic models provides a better representation of the physical processes. Sand-mud interaction may additionally (or consequentially), be used to optimize the morphodynamic model evolution. We show that in order to reproduce the bimodal distribution of the mud content, which is a typical characteristic of the bed composition in the Wadden Sea, one must account for sand-mud interaction. We have provided guidelines to improve schematized model evolution to resemble real-life systems through aggregated morphological metrics. When applying schematized model configurations, one of the main challenges is to translate model-based conclusions to the real world. We strongly advocate the use of morphological validation metrics — representing the shoal and channel properties in terms of geometry and topography, such as the ones that we have presented — as part of future work.

Photograph of the Wadden Sea - by Kevin Krautgartner

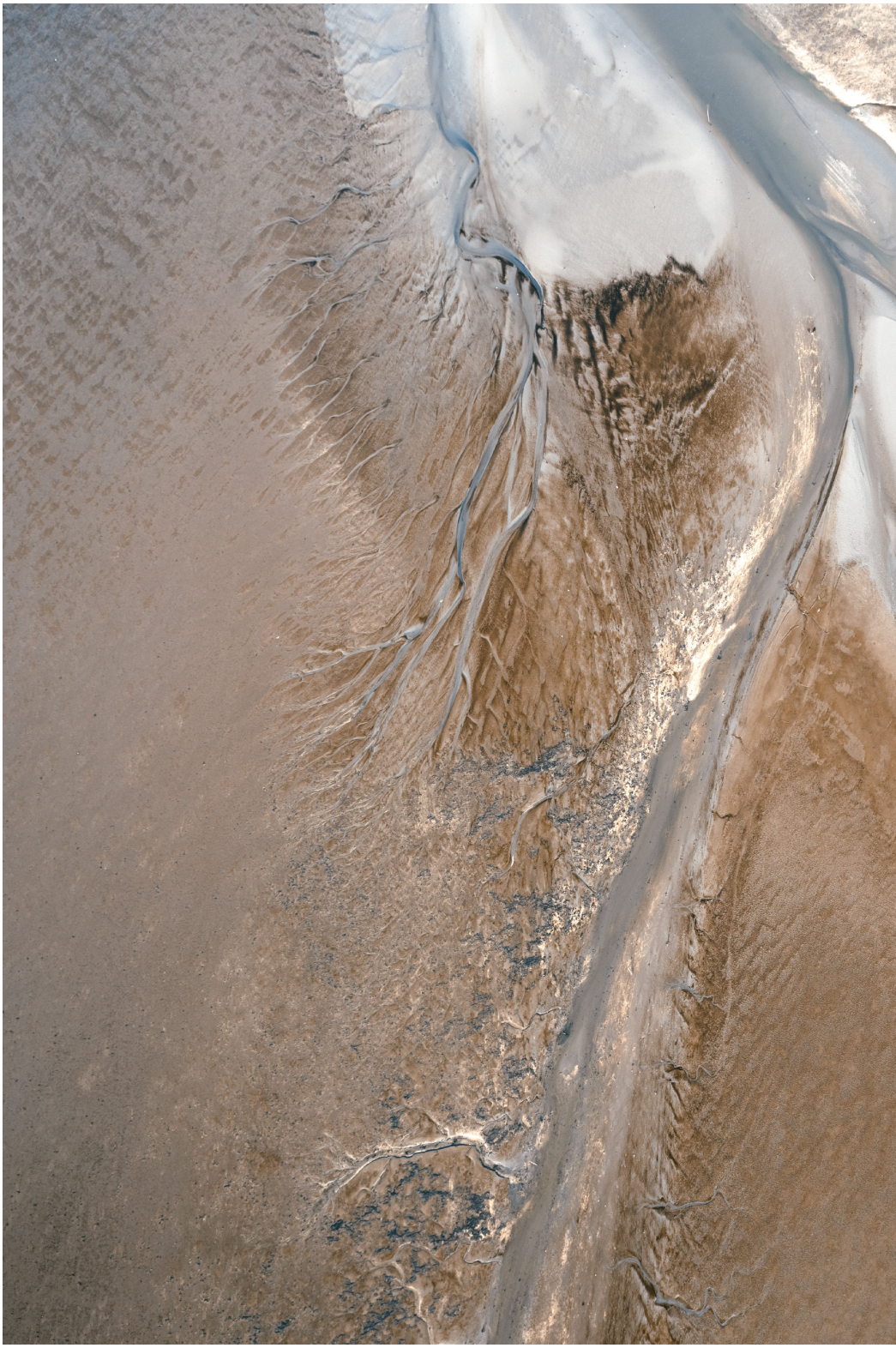

5

COMPOSITION OF THE SEDIMENT BED

Abstract
The sediment composition of the seabed governs its mobility, hence determining sediment transport and morphological evolution of estuaries and tidal basins. Bed sediments often consist of mixtures of sand and mud, with spatial gradients in the sand/mud content. This chapter aims at increasing the understanding of processes driving the sediment composition in tidal basins, focusing on depositional processes. We show that bed sediments in the Wadden Sea tend to be either mud-dominated or sand-dominated, resulting in a bimodal distribution of the mud content where the two modes represent equilibrium conditions. The equilibria depend primarily on the sediment deposition fluxes, with bimodality originating from the dependence of suspended sand/mud concentrations on the local bed composition. Our analysis shows that bimodality is a phenomenon that is not only specific for the Wadden Sea; it can be expected for a wide range of suspended sediment concentrations and thus also in other systems worldwide.

This chapter has been published in *Geophysical Research Letters* as:

Colina Alonso, A., van Maren, D. S., Herman, P. M. J., van Weerdenburg, R. J. A., Huismans, Y., Holthuijsen, S. J., Govers, L. L., Bijleveld, A. I., & Wang, Z. B. (2022). The existence and origin of multiple equilibria in sand-mud sediment beds. *Geophysical Research Letters, 49*, e2022GL101141. [Link]

5.1. INTRODUCTION

Most bed sediments in estuaries and tidal basins are a mixture of sand and mud, with spatial gradients in the sand/mud content, typically with sandy outer areas near the inlet and fining in the landward direction. These gradients may be gradual or abrupt, and cover large spatial scales (e.g., a tidal basin) or small spatial scales (e.g., individual shoals). Especially at small spatial scales the transition in sediment composition may be abrupt (van Straaten & Kuenen, 1957; de Glopper, 1967; Oost, 1995; Braat et al., 2017; de Vet, 2020). The sediment composition in turn governs sediment mobility, hence sediment transport and morphological evolution (Mitchener & Torfs, 1996; Le Hir et al., 2008; Geleynse et al., 2011; Jacobs et al., 2011; van Rijn, 2020). It may also influence hydrodynamics, introducing complex morphodynamic feedback loops (Winterwerp & Wang, 2013; van Maren et al., 2015). Moreover, the bed sediment composition strongly influences biological activity and habitat suitability for many benthic organisms (Brückner et al., 2020). Therefore, understanding and correctly predicting the distribution of sand and mud in tidal basins is important for sustainable management of these systems.

Grain size fractions in the sediment bed of tidal basins are generally sorted along an energy gradient, with a decreasing trend in hydrodynamic energy and grain size from the inlet to the landward side (e.g., Flemming & Nyandwi, 1994; Chang et al., 2006). Above a threshold bed shear stress the mud content is generally low (mud contents <10 %), but the mud content may vary anywhere between 0% and 100 % below this threshold condition (van Ledden, 2003; Braat, 2019). Spatial segregation of sand and mud has often been attributed to erosion processes, identifying a cohesive erosion regime (high mud content) and a non-cohesive erosion regime (low mud content, see e.g., Torfs, 1995; van Ledden, 2003; Jacobs et al., 2011; van Rijn, 2020). Within both regimes, erosion is a bulk process (dominated by mud in the former, by sand in the latter). An implication of this mutual coupling is — as will be discussed in more detail in this chapter — that erosion processes do not lead to sand-mud segregation. Depositional processes, on the other hand, have received much less scientific attention as a driver of sand-mud segregation.

The main objective of this chapter is to increase our understanding of processes driving the sediment composition in tidal basins, focusing on depositional processes. For this purpose, we analyze a large data set containing over 50,000 bed sediment samples collected in the Dutch and German Wadden Sea. The Wadden Sea is the world's largest uninterrupted system of barrier islands and tidal flats, spanning over a distance of nearly 500 km along the North Sea coasts of the Netherlands, Germany and Denmark (Pedersen & Bartholdy, 2006; Elias et al., 2012; Benninghoff & Winter, 2019). Being a mixed-energy tidal system, both tides and waves play an important role in shaping its morphology. The tidal amplitude increases from 1.4 m in the Western Wadden Sea to 3 m in the East. The offshore wave climate mainly consists of locally generated wind waves with an average significant wave height of 1.4 m and corresponding peak wave period of 7 s. The back-barrier basins contain extensive sand- and mudflats (see Figure 5.1) that provide great ecological value. The bed composition is annually sampled on a high spatial resolution, providing a unique data set that, as will be explored in this chapter, provides a signature of sand-mud distribution (bimodality) which has not yet been documented in

literature. These data give important insight into sand-mud patterns and segregation in tidal basins, thereby influencing long-term morphology. The mechanisms responsible for this bimodality will be explored within a theoretical framework supported by numerical models.

5.2. METHODS

5.2.1. FIELD DATA

The Synoptic Intertidal Benthic Survey (*SIBES*) data set contains samples from approximately 7,400 locations, covering the entire Dutch and part of the German Wadden Sea, and most of the Ems Estuary. The Dutch intertidal areas have been annually sampled since 2008, while the Dutch subtidal areas and the German parts of the Wadden Sea have been sampled only once. Sediment samples have been taken with a small core (with a diameter of 33 cm) up to 4 cm depth and freeze dried at -20 °C. After homogenization the samples have been analyzed with a *Coulter LS 13 320*, without prior treatment to extract organic matter or calcium carbonate (see also Bijleveld et al., 2012; Compton et al., 2013). Based on the grain size distribution we derive the clay content (p_{clay}, < 4 μm), silt content (p_{silt}, 4–63 μm) and sand content (p_{sand}, > 63 μm). Mud is defined as all sediment with a grain size smaller than 63 μm (i.e., silt and clay), such that:

$$p_{clay} + p_{silt} + p_{sand} = p_{mud} + p_{sand} = 1. \tag{5.1}$$

By analyzing the averaged sediment composition of the (homogenized) upper layer, we ignore the smaller-scale stratigraphy which is largely determined by the short-term dynamics (caused by for instance spring-neap tide variations) which is out of the scope of this research.

In addition, we make use of the suspended sediment concentration (SSC) data collected in the Wadden Sea since 1973 within the long-term monitoring program (*MWTL*) of the Dutch Ministry of Transport, Public Works and Water Management (Rijkswaterstaat). Measurements have been carried out in over 50 stations on a monthly to bimonthly basis, although currently only 10 stations are still actively maintained. Shipboard measurements are performed at 1 m water depth, where water samples are taken and filtered. After drying, the filter is weighed to determine the amount of suspended sediment. This data gives insight in the overall SSC trends in the Dutch Wadden Sea and more specifically in the large-scale variation of the suspended mud concentrations.

5.2.2. NUMERICAL MODELS

We use two numerical models to determine how concentrations vary in space and how they are related to the local bed composition. First, we use the depth-averaged hydrodynamic model of the Dutch Wadden Sea developed by van Weerdenburg et al. (2021) in Delft3D Flexible Mesh. Near bed sand concentrations during a tidal cycle are calculated using the transport formulations by van Rijn (2007a, 2007b).

In addition, we have set up a generalized, schematized depth-averaged (2DH) Delft3D morphodynamic model (Lesser et al., 2004) of a tidal inlet. The model domain consists

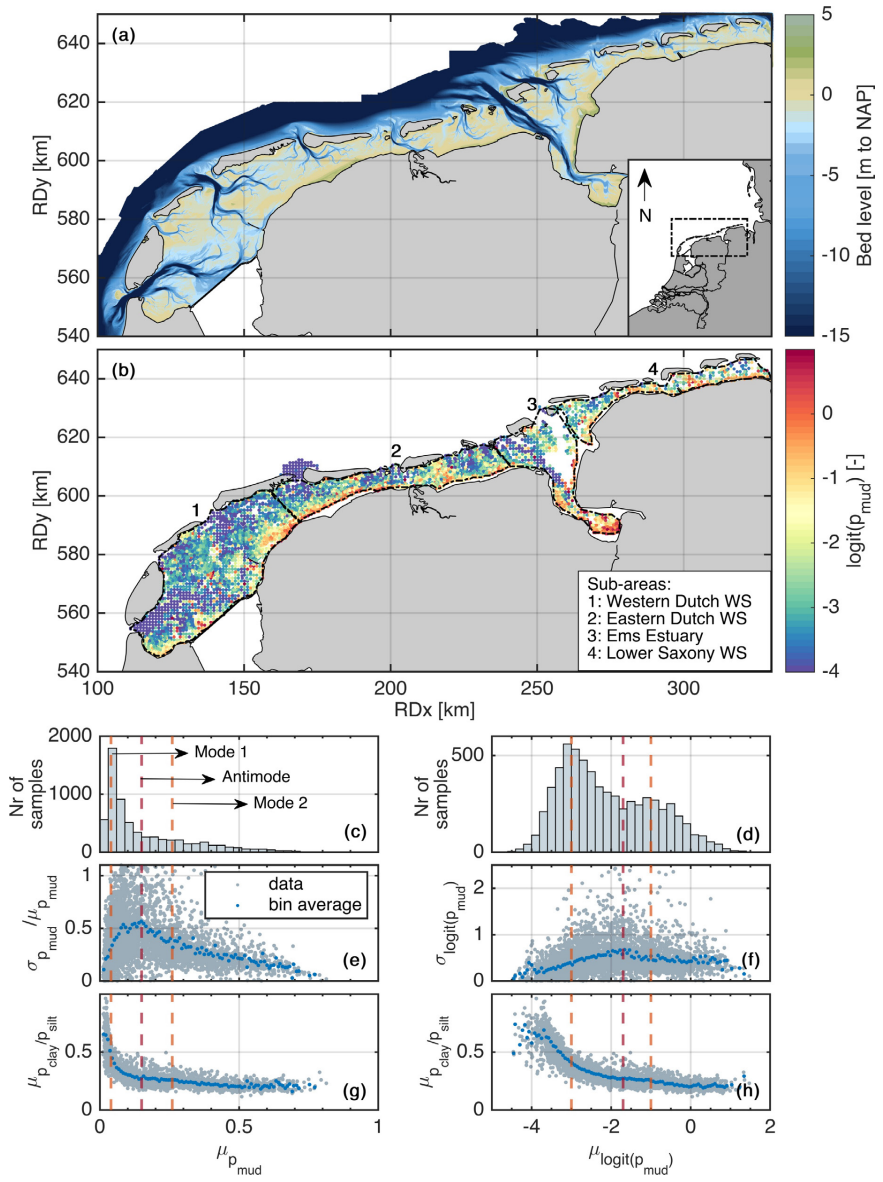

Figure 5.1: (a) Bathymetry of the Wadden Sea (WS) including the Ems Estuary in m to NAP (Dutch Ordnance Datum). (b) Mean mud content for each location, after logit transformation, over the period 2009–2018. (c–d) Number of samples per mud content (prior to and after logit transformation). (e) Coefficient of variation of the mud content. Standard deviations ($\sigma_{p_{mud}}$) and means ($\mu_{p_{mud}}$) are computed for each sample site (every gray dot represents one site). Bin average values (blue dots) have been calculated for 300 bins. (f) Standard deviation of $logit(p_{mud})$. (g–h) Dependence of the clay/silt ratio on the mud content.

of a tidal inlet in between two islands and a back-barrier basin with dimensions of 15 × 10 km and a rectangular computational grid with a mesh size of 100 × 100 m. The initial topography is a gradually sloping bed with a uniform sediment composition ($p_{sand} = 0.95, p_{mud} = 0.05$). The model has a stratified bed with an active transport layer of 0.1 m. Below the transport layer, 20 Eulerian sediment layers of 1 m thickness are prescribed. Initially, all bed layers have the same sediment composition. The model is run for a period of 50 years, forced by a semi-diurnal and quarter-diurnal tide with an amplitude of 1.5 m (S2+S4) prescribed at the northern open boundary (15 km from the inlet), and a wave-climate created by locally generated wind-waves of varying strength and direction. Sand-mud interaction is accounted for using the formulations by van Ledden (2003), in which non-cohesive sediment transport is calculated with van Rijn (1993) transport formulations, and cohesive sediment transport with the Partheniades-Krone formulation (Partheniades, 1965). Details on the model settings of both models are provided in Appendix C.

5.3. FIELD DATA REVEAL A BIMODAL MUD CONTENT

5.3.1. THE COMPOSITION OF THE SEDIMENT BED IS STRONGLY SEGREGATED

The overall sediment distribution in the Wadden Sea and Ems Estuary is characterized by a pronounced sand-mud segregation. Sandy channels with a low mud content ($p_{mud} < 10\%$) dominate the central part of the basins (see Figure 5.1b). The mud content sharply increases to more than 40% on the mudflats bordering the mainland coastlines, in sheltered bays, and across the tidal divides behind the islands.

The statistical distribution of the mud content in the Wadden Sea bed is positively skewed with mostly sandy samples (see Figure 5.1c). Because of this log-normal distribution, we convert the mean mud content p_{mud} using a logit transformation ($logit(p_{mud})$). We use the logit transformation rather than a conventional log transformation ($log(p_{mud})$), because the range of p_{mud}/p_{sand} can be infinite whereas p_{mud} is bounded between 0 and 1. This transformation is defined as:

$$logit(p_{mud}) = ln(p_{mud}/(1 - p_{mud})) = ln(p_{mud}/p_{sand}). \tag{5.2}$$

Logit-transformed mud contents reveal a striking bimodality: most frequent observations occur for either low or high $logit(p_{mud})$, with fewer observations in between (see Figures 5.1d and 5.2). This bimodality is not simply the result of large-scale spatial segregation, which would for instance be the case in a system with mainly sandy channels and muddy shoals. This is evidenced by its presence in both the subtidal and the intertidal areas (Figure 5.2). Especially the mud content in the intertidal areas shows that flats tend to be either sand-dominated or mud-dominated. The Eastern Wadden Sea, the Ems estuary and Lower Saxony have an approximately equal number of sandy and muddy flats, but the intertidal areas in the Western Dutch Wadden Sea are largely sandy. The subtidal areas in the Wadden Sea are mainly sand-dominated but in the Ems Estuary the subtidal areas are as frequently muddy as they are sandy, showing that also channels may be muddy.

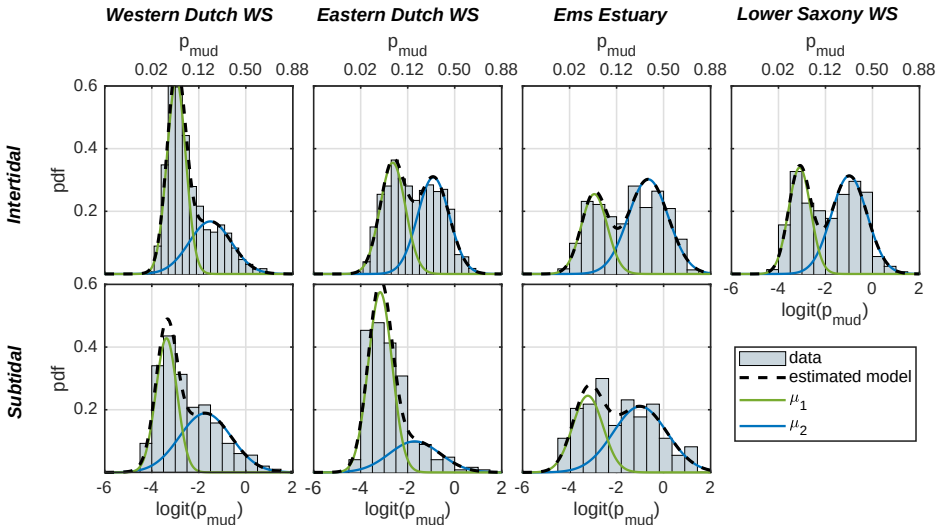

Figure 5.2: Distribution of the mud content p_{mud} [-] after logit transformation and data-fit for the sub-areas (of which the polygons are defined in Figure 5.1b). The upper panels show the results for the intertidal areas, the lower panels for the subtidal areas (no subtidal data is available for the German Lower Saxony Wadden Sea). The bin size is based on the number of observations. Distributions are fitted with a Gaussian mixture model using the Expectation Maximization algorithm (Roughan, 2021).

The location of the first mode is remarkably stable: all sub-systems show a mode corresponding to approximately 4% mud. In contrast to the first mode, the mud content (value of $logit(p_{mud})$) and frequency of occurrence of more muddy areas (i.e., the second mode) can largely vary per sub-area of the Wadden Sea (as defined in Figure 5.1b). Comparison with data from the 1990s (Rijkswaterstaat, 1998) reveals that the bimodal distribution of the mud content in the Wadden Sea has remained largely stable over the past decades (see also Chapter 2; Colina Alonso et al., 2021). Apparently, the second mode is more sensitive to local conditions compared to the first mode, but does remain fairly constant over time.

5.3.2. TWO EQUILIBRIUM STATES

The intertidal locations in the Dutch Wadden Sea (n = 5,935) are sampled every year, allowing the determination of the variability of $logit(p_{mud})$ using a standard deviation. Beds with a mean mud content close to any of the modes ($\mu_1 \approx$ -3, $\mu_2 \approx$ -1) are relatively stable in time, reflected in a relatively lower standard deviation (Figure 5.1e and Figure 5.1f); the standard deviation of samples with a mean mud content in between the two modes is substantially higher. Apparently, the two frequently occurring modes are fairly constant in time, while sediments with a mud content in between tend to switch to either of the modes. We believe this reflects the stability of the different states, where both modes can be characterized as stable conditions (equilibrium mud contents), whereas a mud content in between the two modes is unstable. In the next section, we investigate the mechanisms controlling the existence of multiple equilibria.

5.4. THEORETICAL ANALYSIS ON THE BED SEDIMENT COMPOSITION

5.4.1. SEDIMENT BED DYNAMICS

Bed sediments are continuously eroded, transported and deposited, resulting in bed level and bed composition changes. The change of the sediment composition, expressed as the change in mud content, can be described by:

$$\frac{\partial p_{mud}}{\partial t} = \frac{\partial \frac{M}{M+S}}{\partial t} = \frac{S}{(M+S)^2}\frac{\partial M}{\partial t} - \frac{M}{(M+S)^2}\frac{\partial S}{\partial t} \tag{5.3}$$

in which M is the total mass of mud in the bed and S the total mass of sand. Equilibrium corresponds to $\frac{\partial p_{mud}}{\partial t} = 0$. Since

$$M + S > 0 \tag{5.4}$$

and

$$\frac{S}{(M+S)} = p_{sand} = 1 - p_{mud} \tag{5.5}$$

and

$$\frac{M}{(M+S)} = p_{mud}, \tag{5.6}$$

equilibrium corresponds to:

$$(1 - p_{mud})\frac{\partial M}{\partial t} - p_{mud}\frac{\partial S}{\partial t} = 0. \tag{5.7}$$

For both mud and sand, the change of mass in time ($\frac{\partial M}{\partial t}$, $\frac{\partial S}{\partial t}$) is given by the sum of the deposition rate (D_{mud}, D_{sand}) and the erosion rate (E_{mud}, E_{sand}). Herein, with deposition and erosion we refer to the gross sediment fluxes, which can occur simultaneously (Winterwerp, 2007), and of which the net result can be either accretion or erosion. Equilibrium is defined by:

$$(1 - p_{mud})(D_{mud} - E_{mud}) - p_{mud}(D_{sand} - E_{sand}) = 0. \tag{5.8}$$

The deposition of sand and mud can be treated as two independent processes when neglecting flocculation interaction (Manning et al., 2011; Spearman et al., 2011), which we do here for simplicity reasons, and as long as the near bed concentration c_b is less than the gelling concentration (Torfs et al., 1996), which is the case for most tidal systems including the Wadden Sea. However, erosion of sand and mud in the bed is generally coupled and proportional, as elaborated in the next section.

5.4.2. INTERACTIVE EROSION OF SAND-MUD MIXTURES

Sand-mud mixtures are either non-cohesive or cohesive, depending on the small-scale structure of the bed. In a sand-dominated bed (non-cohesive), the internal structure is determined by the inter-particle locking of sand grains. For a high mud content, sand grains lose contact and sand particles become part of a (cohesive) mud matrix (Torfs, 1995; van Ledden et al., 2004a; Jacobs et al., 2011).

The erosion behavior of sand-mud mixtures has been topic of several experimental studies (e.g., Mitchener & Torfs, 1996; Jacobs, 2011; van Rijn, 2020) and parameterized in erosion models (e.g., van Ledden, 2003; Le Hir et al., 2011). This earlier work reveals that for non-cohesive mixtures, erosion of both sand and mud depends on the erosion properties of sand, as sand determines the skeleton structure. In the cohesive regime, erosion of sand and mud is determined by the erosion properties of mud. Consequently, the gross erosion fluxes of sand and mud are proportionally coupled (Mitchener & Torfs, 1996; van Ledden et al., 2004a; Winterwerp & van Kesteren, 2004; Jacobs et al., 2011; Le Hir et al., 2011; Chen et al., 2021a). Therefore we can express erosion of mud as follows:

$$E_{mud} = E_{sand} \frac{p_{mud}}{(1 - p_{mud})}. \tag{5.9}$$

This equation reveals that erosion of sand and mud is coupled following a ratio governed by p_{mud}, which strikingly implies that p_{mud} remains constant. Erosion does therefore not lead to a change in mud content $\frac{\partial p_{mud}}{\partial t}$. Field observations in which higher bed shear stresses lead to coarsening of the bed are therefore not the result of preferential erosion of mud relative to sand, but reflect a reduction in the deposition of the mud particles relative to sand particles after erosion. The equilibrium mud content (Equation 5.8) is therefore redefined as:

$$(1 - p_{mud})D_{mud} - p_{mud}D_{sand} = 0. \tag{5.10}$$

5.4.3. DEPOSITION OF SAND-MUD MIXTURES

The sediment deposition rate can be approximated as the product of the near-bed settling velocity ($w_{s,b}$) and the near-bed SSC (c_b). In general, the settling velocity of sand is at least an order of magnitude larger than that of mud. Local sand concentrations mostly depend on the local hydrodynamic conditions, whereas local mud concentrations are often supply-limited and (because of the small settling velocity) determined by conditions elsewhere or by the hydrodynamic history (Colosimo et al., 2020; Pearson et al., 2021). This typically results in high sand concentrations in the channels and low sand concentrations over the flats, while the suspended mud concentration is more uniformly distributed over the channels and the flats. We can simplify this to an overall constant mud concentration, regardless of the local mud content in the bed, whereas sand concentrations in the water column would decrease with increasing mud content in the bed. This is supported by the findings of Colosimo et al. (2020) and Pearson et al. (2021), combined with the fact that muddy beds mainly prevail in calm environments. In the next section we test this simplification of the deposition fluxes, for the Wadden Sea and for tidal basins in general, and we explore its relevance for the observed bimodality of p_{mud} in the sediment bed.

5.5. ANALYSIS OF SAND-MUD DEPOSITION FLUXES

5.5.1. DEPENDENCY OF THE DEPOSITION FLUXES ON THE LOCAL CONDITIONS

We illustrate the spatial variability of $c_{b,sand}$ and $c_{b,mud}$ with two numerical models (one model of the Wadden Sea and one model of a generalized tidal basin) in combination with field data (see also Section 5.2). The Wadden Sea model (van Weerdenburg et al., 2021) is used to calculate tide-averaged near-bed sand concentrations. These are compared to

the observed mud content in the bed, derived from *SIBES* data. Figure 5.3a shows that $c_{b,sand}$ indeed sharply decreases for increasing p_{mud}. However at very small p_{mud} values, $c_{b,sand}$ seems to reach a maximum, revealing a sigmoidal type of relation rather than a purely inverse one. This is especially clear after logit transformation (see the inset plot in Figure 5.3a). The results of the schematized model, in which both $c_{b,sand}$ and p_{mud} are computed, show a very similar relation (Figure 5.3b, see bin-averaged values for a comparison with Figure 5.3a). In both models sand concentrations are very low for high mud contents, but still exceed 0. For both the model and the data, the sigmoidal relation between $c_{b,sand}$ and p_{mud} can be described with the same sigmoid fit. Our model data shows slight deviations from a purely sigmoidal character around $0.1 < p_{mud} < 0.15$, but we believe this may originate from model artifacts rather than having a physical cause.

The schematized model also gives insight into the tide-averaged mud concentrations: these are more or less constant, regardless of the local sediment composition (Figure 5.3c). But although $c_{b,mud}$ does not depend on local p_{mud}, long-term SSC observations in the Dutch Wadden Sea reveal that there is considerable variation over larger spatial scales (see Figure C.5 of Appendix C). Concentrations are generally lower in the western part and higher in the eastern part and the Ems Estuary, and are around 67 mg/l on average. Since SSC is herein measured close to the water surface in relatively deep areas (depth > 5 m), the observed suspended sediment is assumed to be mainly mud. The near-bed mud concentrations are assumed to be a factor 2–3 higher, following a Rouse profile (see e.g., van Maren et al., 2020). The observations in the Wadden Sea illustrate that the concentrations computed with the schematized model (Figure 5.3c) reasonably represent the mud concentrations in the western part of the Wadden Sea.

As shown above, a local dependency exists between D_{sand} and p_{mud}. In order to determine the spatial scale associated with D_{sand}, we calculate a transport length scale as:

$$L = \frac{hu}{w_s}, \tag{5.11}$$

in which h is the depth, u the depth-averaged velocity and w_s the settling velocity of the corresponding sediment type. This length scale is compared against the variogram of p_{mud}, representing the inter-dependency of the observed mud content as a function of distance (for details, see Appendix C). The distance at which the sediment data are no longer spatially correlated is 5,464 m. This value is much larger than the 95 percentile transport length scales of coarse and fine sand (which are in the order of 400 and 1,400 m, respectively), showing that transport of sand is determined by local conditions. This validates the assumption of correlation between local D_{sand} and p_{mud}. The transport length scale of mud is an order of magnitude larger. This confirms our findings in Figure 5.3 that sand concentrations largely depend on local hydrogeomorphic conditions (explaining the correlation between D_{sand} and p_{sand}), while local mud concentrations are much more affected by conditions elsewhere and/or earlier (since mud can be transported over much larger distances).

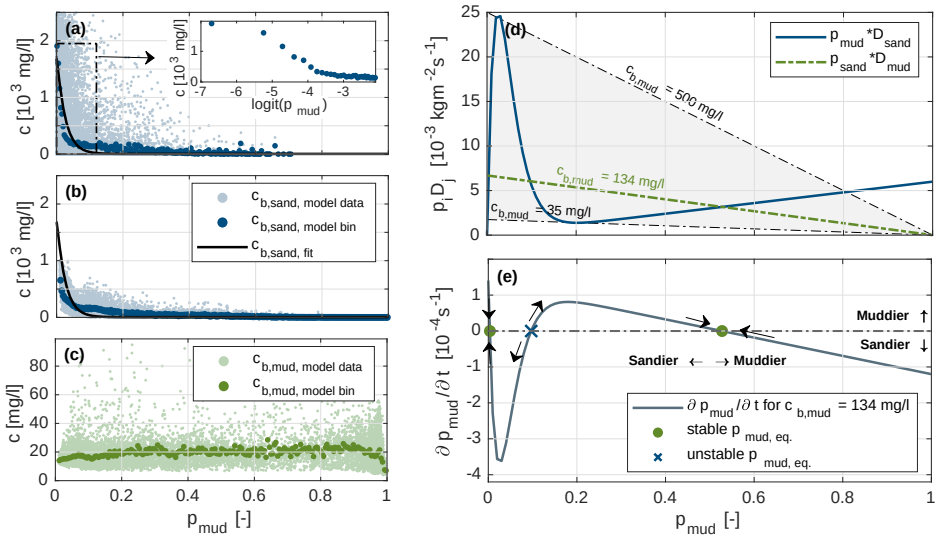

Figure 5.3: Suspended sediment concentrations, deposition fluxes and corresponding equilibrium sediment composition. (a) Relation between p_{mud} in the bed (derived from *SIBES* data) and the tide averaged $c_{b,sand}$ in the Wadden Sea (calculated with a numerical model, see (b) for legend). (b–c) Relation between p_{mud}, $c_{b,sand}$ and $c_{b,mud}$, derived from a schematized model. (d) Product of the deposition fluxes (fits based on model data) and the local sediment composition (Equation 5.10). Multiple equilibria are possible for 35 mg/l $< c_{b,mud} <$ 500 mg/l. (e) $\frac{\partial p_{mud}}{\partial t}$ for $c_{b,mud} = 134$ mg/l and the theoretical fit of c_{sand}, and corresponding equilibria of p_{mud} at $\frac{\partial p_{mud}}{\partial t} = 0$.

5.5.2. EQUILIBRIUM MUD CONTENTS

The theoretical fits of $c_{b,sand}$ (sigmoid) and $c_{b,mud}$ (constant, using 134 mg/l) to p_{mud} are subsequently used to calculate $p_{mud} \times D_{sand}$ and $p_{sand} \times D_{mud}$ (Equation 5.10, Figure 5.3d) and the resulting temporal change in p_{mud} (Figure 5.3e). Figure 5.3e reveals three equilibrium conditions in the Wadden Sea, of which two are stable and one is unstable. Stable equilibrium conditions are characterized by convergence: an increase in p_{mud} leads to a negative $\frac{\partial p_{mud}}{\partial t}$ while a decrease in p_{mud} results in a positive $\frac{\partial p_{mud}}{\partial t}$. Unstable conditions prevail in-between, in agreement with our theory but also suggested by the large standard deviation of the mud content for conditions in-between the bimodal peaks (Figure 5.1e, f). We believe that the bimodality in the bed sediment of the Wadden Sea is the result of these stable equilibrium conditions. Our analysis then suggests that bimodality is expected for many $c_{b,mud}$ conditions (tide averaged values of 35–500 mg/l), which is a much wider range than the conditions observed in the Wadden Sea.

The first equilibrium condition is in all cases located near $p_{mud} \approx 0$, showing that this condition is not sensitive to the suspended sediment concentrations. Note that in reality we observe a mode at slightly higher values of $p_{mud} \approx 0.04$ (see Figure 5.2). We believe this results from mud-burial mechanisms such as the trapping of mud in local bedforms and bioturbation, which are beyond the scope of our analysis (Terwindt & Breusers, 1972;

Le Hir et al., 2007; Kristensen et al., 2012). In contrast, the location of the second stable equilibrium condition is sensitive to the suspended sediment concentrations.

For an increasing mud concentration $c_{b,mud}$, the second stable equilibrium shifts to higher values of $p_{mud,\ eq.}$. This corresponds well with our data, where $c_{b,mud}$ increases in the eastern direction (Western Dutch Wadden Sea to Eastern Dutch Wadden Sea to Ems Estuary) while the second mode of the bimodal distribution shifts to the right (Figure 5.2). A second factor influencing the location of the second equilibrium is the sand concentration above muddy beds. The higher $c_{b,sand}$ at high p_{mud} (Figure 5.3a), the lower the value of the second stable $p_{mud,eq.}$ in Figure 5.3e. Sand transport rates over muddy beds will differ per system because it is probably mostly influenced by sand characteristics (D_{50}) and storm conditions. During storms sand may be transported to low-energy (muddy) locations, so the second bimodality peak is expected at lower p_{mud} values when the muddy areas are close to energetic sandy shorelines.

Our analysis explains the occurrence of bimodality, but also the spatial trends in bimodality for a range of sedimentary conditions in the Wadden Sea. In this environment, the time and spatially average SSC varies (from East to West) by a factor of $\sim$2. Therefore, we strongly encourage to expand this analysis to field conditions covering a wider range in SSC (both more and less turbid environments).

5.5.3. CRITERIA FOR BIMODALITY

Based on our findings, we can define three general criteria for the suspended sediment concentrations with respect to p_{mud}, in order to have two stable equilibria, and thus a bimodal mud content in the bed:

1. $c_{b,mud} > 0$ at $p_{mud} = 0$: mud is always available for deposition, also in fully sandy environments.

2. $c_{b,sand} > 0$ at $p_{mud} = 1$: sand is always available for deposition, also in fully muddy environments. This likely suggests transport of fine sand, since hydrodynamic conditions here are mostly not sufficiently energetic to transport coarse sediments.

3. The lines $p_{mud} \times D_{sand}$ and $(1 - p_{mud}) \times D_{mud}$ should cross three times: two crossings will define the stable equilibria and one crossing in between will define the unstable equilibrium. This gives requirements for the character of the relations between $c_{b,sand}$ and p_{mud} (in our case sigmoid), $c_{b,mud}$ and p_{mud} (in our case constant) and for the magnitude of $c_{b,mud}$. The latter should be within a range in which three crossings are possible.

5.6. CONCLUSIONS

Bed sediments in estuaries and tidal basins are often a mixture of sand and mud. The sediment composition is a key component influencing morphological evolution, hydrodynamics, biological activity and habitat suitability. Consequently, understanding the distribution of sand and mud in tidal basins is important for sustainable management. Analysis of bed sediments in the Wadden Sea has revealed that the mud content is bimodally

distributed, with sediment mixtures being either sand-dominated or mud-dominated. Beds with a mean mud content close to one of the modes are relatively stable in time, whereas those with a mean mud content in between are more variable in time. This suggests that the system is bistable with an unstable state between the two stable equilibrium conditions.

Using numerical models and field data, we have shown that the existence of multiple equilibrium conditions can be explained theoretically with the gross sediment deposition flux. Since in most cases gross sand and mud erosion fluxes are interdependent (erodibility interaction), the equilibrium mud contents depend primarily on the sediment deposition fluxes. The deposition fluxes are the product of the near-bed SSC and the settling velocity. Model simulations show that suspended concentrations of mud only weakly depend on the local bed composition, whereas we observe a sigmoidal relation between the concentrations of sand and the local mud content in the sediment bed. Herein, sand concentrations rapidly decrease with increasing mud content, but never become zero.

The difference in the suspended sand and mud concentration leads to multiple equilibria in bed composition — of which two are stable and one is unstable — for a wide range of conditions. This explains why bimodality is observed in the entire analyzed Wadden Sea system, even though average suspended sediment concentrations may largely differ per sub-system. The value of the first equilibrium (sandy mode) is relatively robust and stable, whereas the second equilibrium (muddy mode) may largely vary depending on the local mud concentrations and the mobility of sand in muddy areas. Our analysis shows that bistability is a generic phenomenon, so it can be expected in other systems as well. We advocate to study this for other systems worldwide in which sufficient bed sediment data is available to determine a representative statistical distribution of the sediment composition.

Our conclusion that sand-mud segregation results from deposition processes has implications for the understanding of sediment transport processes and modeling of coastal evolution. Predicting the sediment composition in the bed not only requires accounting for sand-mud erodibility interaction, but also a realistic spatial distribution of SSC (and hence the deposition flux). Our findings advance on our understanding of the distribution of sand and mud in tidal basins, and we recommend further analysis of these interaction processes using numerical morphological models.

Photograph of the Wadden Sea - by Kevin Krautgartner

6

SYNTHESIS

This dissertation aims to improve the understanding of large-scale morphodynamics in sand-mud tidal systems by investigating processes related to segregation of sand and mud, sand-mud interaction processes, sediment supply, and long-term deposition. This aim has been reformulated into a set of overarching research questions. The first section of this concluding chapter addresses these research questions. The findings are subsequently synthesized into generic advancements in sand-mud morphodynamics. Lastly, an outlook is presented including recommendations for future work.

6.1. CONCLUSIONS

RQ 1: What is the relative role of sand and mud deposition in the morphodynamic evolution of tidal basins in response to human interventions?

The answer to this question is explored for the case of the Western Dutch Wadden Sea, where closure of the South Sea (*Zuiderzee*) in 1932 largely changed the morphology of the remaining tidal basins. The responses of sand and mud to the intervention have been very different in time and in space. The closure triggered sediment infilling with a substantial contribution of mud (21%–42%). The contribution of mud to the total sediment infilling volume is much larger than the average mud content in the top layer of the bed, because muddy areas accrete faster than sandy areas. This was also observed in a basin of the Eastern Dutch Wadden Sea after closure of the Lauwers Sea (*Lauwerszee;* van Ledden et al., 2006; van Maren et al., 2023).

During the initial response of the basins, large sand and mud volumes accreted in abandoned channels (which also occurred in the Lauwers Sea case). At present, mud sedimentation along the mainland coast is still ongoing in the Western Dutch Wadden Sea with fairly constant import rates, while the net import of sand significantly decreased over time and has been fluctuating around 0 in the past two decades. Gross volume changes are however much larger for sand than for mud, and result from the migration of predominantly sandy channels.

RQ 2: How much mud is delivered to the Wadden Sea by marine and fluvial sources, where does it accumulate and how do human interventions influence source and sink terms?

The marine North Sea Continental Flow (NSCF) transports mud from the Dover Strait along the French, Belgian and Dutch coasts, later following the Wadden Sea coastline. This current is the main mud source for the Wadden Sea, delivering approximately 10–14.4 million (M) ton/year. Several rivers (from Lake IJssel and the Ems, Weser and Elbe estuaries) constitute additional sediment sources, adding a total amount of mud of 1.5 M ton/year.

Mud is imported into the Wadden Sea basins, where it deposits on the low-energy areas (especially along the mainland coast). Both the basins and the salt-marshes act as important mud sinks. The former constitute the largest mud sink, with an average deposition of 7.95 M ton/year. The latter are a smaller sink (1.84 M ton/year), although deposition rates per km^2 tend to be much larger, making them more efficient mud traps. A small amount of mud (0.5 M ton/year) additionally deposits offshore near Helgoland. Mud is

also artificially extracted from the system by dredging activities after which the sediments are disposed on land (1.98 M ton/year).

Combining these findings shows that the mud budget of the Wadden Sea is nearly closed: ∼14 M ton/year is supplied by the NSCF and local rivers, while a similar mass deposits in the basins and marshes, and is extracted by dredging. Anthropogenic sediment extraction provides large sinks, even surpassing salt marsh deposition. Both the alongshore change in deposition rates and in sediment composition data indicate that mud deficits may exist in the northern German and Danish parts of the Wadden Sea.

RQ 3: What is the large-scale impact of small-scale sand-mud interactions and how do these interactions influence predictions of the morphodynamic evolution?
Tidal basin evolution was studied including two abiotic sand-mud interaction mechanisms, namely erosion interaction and roughness interaction. Erosion interaction results from the influence of sand and mud on the sediment matrix of the sediment bed. Sand-mud mixtures may be non-cohesive, in which erosion of the mixture is determined by the sand skeleton, or cohesive, in which the mud matrix determines the erosive behavior of the mixture. Roughness interaction results from the effect of the sediment composition on the hydraulic roughness of the sediment bed — and therefore also the near-bed turbulence and thus the bed shear stresses. An increase in the mud content of the bed herein lowers the bed shear stresses and thus weakens erosion forces.

Sand-mud interaction can significantly impact tidal basin evolution, with erosion interaction generally having a much larger effect than roughness interaction. Especially the intertidal flat shape, size and composition widely vary with the considered sand-mud interactions (as well as with mud erodibility settings). While both interactions can enhance mudflat formation, their effects are maximized under different circumstances. Including sand-mud interaction in numerical simulations has limited effect on the modeled hypsometry and channel depths. It is however crucial for correctly reproducing the bimodal character of the bed sediment composition (see RQ 4).

Including sand-mud interaction in morphodynamic models thus provides a better representation of the physical processes. In addition, it can be used to optimize the morphodynamic model evolution following the guidelines that have been presented.

RQ 4: Which processes lead to the spatial segregation of sand and mud, and how can the sediment composition be better predicted?
Analysis of a large data set containing bed sediment samples collected in the Dutch and German Wadden Sea shows that bed sediments in the Wadden Sea tend to be either sand-dominated or mud-dominated. This results in a bimodal distribution of the mud content in the upper bed (either very low, or relatively high), where the two modes represent two equilibrium conditions (and therefore revealing a bistability).

While spatial segregation of sand and mud has often been attributed to erosion processes, it is shown that because of sand-mud erosion interaction — where erosion is a bulk process determined by either the sand or the mud skeleton — erosion processes do not lead

to sand-mud segregation. Instead, the equilibrium bed composition primarily depends on the sediment deposition fluxes, and bimodality originates from the dependence of suspended sand/mud concentrations on the local bed composition. Our findings suggest that bimodality strongly depends on the availability of mud and transport capacity of sand.

In order to reproduce a bimodal distribution of the mud content with process-based morphodynamic models, one must account for sand-mud interaction in the model set-up. In addition, the modeled sediment composition will largely depend on the overall mud availability and the suspended sand concentrations along the model domain. The former mainly depends on the imposed initial bed composition and suspended mud concentrations along the boundaries. The latter is influenced by hydrodynamic conditions (e.g., storminess) and by the mobility of the sand fraction (which is affected by e.g., D_{50}).

6.2. ADVANCEMENTS IN SAND-MUD MORPHODYNAMICS

6.2.1. THE NEED FOR A COMBINED APPROACH

This thesis illustrates the importance of a combined sand-mud approach in morphodynamic studies of areas where both sediment types prevail. Both sand and mud contribute to the morphodynamic development of the sediment bed, but each at its own spatial and temporal scale. Their quantitative contribution to morphological development cannot be simply predicted by the average surface bed composition. In the Wadden Sea for instance, mud is preferentially depositing in areas with high net sedimentation rates, whereas large volumes of sand are redistributed by channel migration without necessarily altering net sediment volumes. Moreover, the combined behavior of mixed sand-mud beds is not a superposition of their individual sediment dynamics, because of the small-scale interactions involved which can significantly influence large-scale evolution. This is especially relevant in estuaries and tidal basins as the Wadden Sea, where the sediment bed is generally composed of sand-mud mixtures — despite the clear segregation between dominantly sandy and muddy areas.

Advancing our understanding of sand-mud morphodynamics requires combined data-based and modeling approaches. Historical bathymetrical and sedimentological data of the Wadden Sea have provided new insights into the morphodynamic response to basin closures. These new insights may be used to improve and/or validate numerical models to better predict the impact of future interventions in similar areas. Analysis of data collected as part of recent field campaigns (such as *SIBES*) have also improved our understanding of sand-mud dynamics. Novel analysis methods revealed the importance of deposition processes determining the sediment composition, but also new properties (such as the bimodality of the mud content) with which we can validate model results. Numerical models are, in turn, important to interpret our data, as illustrated with the origin of the bimodality.

The morphodynamics of coastal systems shaped by sand and mud is complex, driven by many processes that act simultaneously (see Figure 1.1). Improving our understanding of, but also communicating about the morphodynamics of such systems, is facilitated by

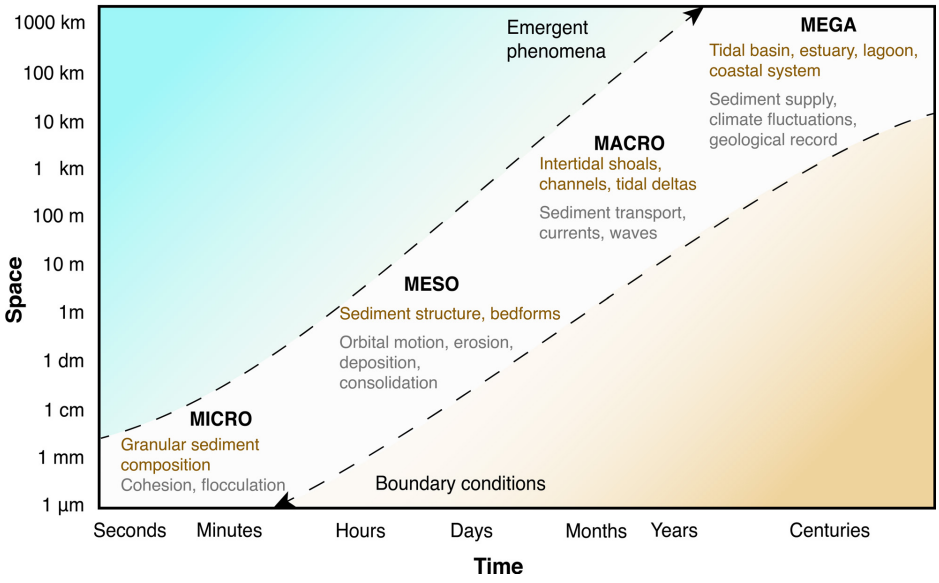

Figure 6.1: Space and time scales of processes (in gray) and phenomena (in brown) in sand-mud morphodynamics, after de Vriend (1991), Jacobs (2011), and Pearson (2022).

conceptual models. Conceptual models integrate our understanding based on models as well as data, focusing only on those findings that are important for a specific purpose, and deliberately abstracting from irrelevant details. The Wadden Sea case also illustrates that a system-wide (and therefore sometimes cross-bordering) perspective is not only desired, but even essential. This especially holds for the management of sand-mud systems in which sediment availability is finite. Local interventions may have implications elsewhere (e.g, due to the limited availability of mud). Such a response may be slow, among others because of a system's buffer capacity temporarily obscuring the effects of an intervention. The response of a system to interventions may therefore only be accurately predicted when the system is well understood at all spatial and temporal scales.

6.2.2. INTERACTING SCALES

Physical processes and phenomena in the field of sand-mud morphodynamics cover a wide range of spatial and temporal scales (see Figure 6.1). The relevance of the processes and phenomena depend on the scale of the research or management question. By placing these processes in a scale-cascade, one can determine how they might affect each-other: emergent phenomena at smaller scales affect the larger scales by propagating upward trough non-linearities, whereas phenomena at larger scales serve as boundary conditions for the smaller scales.

This work has shown that the scales are strongly connected. Chapter 4 reveals, for instance, that sand-mud interaction mechanisms taking place at particle scale can eventually steer tidal basin evolution. As a consequence, a correct representation of these

small-scale processes might be necessary to correctly model large-scale evolution. Chapter 5 illustrates that sand and mud concentrations influence the sediment bed on different scales. Sand concentrations are mostly determined by the local conditions at a certain moment, whereas mud concentrations are much more influenced by conditions that have occurred previously and elsewhere, and are more evenly spread along larger areas and longer timescales. These spatial differences in concentration directly influence the deposition fluxes, triggering another large-scale phenomenon — the bimodality of the mud content.

6.2.3. DEFINING METRICS

Morphological metrics, such as the ones we have presented in Chapter 4, may contribute to evaluation and comparison of coastal morphology worldwide. Figure 6.2 shows morphological metrics of sand-mud systems that can be used to evaluate coastal systems or model results depending on the relevant time and spatial scale of the question.

These metrics may facilitate a quantitative comparison of schematized model results with the real world. The morphodynamic impacts of climate change and human interventions play a role on decades to centuries, and forecasting these impacts requires tools that can handle such long timescales. Many realistic numerical models are not suitable for this purpose because they are not in morphodynamic equilibrium. Schematized models have a great potential to model such large-scale long-term impacts because their simplifications more easily allows morphodynamic equilibrium. It is however a challenge to capture the fundamental aspects of real-world systems in such low-complexity models, and to quantitatively validate the schematized model performance. Morphological metrics can be used to overcome these challenges.

Morphological metrics may be additionally used to analyze the state and development of a specific area, revealing trends, transitions, and even tipping points. For example, the overall distribution of the mud content in the Wadden Sea has been relatively stable over the past decades, while it does differ between individual parts. Even though bimodality is observed in most basins, the distribution of the mud content in the northern German and Danish parts of the Wadden Sea is not bimodal, suggesting a mud deficit (and therefore a supply limitation in the basins). Similarly, the modes of the bimodality can be used as a metric to analyze spatial and temporal suspended sediment concentration trends. In addition to morphological trends, response timescales to interventions can provide crucial information about the current state and to be expected behavior of coasts and deltas in transition (van Maren et al., 2023).

6.3. OUTLOOK

6.3.1. RECOMMENDATIONS FOR FUTURE MEASUREMENTS

An important assumption when using the approach of van Ledden (2003), is the choice for $p_{mud,crit}$ at which the sediment mixture switches form non-cohesive to cohesive behavior. Its exact value is an important model input parameter, but cannot be directly determined from field observations. Even more, the transition from non-cohesive to cohesive behavior is probably gradual rather than abrupt. Note that in reality, the threshold

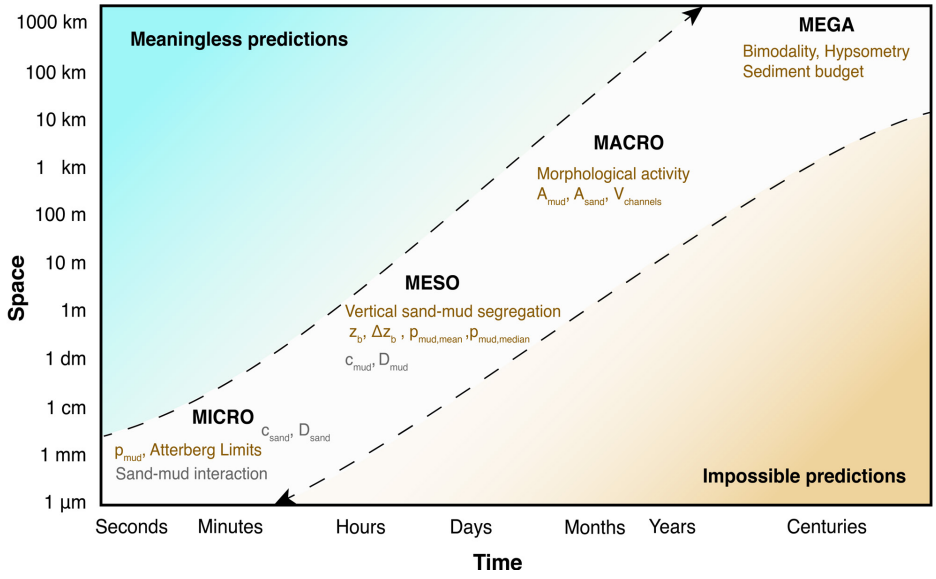

Figure 6.2: Processes (gray) and metrics (brown) to be validated depending on the analyzed scales.

between both regimes is determined by the critical clay content $p_{clay,crit}$, which can be converted to $p_{mud,crit}$ for systems where the clay/silt ratio is constant (at least in the cohesive regime).

Another important unknown is related to the (skin friction related) roughness height that is used to calculate bed shear stresses. In Chapter 4 we imposed, as a first assumption, a gradual transition between the roughness height of sand (approximated by $k_{s,sand} = 2.5D_{50,sand}$ for a bed consisting for 90% out of sand) and the roughness height of mud ($k_{s,mud} = 2.5D_{50,mud}$ for a bed with 90% mud). Further research is needed on the value of the roughness heights of both sediment fractions (although especially that of mud), but also on the transition speed depending on the sediment composition of sand-mud mixtures.

In the past decade, the most extensive field campaigns regarding the bed sediment composition of the Wadden Sea (within the project of *SIBES*) have provided crucial insight for this thesis. The combined continuity, spatial coverage, and resolution over time and space of these measurements make them worldwide unique. Measurements are, however, only executed in the summer months, leaving a potentially important lack of knowledge. Mud contents are, for instance, expected to be lower in winter months, especially during high-energy conditions. Also the recovery period after a storm is poorly known. It is therefore strongly advised to execute similar experiments year-round, starting with a smaller area that is well accessible (such as a fringing flat as the *Balgzand* area) to gain first insights in the effects of seasonality.

A deeper analysis of the Wadden Sea's mud budget would largely benefit from suspended sediment concentration (SSC) measurements. Although SSC time series in the Wadden Sea show that there is a consistency in relative seasonality trends (being almost independent of station location, depth and salinity, see Herman et al., 2018), there is a great spatial and temporal variability in absolute SSC values. Further analyzing the potential supply-limitation of mud in parts of the Wadden Sea would therefore require long-term and high-resolution (ideally continuous) measurements in a great number of stations in the Dutch, German and Danish parts of the Wadden Sea.

6.3.2. MODELING SAND-MUD MORPHODYNAMICS

Understanding and predicting the dynamics of sand-mud mixtures strongly benefits from simultaneous application of analytical and (multiple) numerical models. Process-based mud transport models are, for instance, capable of either addressing morphological changes or sediment concentrations, while models that are accurate for both purposes are rare. The reason for this is the large number of variables, timescales and unknown processes, which make it very difficult to derive a mathematical representation that perfectly mimics all governing processes (Winterwerp et al., 2021).

In addition, questions related to processes slowly operating over long periods are especially challenging to answer. An example is the extent to which tidal basins keep pace with SLR. Process-based models such as Delft3D are very well capable of predicting the morphodynamic evolution after large-scale distortion of the system (e.g., after a basin closure), but are less suitable to predict the smaller-scale (natural) evolution of inlets, unless abundant field data are available (Lesser, 2009). This is even more relevant for sand-mud systems than for pure sandy systems, in which a wide range of additional parameters exists controlling its morphodynamic behavior. The absence of calibration and validation data under the foreseen SLR conditions thus introduces major uncertainties for accurate predictions of the morphological response. Consequently, management decisions should be backed with a wide range of methodologies.

This thesis illustrates that the predicted morphological evolution of sand-mud environments is strongly influenced by choices for erosion formulations and mud parameters. Some combinations provide unrealistic model results, even though the individual choices may seem realistic themselves. It is therefore advised to not only follow the guidelines provided in Chapter 4, but especially to also remain critical toward the accuracy of the model results. Whenever possible, model output should be quantified trough metrics describing the morphology (Chapter 4), but also to data-based timescales of the morphological response (van Maren et al., 2023). Developing a system understanding should be at the heart of all modelling studies.

6.3.3. PRESSING CHALLENGES

In Chapter 1 of this thesis it was postulated that a better understanding of sand-mud morphodynamics is needed to enable successful and sustainable management of coasts and deltas. Worldwide, these systems are under pressure by human activities and climate change, both threatening their existence. We have zoomed in on the Wadden Sea — a

unique area providing crucial ecosystem services, but whose fate is determined by a delicate balance between relative SLR and sediment accretion (Wang et al., 2018). SLR may lead to drowning of the intertidal area, which would result in a (partial) loss of its ecosystems (Timmerman et al., 2021) and of its carbon storage potential. Degradation of the intertidal flats could even lead to a release of CO_2 into the oceans and the atmosphere, enhancing global warming (UNESCO, 2020). On the other hand, the Wadden Sea is currently accumulating sediments at a rate that outpaces SLR, which is causing maintenance problems of several navigation routes (Herman et al., 2016; Smits et al., 2022). Moreover, coastal systems such as the Wadden Sea have multiple purposes (e.g., flood safety, recreation, navigation and ecology), which may result in conflicting interests. Management of these systems is therefore not an easy task.

The challenges regarding the current state of our coasts and deltas are more pressing than ever (IPCC, 2023). In the current Anthropocene, we are facing the consequences of human interventions, and simultaneously also experiencing the tip of the iceberg of what climate change might bring. While writing these lasts words, I look back on a summer full of natural disasters; El Niño has amplified extreme weathers, further exposing the already present effects of climate change ("Rough years ahead", 2023). The climate change crisis has triggered a biodiversity crisis. Overcoming both crises and securing a livable future will require a dual focus: both substantially reducing emissions, and making sustainable adaptions to the already existing changes in our climate, embracing nature-based solutions (Pörtner et al., 2023). Doing nothing is no longer an option. We must act now.

Photograph of the Wadden Sea - by Kevin Krautgartner

REFERENCES

Ackermann, F., & Schubert, B. (2007). Trace Metals as Indicators for the Dynamics of (Suspended) Particulate Matter in the Tidal Reach of the River Elbe. In Springer (Ed.), *Sediment dynamics and pollutant mobility in rivers. an interdisciplinary approach.* (pp. 296–394). https://doi.org/10.1139/l91-019

Baart, F., van Gelder, P. H., de Ronde, J., van Koningsveld, M., & Wouters, B. (2012). The effect of the 18.6-year lunar nodal cycle on regional sea-level rise estimates. *Journal of Coastal Research*, *28*(2), 511–516. https://doi.org/10.2112/JCOASTRES-D-11-00169.1

Baas, J. H., Davies, A. G., & Malarkey, J. (2013). Bedform development in mixed sand-mud: The contrasting role of cohesive forces in flow and bed. *Geomorphology*, *182*, 19–32. https://doi.org/10.1016/j.geomorph.2012.10.025

Baas, J. H., Malarkey, J., Lichtman, I. D., Amoudry, l. O., Thorne, P. D., Hope, j. A., Peakall, J., Paterson, D. M., Bass, S. J., Cooke, R. D., Manning, A. J., Parsons, D. R., & Ye, L. (2021). Current- and Wave-Generated Bedforms on Mixed Sand–Clay Intertidal Flats: A New Bedform Phase Diagram and Implications for Bed Roughness and Preservation Potential. *Frontiers in Earth Science*, *9*, 1–27. https://doi.org/10.3389/feart.2021.747567

Barbier, E. B., Hacker, S. D., Kennedy, C., Koch, E. W., Stier, A. C., & Silliman, B. R. (2011). The value of estuarine and coastal ecosystem services. *Ecological Monographs*, *81(2)*(2), 169–193.

Beets, D. J., van der Valk, L., & Stive, M. J. (1992). Holocene evolution of the coast of Holland. *Marine Geology*, *103*(1-3), 423–443. https://doi.org/10.1016/0025-3227(92)90030-L

Beets, D. J., & van der Spek, A. J. F. (2000). The Holocene evolution of the barrier and the back-barrier basins of Belgium and the Netherlands as a function of late Weichselian morphology, relative sea-level rise and sediment supply. *Geologie en Mijnbouw/Netherlands Journal of Geosciences*, *79*(1), 3–16. https://doi.org/10.1017/S0016774600021533

Benninghoff, M., & Winter, C. (2018). Decadal evolution of tidal flats and channels in the Outer Weser estuary, Germany. *Ocean Dynamics*, *68*(9), 1181–1190. https://doi.org/10.1007/s10236-018-1184-2

Benninghoff, M., & Winter, C. (2019). Recent morphologic evolution of the German Wadden Sea. *Scientific Reports*, *9*(1), 9293. https://doi.org/10.1038/s41598-019-45683-1

Bi, Q., & Toorman, E. A. (2015). *Mixed-sediment transport modelling in Scheldt estuary with a physics-based bottom friction law* (Vol. 65). https://doi.org/10.1007/s10236-015-0816-z

Bijleveld, A. I., van Gils, J. A., van der Meer, J., Dekinga, A., Kraan, C., van der Veer, H. W., & Piersma, T. (2012). Designing a benthic monitoring programme with

multiple conflicting objectives. *Methods in Ecology and Evolution*, *3*(3), 526–536. https://doi.org/10.1111/j.2041-210X.2012.00192.x

Bilskie, M. V., Hagen, S. C., Medeiros, S. C., & Passeri, D. L. (2014). Dynamics of sea level rise and coastal flooding on a changing landscape. *Geophysical Research Letters*, *41*(3), 927–934. https://doi.org/10.1002/2013GL058759

BIOCONSULT & Coastal Defence and Nature Conservation Agency (NLWKN). (2012). Sediment Management Strategies in the Weser Estuary – Study in the framework of the Interreg IVB project TIDE Long version. *rapport projet Interreg IVB TIDE*, (December), 56.

BIOCONSULT, GbR, S., & Scholle. (2018). *Umwelt- und naturschutzfachliche Studie zum Sedimentmanagementkonzept für die bremischen Häfen* (tech. rep.).

Boechat Albernaz, M., Brückner, M. Z., van Maanen, B., van der Spek, A. J., & Kleinhans, M. G. (2023). Vegetation Reconfigures Barrier Coasts and Affects Tidal Basin Infilling Under Sea Level Rise. *Journal of Geophysical Research: Earth Surface*, *128*(4). https://doi.org/10.1029/2022JF006703

Bowen, A., & Inman, D. (1966). *Budget of littoral sands in the vicinity of Point Arguello, California. U.S. Army Corps of Engineers, Coastal Engineering Research Center, Technical Memorandum No. 19* (tech. rep.).

Braat, L. (2019). *Morphodynamics and Sedimentology of Estuaries with Sand and Mud* [PhD thesis]. Utrecht University.

Braat, L., Leuven, J. R., Lokhorst, I. R., & Kleinhans, M. G. (2019). Effects of estuarine mudflat formation on tidal prism and large-scale morphology in experiments. *Earth Surface Processes and Landforms*, *44*(2), 417–432. https://doi.org/10.1002/esp.4504

Braat, L., van Kessel, T., Leuven, J. R. F. W., & Kleinhans, M. G. (2017). Effects of mud supply on large-scale estuary morphology and development over centuries to millennia. *Earth Surf. Dynam.*, *5*, 617–652.

Broaddus, C. M., Vulis, L. M., Nienhuis, J. H., Tejedor, A., Brown, J., Foufoula-Georgiou, E., & Edmonds, D. A. (2022). First⊠Order River Delta Morphology Is Explained by the Sediment Flux Balance From Rivers, Waves, and Tides. *Geophysical Research Letters*, *49*(22). https://doi.org/10.1029/2022GL100355

Brown, S., & Nicholls, R. J. (2015). Subsidence and human influences in mega deltas: The case of the Ganges-Brahmaputra-Meghna. *Science of the Total Environment*, *527-528*, 362–374. https://doi.org/10.1016/j.scitotenv.2015.04.124

Brückner, M. Z. M., Braat, L., Schwarz, C., & Kleinhans, M. G. (2020). What Came First, Mud or Biostabilizers? Elucidating Interacting Effects in a Coupled Model of Mud, Saltmarsh, Microphytobenthos, and Estuarine Morphology. *Water Resources Research*, *56*(9). https://doi.org/10.1029/2019WR026945

Brückner, M. Z. M., Schwarz, C., Coco, G., Baar, A., Boechat Albernaz, M., & Kleinhans, M. G. (2021). Benthic species as mud patrol - modelled effects of bioturbators and biofilms on large-scale estuarine mud and morphology. *Earth Surface Processes and Landforms*, (January), 1–17. https://doi.org/10.1002/esp.5080

Bundesanstalt Für Wasserbau. (2020). EasyGSH-DB: Bathymetrie (1996-2016) [Dataset]. https://doi.org/10.48437/02.2020.K2.7000.0002

Caldwell, R. L., & Edmonds, D. A. (2014). The effects of sediment properties on deltaic processes and morphologies: A numerical modeling study. *Journal of Geophysical Research: Earth Surface*, *119*(5), 961–982. https://doi.org/10.1002/2013JF002965

Chang, T. S., Bartholomä, A., & Flemming, B. W. (2006). Seasonal dynamics of fine-grained sediments in a back-barrier tidal basin of the German Wadden Sea (southern North Sea). *Journal of Coastal Research*, *22*(2), 328–338. https://doi.org/10.2112/03-0085.1

Chen, D., Zheng, J., Zhang, C., Guan, D., Li, Y., & Wang, Y. (2021a). Critical Shear Stress for Erosion of Sand-Mud Mixtures and Pure Mud. *Frontiers in Marine Science*, *8*. https://doi.org/10.3389/fmars.2021.713039

Chen, X., Zhang, C., Townend, I. H., Paterson, D. M., Gong, Z., Jiang, Q., Feng, Q., & Yu, X. (2021b). Biological Cohesion as the Architect of Bed Movement Under Wave Action. *Geophysical Research Letters*, *48*(5), 1–9. https://doi.org/10.1029/2020GL092137

Chirol, C., Haigh, I. D., Pontee, N., Thompson, C. E., & Gallop, S. L. (2018). Parametrizing tidal creek morphology in mature saltmarshes using semi-automated extraction from lidar. *Remote Sensing of Environment*, *209*(March 2017), 291–311. https://doi.org/10.1016/j.rse.2017.11.012

Chirol, C., Haigh, I. D., Pontee, N., Thompson, C. E. L., & Gallop, S. L. (2022). Morphological evolution of creek networks in 10 restored coastal wetlands in the UK. *Scientific Data*, *9*(1), 1–16. https://doi.org/10.1038/s41597-022-01199-4

Cleveringa, J., & Oost, A. P. (1999). The fractal geometry of tidal-channel systems in the Dutch Wadden Sea. *Geologie en Mijnbouw/Netherlands Journal of Geosciences*, *78*(1), 21–30. https://doi.org/10.1023/A:1003779015372

Coco, G., Zhou, Z., van Maanen, B., Olabarrieta, M., Tinoco, R., & Townend, I. (2013). Morphodynamics of tidal networks: Advances and challenges. *Marine Geology*, *346*, 1–16. https://doi.org/10.1016/j.margeo.2013.08.005

Colina Alonso, A., van Maren, D. S., Elias, E. P. L., Holthuijsen, S. J., & Wang, Z. B. (2021). The contribution of sand and mud to infilling of tidal basins in response to a closure dam. *Marine Geology*, *439*(September). https://doi.org/10.1016/j.margeo.2021.106544

Colina Alonso, A., van Maren, D. S., Herman, P. M. J., van Weerdenburg, R. J. A., Huismans, Y., Holthuijsen, S. J., Govers, L. L., Bijleveld, A. I., & Wang, Z. B. (2022). The Existence and Origin of Multiple Equilibria in Sand-Mud Sediment Beds. *Geophysical Research Letters*, *49*(22). https://doi.org/10.1029/2022GL101141

Colina Alonso, A., van Maren, D. S., van Weerdenburg, R. J. A., Huismans, Y., & Wang, Z. B. (2023). Morphodynamic modeling of tidal basins: The role of sand-mud interaction. *Journal of Geophysical Research: Earth Surface*. https://doi.org/10.1029/2023JF007391

Colosimo, I., de Vet, P. L., van Maren, D. S., Reniers, A. J., Winterwerp, J. C., & van Prooijen, B. C. (2020). The impact of wind on flow and sediment transport over intertidal flats. *Journal of Marine Science and Engineering*, *8*(11), 1–26. https://doi.org/10.3390/jmse8110910

Compton, T. J., Holthuijsen, S., Koolhaas, A., Dekinga, A., ten Horn, J., Smith, J., Galama, Y., Brugge, M., van der Wal, D., van der Meer, J., van der Veer, H. W., & Piersma,

T. (2013). Distinctly variable mudscapes: Distribution gradients of intertidal macrofauna across the Dutch Wadden Sea. *Journal of Sea Research*, *82*(September 2013), 103–116. https://doi.org/10.1016/j.seares.2013.02.002

Cooper, J. A., Masselink, G., Coco, G., Short, A. D., Castelle, B., Rogers, K., Anthony, E., Green, A. N., Kelley, J. T., Pilkey, O. H., & Jackson, D. W. (2020). Sandy beaches can survive sea-level rise. *Nature Climate Change*, *10*(11), 993–995. https://doi.org/10.1038/s41558-020-00934-2

Dangendorf, S., Hay, C., Calafat, F. M., Marcos, M., Piecuch, C. G., Berk, K., & Jensen, J. (2019). Persistent acceleration in global sea-level rise since the 1960s. *Nature Climate Change*, *9*(9), 705–710. https://doi.org/10.1038/s41558-019-0531-8

Dastgheib, A., Roelvink, J. A., & Wang, Z. B. (2008). Long-term process-based morphological modeling of the Marsdiep Tidal Basin. *Marine Geology*, *256*(1-4), 90–100. https://doi.org/10.1016/j.margeo.2008.10.003

Dastgheib, A. (2012). *Long-term process-based morphological modeling of large tidal basins* [PhD thesis]. UNESCO-IHE Institute for Water Education.

Davis, R. A., & Hayes, M. O. (1984). What is a Wave-Dominated Coast? *Developments in Sedimentology*, *39*(100), 313–329. https://doi.org/10.1016/S0070-4571(08)70152-3

de Glopper, R. J. (1967). Over de bodemgesteldheid van het waddengebied. *Van zee tot land*, 5–61.

de Jonge, V. N., Essink, K., & Boddeke, R. (1993). The Dutch Wadden Sea: a changed ecosystem. *Hydrobiologia*, *265*(1-3), 45–71. https://doi.org/10.1007/BF00007262

de Kok, J. (2004). *Slibtransport langs de Nederlandse kust Slibtransport langs de Nederlandse kust* (tech. rep. No. december). RIKZ.

de Kruif, A. (2001). *Bodemdieptegegevens van het Nederlandse Kustsysteem* (tech. rep.). Rijkswaterstaat, National Institute for Coastal and Marine Management RIKZ. The Hague.

Deltacommissie. (1960). Rapport Deltacommissie. Deel. 1. Eindverslag en interim - adviezen (in Dutch).

de Vet, P. L. M. (2020). *Intertidal Flats in Engineered Estuaries: On the Hydrodynamics, Morphodynamics, and Implications for Ecology and System Management* [PhD thesis]. Delft University of Technology. https://doi.org/10.4233/uuid:2b392951-3781-4aed-b093-547c70cc581d

de Vet, P. L. M., van Prooijen, B. C., Schrijvershof, R. A., van der Werf, J. J., Ysebaert, T., Schrijver, M. C., & Wang, Z. B. (2018). The Importance of Combined Tidal and Meteorological Forces for the Flow and Sediment Transport on Intertidal Shoals. *Journal of Geophysical Research: Earth Surface*. https://doi.org/10.1029/2018JF004605

de Vriend, H. J. (1991). Mathematical modelling and large-scale coastal behaviour Part 1: Physical processes. *Journal of Hydraulic Research*, *29*(6), 727–740.

de Vriend, H. J., Wang, Z. B., Ysebaert, T., Herman, P. M. J., & Ding, P. (2011). Eco-morphological problems in the yangtze estuary and the western scheldt. *Wetlands*, *31*(6), 1033–1042. https://doi.org/10.1007/s13157-011-0239-7

Dijkstra, Y. M., Schuttelaars, H. M., & Schramkowski, G. P. (2019). A Regime Shift From Low to High Sediment Concentrations in a Tide-Dominated Estuary. *Geophysical Research Letters*, *46*(8), 4338–4345. https://doi.org/10.1029/2019GL082302

Dissanayake, D. M. P. K., Ranasinghe, R., & Roelvink, J. A. (2012). The morphological response of large tidal inlet/basin systems to relative sea level rise. *Climatic Change*, *113*(2), 253–276. https://doi.org/10.1007/s10584-012-0402-z

Dissanayake, D. M. P. K., Roelvink, J. A., & van der Wegen, M. (2009). Modelled channel patterns in a schematized tidal inlet. *Coastal Engineering*, *56*(11-12), 1069–1083. https://doi.org/10.1016/j.coastaleng.2009.08.008

Duran-Matute, M., Gerkema, T., Boer, G. J. D., Nauw, J. J., & Gräwe, U. (2014). Residual circulation and freshwater transport in the Dutch Wadden Sea : a numerical modelling study. *Ocean Sci.*, *10*, 611–632. https://doi.org/10.5194/os-10-611-2014

Duran-Matute, M., Gerkema, T., & Sassi, M. G. (2016). Quantifying the residual volume transport through a multiple- inlet system in response to wind forcing: The case of the western Dutch Wadden Sea. *Journal of Geophysical Research: Oceans*, 8888–8903. https://doi.org/10.1002/2016JC011807.Received

Edmonds, D. A., Paola, C., Hoyal, D. C., & Sheets, B. A. (2011). Quantitative metrics that describe river deltas and their channel networks. *Journal of Geophysical Research: Earth Surface*, *116*(4), 1–15. https://doi.org/10.1029/2010JF001955

Edmonds, D. A., & Slingerland, R. L. (2010). Significant effect of sediment cohesion on delta morphology. *Nature Geoscience*, *3*(2), 105–109. https://doi.org/10.1038/ngeo730

Elias, E. P. L., Van Der Spek, A. J. F., Wang, Z. B., & de Ronde, J. (2012). Morphodynamic development and sediment budget of the Dutch Wadden Sea over the last century. *Geologie en Mijnbouw/Netherlands Journal of Geosciences*, *91*(3), 293–310. https://doi.org/10.1017/S0016774600000457

Elias, E. P. L., & van der Spek, A. J. F. (2006). Long-term morphodynamic evolution of Texel Inlet and its ebb-tidal delta (The Netherlands). *Marine Geology*, *225*(1-4), 5–21. https://doi.org/10.1016/j.margeo.2005.09.008

Elias, E. P. L., van der Spek, A. J. F., & Lazar, M. (2016). The 'Voordelta', the contiguous ebb-tidal deltas in the SW Netherlands: Large-scale morphological changes and sediment budget 1965-2013 ; impacts of large-scale engineering. *Netherlands Journal of Geosciences*. https://doi.org/10.1017/njg.2016.37.

Elias, E. P. L. (2006). *Morphodynamics of Texel Inlet* [PhD thesis]. Delft University of Technology.

Elias, E. P. L., Stive, M. C., Bonekamp, J. G., & Cleveringa, J. (2003). Tidal Inlet Dynamics in Response To Human Intervention. *Coastal Engineering Journal*, *45*(04), 629–658. https://doi.org/10.1142/S0578563403000932

Elliott, M., Whitfield, A. K., Potter, I. C., Blaber, S. J., Cyrus, D. P., Nordlie, F. G., & Harrison, T. D. (2007). The guild approach to categorizing estuarine fish assemblages: A global review. *Fish and Fisheries*, *8*(3), 241–268. https://doi.org/10.1111/j.1467-2679.2007.00253.x

Elmilady, H., van der Wegen, M., Roelvink, D., & van der Spek, A. (2020). Morphodynamic Evolution of a Fringing Sandy Shoal: From Tidal Levees to Sea Level Rise.

Journal of Geophysical Research: Earth Surface, *125*(6), 1–21. https://doi.org/10.1029/2019JF005397

Elmilady, H., Wegen, M., Roelvink, D., & Spek, A. (2022). Modeling the Morphodynamic Response of Estuarine Intertidal Shoals to Sea-Level Rise. *Journal of Geophysical Research: Earth Surface*, *127*(1). https://doi.org/10.1029/2021JF006152

Eslami, S., Hoekstra, P., Nguyen Trung, N., Ahmed Kantoush, S., Van Binh, D., Duc Dung, D., Tran Quang, T., & van der Vegt, M. (2019). Tidal amplification and salt intrusion in the Mekong Delta driven by anthropogenic sediment starvation. *Scientific Reports*, *9*(1), 1–10. https://doi.org/10.1038/s41598-019-55018-9

Esselink, P., van Duin, W., Bunje, J., Cremer, J., Folmer, E., Frikke, J., Glahn, M., de Groot, A., Hecker, N., Hellwig, U., Jensen, K., Körber, P., Petersen, J., & Stock, M. (2017). *Wadden Sea Quality Status Report: Salt Marshes* (tech. rep.).

Eysink, W., & Biegel, E. J. (1992). *Impact of sea level rise on the morphology of the Wadden Sea in the scope of its ecological function. ISOS*2 Project, phase 2* (tech. rep.). Delft Hydraulics. Delft.

Fettweis, M., Nechad, B., & van den Eynde, D. (2007). An estimate of the suspended particulate matter (SPM) transport in the southern North Sea using SeaWiFS images, in situ measurements and numerical model results. *Continental Shelf Research*, *27*(10-11), 1568–1583. https://doi.org/10.1016/j.csr.2007.01.017

Fettweis, M., & van den Eynde, D. (2003). The mud deposits and the high turbidity in the Belgian-Dutch coastal zone, southern bight of the North Sea. *Continental Shelf Research*, *23*(7), 669–691. https://doi.org/10.1016/S0278-4343(03)00027-X

Flemming, B. W., & Nyandwi, N. (1994). Land reclamation as a cause of fine-grained sediment depletion in backbarrier tidal flats (Southern North Sea). *Netherlands Journal of Aquatic Ecology*, *28*(3-4), 299–307. https://doi.org/10.1007/BF02334198

Flemming, B. W., & Ziegler, K. (1995). High-resolution grain size distribution patterns and textural trends in the backbarrier environment of Spiekeroog Island (Southern North Sea). *Senckenberg Maritima*, *26*, 1–24.

Folmer, E. O., Bijleveld, A. I., Holthuijsen, S., van der Meer, J., Piersma, T., & van der Veer, H. W. (2023). Space–time analyses of sediment composition reveals synchronized dynamics at all intertidal flats in the Dutch Wadden Sea. *Estuarine, Coastal and Shelf Science*, *285*(February), 108308. https://doi.org/10.1016/j.ecss.2023.108308

Fredsoe, J., & Deigaard, R. (1992). *Mechanics of coastal sediment transport Vol. 3*. World scientific publishing company.

Galiforni-Silva, F., Wijnberg, K. M., & Hulscher, S. J. (2020). Storm-induced sediment supply to coastal dunes on sand flats. *Earth Surface Dynamics*, *8*(2), 335–350. https://doi.org/10.5194/esurf-8-335-2020

Geleynse, N., Storms, J. E., Walstra, D. J. R., Jagers, H. R., Wang, Z. B., & Stive, M. J. (2011). Controls on river delta formation; insights from numerical modelling. *Earth and Planetary Science Letters*, *302*(1-2), 217–226. https://doi.org/10.1016/j.epsl.2010.12.013

Gerritsen, H., Boon, J. G., Van der Kaaij, T., & Vos, R. J. (2001). Integrated modelling of suspended matter in the North Sea. *Estuarine, Coastal and Shelf Science*, *53*(4), 581–594. https://doi.org/10.1006/ecss.2000.0633

Grabemann, I., & Krause, G. (1998). Response of the turbidity maximum in the Weser Estuary to pulses in freshwater runoff and to storms. In J. Dronkers & M. Scheffers (Eds.), *Physics of estuaries and coastal seas* (pp. 83–92).

Grabemann, I., & Krause, G. (2001). On different time scales of suspended matter dynamics in the Weser estuary. *Estuaries*, *24*(5), 688–698. https://doi.org/10.2307/1352877

Grabowski, R. C., Droppo, I. G., & Wharton, G. (2011). Erodibility of cohesive sediment: The importance of sediment properties. *Earth-Science Reviews*, *105*(3-4), 101–120. https://doi.org/10.1016/j.earscirev.2011.01.008

Grasmeijer, B., Huisman, B., Luijendijk, A., Schrijvershof, R., van der Werf, J., Zijl, F., de Looff, H., & de Vries, W. (2022). Modelling of annual sand transports at the Dutch lower shoreface. *Ocean and Coastal Management*, *217*(July 2021), 105984. https://doi.org/10.1016/j.ocecoaman.2021.105984

Gräwe, U., Flöser, G., Gerkema, T., Duran□Matute, M., Badewien, T. H., Schulz, E., & Burchard, H. (2016). A numerical model for the entire Wadden Sea: Skill assessment and analysis of hydrodynamics. *Journal of Geophysical Research: Oceans*, *121*(7), 5231–5251. https://doi.org/10.1002/2016JC011655

Guo, L., van der Wegen, M., Roelvink, D. J., Wang, Z. B., & He, Q. (2015). Long-term, process-based morphodynamic modeling of a fluvio-deltaic system, part I: The role of river discharge. *Continental Shelf Research*, *109*, 95–111. https://doi.org/10.1016/j.csr.2015.09.002

Hajek, E., Edmonds, D., Millard, C., Toms, L., & Fogaren, C. (2012). Records of transient avulsion-related river patterns in ancient deposits: evidence for different styles of channel-floodplain coupling. *AGU fall meeting abstracts*.

Hebbeln, D., Scheurle, C., & Lamy, F. (2003). Depositional history of the Helgoland mud area, German Bight, North Sea. *Geo-Marine Letters*, *23*(2), 81–90. https://doi.org/10.1007/s00367-003-0127-0

Hendriks, H. C., van Prooijen, B. C., Aarninkhof, S. G., & Winterwerp, J. C. (2020). How human activities affect the fine sediment distribution in the Dutch Coastal Zone seabed. *Geomorphology*, *367*, 107314. https://doi.org/10.1016/j.geomorph.2020.107314

Herman, P. M. J., Villars, N., Winterwerp, H., van Kessel, T., Wang, Z. B., Briere, C., van Rijn, L. C., & Cleveringa, J. (2016). *Analyse Vaargeul Holwerd- Ameland. Deltares report 1230378-005* (tech. rep.). Deltares. Delft.

Herman, P. M. J., van Kessel, T., Vroom, J., Dankers, P., Cleveringa, J., de Vries, B., & Villars, N. (2018). *Mud dynamics in the Wadden Sea: Towards a conceptual model* (tech. rep.). Deltares. Delft.

Herman, P. M., Middelburg, J. J., & Heip, C. H. (2001). Benthic community structure and sediment processes on an intertidal flat: Results from the ECOFLAT project. *Continental Shelf Research*, *21*(18-19), 2055–2071. https://doi.org/10.1016/S0278-4343(01)00042-5

Herrling, G., Becker, M., Lefebvre, A., Zorndt, A., Krämer, K., & Winter, C. (2021). The effect of asymmetric dune roughness on tidal asymmetry in the Weser estuary. *Earth Surface Processes and Landforms*, *46*(11), 2211–2228. https://doi.org/10.1002/esp.5170

Hibma, A., De Vriend, H. J., & Stive, M. J. (2003). Numerical modelling of shoal pattern formation in well-mixed elongated estuaries. *Estuarine, Coastal and Shelf Science*, *57*(5-6), 981–991. https://doi.org/10.1016/S0272-7714(03)00004-0

Hijma, M., & Kooi, H. (2018a). *Bodemdaling in het kustfundament en de getijdenbekkens (deel 2): Een update, case IJmuiden en kwantificering. Deltares report 11202190-001-ZKS-0001* (tech. rep.). Deltares. Delft, the Netherlands.

Hijma, M., & Kooi, H. (2018b). *Bodemdaling in het kustfundament en de getijdenbekkens: Door geologische processen en menselijke activiteiten. Deltares report 11200538-008-ZKS-0001* (tech. rep.). Deltares. Delft, the Netherlands.

Hofstee, J. (1980). *Toelichting op de analysemethoden voor grond, gewas, water en bodemvocht* (tech. rep.). Rapport Rijksdienst voor de IJsselmeerpolders. Lelystad.

Hoitink, A. J., Nittrouer, J. A., Passalacqua, P., Shaw, J. B., Langendoen, E. J., Huismans, Y., & van Maren, D. S. (2020). Resilience of River Deltas in the Anthropocene. *Journal of Geophysical Research: Earth Surface*, *125*(3), 1–24. https://doi.org/10.1029/2019JF005201

Hollebrandse, F. A. P. (2005). *Temporal development of the tidal range in the southern North Sea* [MSc. thesis]. Delft University of Technology.

HPA & WSA. (2011). *River Elbe River Engineering and Sediment Management Concept - Review of sediment management strategy in the context of other European estuaries from a morphological perspective* (tech. rep. No. May). Hamburg Port Authority (HPA) & Federal Waterways and Shipping Administration (WSA).

Huismans, Y., van der Spek, A., Lodder, Q., Zijlstra, R., Elias, E., & Wang, Z. B. (2022). Development of intertidal flats in the Dutch Wadden Sea in response to a rising sea level: Spatial differentiation and sensitivity to the rate of sea level rise. *Ocean and Coastal Management*, *216*(February), 105969. https://doi.org/10.1016/j.ocecoaman.2021.105969

IPCC. (2021). *Climate Change 2021: The Physical Science Basis. Contribution of Working Group I to the Sixth Assessment Report of the Intergovernmental Panel Climate Change [Masson-Delmotte, V., P. Zhai, A. Pirani, S.L. Connors, C. Péan, S. Berger, N. Caud, Y. Chen*. Cambridge University Press. https://doi.org/10.1017/9781009157896

IPCC. (2022). *Climate Change 2022: Impacts, Adaptation and Vulnerability. Contribution of Working Group II to the Sixth Assessment Report of the Intergovernmental Panel on Climate Change [H.-O. Pörtner, D.C. Roberts, M. Tignor, E.S. Poloczanska, K. Mintenbeck, A. Alegr*. Cambridge University Press. Cambridge. https://doi.org/doi:10.1017/9781009325844

IPCC. (2019). *IPCC Special Report on the Ocean and Cryosphere in a Changing Climate [H.-O. Pörtner, D.C. Roberts, V. Masson-Delmotte, P. Zhai, M. Tignor, E. Poloczanska, K. Mintenbeck, A. Alegría, M. Nicolai, A. Okem, J. Petzold, B. Rama, N.M. Weyer (eds.)]* Cambridge University Press. https://doi.org/10.1017/9781009157964

IPCC. (2023). *IPCC, 2023: Climate Change 2023: Synthesis Report. Contribution of Working Groups I, II and III to the Sixth Assessment Report of the Intergovernmental Panel on Climate Change [Core Writing Team, H. Lee and J. Romero (eds.)]. IPCC, Geneva, Switzerland.* (P. Arias, M. Bustamante, I. Elgizouli, G. Flato, M. Howden, C. Méndez-Vallejo, J. J. Pereira, R. Pichs-Madruga, S. K. Rose, Y. Saheb, R. Sánchez Rodríguez, D. Ürge-Vorsatz, C. Xiao, N. Yassaa, J. Romero, J. Kim, E. F. Haites, Y. Jung, R. Stavins, … C. Péan, Eds.; tech. rep.). Intergovernmental Panel on Climate Change. https://doi.org/10.59327/IPCC/AR6-9789291691647

Jacobs, W. (2011). *Sand-mud erosion from a soil mechanical perspective* [PhD thesis]. Delft University of Technology.

Jacobs, W., Le Hir, P., van Kesteren, W., & Cann, P. (2011). Erosion threshold of sand–mud mixtures. *Continental Shelf Research*, *31*(10), S14–S25. https://doi.org/10.1016/j.csr.2010.05.012

Jordan, C., Tiede, J., Lojek, O., Visscher, J., Apel, H., Nguyen, H. Q., Quang, C. N. X., & Schlurmann, T. (2019). Sand mining in the Mekong Delta revisited - current scales of local sediment deficits. *Scientific Reports*, *9*(1), 1–14. https://doi.org/10.1038/s41598-019-53804-z

Komar, P. D. (1996). The budget of littoral sediments: concepts and applications. *Shore and Beach*, *64*(3), 18–26.

Kristensen, E., Penha-Lopes, G., Delefosse, M., Valdemarsen, T., Quintana, C. O., & Banta, G. T. (2012). What is bioturbation? the need for a precise definition for fauna in aquatic sciences. *Marine Ecology Progress Series*, *446*(February), 285–302. https://doi.org/10.3354/meps09506

Laursen, K., Bregnballe, T., Kleefstra, R., Frikke, J., Günther, K., Hornman, M., Pedersen, C. L., Blew, J., & Pape Møller, A. (2023). Regime shift and changes in sediment morphology driven by sea level rise affect abundance of migratory waders. *Journal of Ornithology*, *164*(3), 573–582. https://doi.org/10.1007/s10336-023-02056-w

Le Hir, P., Monbet, Y., & Orvain, F. (2007). Sediment erodability in sediment transport modelling: Can we account for biota effects? *Continental Shelf Research*, *27*(8), 1116–1142. https://doi.org/10.1016/j.csr.2005.11.016

Le Hir, P., Cann, P., Waeles, B., Jestin, H., & Bassoullet, P. (2008). Chapter 11 Erodibility of natural sediments: experiments on sand/mud mixtures from laboratory and field erosion tests. *Proceedings in Marine Science*, *9*, 137–153. https://doi.org/10.1016/S1568-2692(08)80013-7

Le Hir, P., Cayocca, F., & Waeles, B. (2011). Dynamics of sand and mud mixtures: A multiprocess-based modelling strategy. *Continental Shelf Research*, *31*(10 SUPPL.), 135–149. https://doi.org/10.1016/j.csr.2010.12.009

Leecaster, M. (2003). Spatial analysis of grain size in Santa Monica Bay. *Marine Environmental Research*, *56*(1-2), 67–78. https://doi.org/10.1016/S0141-1136(02)00325-2

Lely, C. (1892). Resultaten van het Technisch Onderzoek, Zuiderzee-Vereniging. Nota 1-8.

Lesser, G. R., Roelvink, J. A., van Kester, J. A., & Stelling, G. S. (2004). Development and validation of a three-dimensional morphological model. *Coastal Engineering*, *51*(8-9), 883–915. https://doi.org/10.1016/j.coastaleng.2004.07.014

Lesser, G. (2009). *An Approach to Medium-term Coastal Morphological Modelling* [Phd]. Delft University of Technology, UNESCO-IHE Institute for Water Education. http://www.narcis.nl/publication/RecordID/oai:tudelft.nl:uuid:62caa573-4fc0-428e-8768-0aa47ab612a9

Lodder, Q., & Slinger, J. (2022). The 'Research for Policy' cycle in Dutch coastal flood risk management: The Coastal Genesis 2 research programme. *Ocean and Coastal Management*, *219*(July 2021), 106066. https://doi.org/10.1016/j.ocecoaman.2022.106066

Lodder, Wang, Elias, van der Spek, de Looff, & Townend. (2019). Future Response of the Wadden Sea Tidal Basins to Relative Sea-Level rise—An Aggregated Modelling Approach. *Water*, *11*(10), 2198. https://doi.org/10.3390/w11102198

Lotze, H. K. (2007). Rise and fall of fishing and marine resource use in the Wadden Sea, southern North Sea. *Fisheries Research*, *87*(2-3), 208–218. https://doi.org/10.1016/j.fishres.2006.12.009

Luan, H. L., Ding, P. X., Wang, Z. B., Ge, J. Z., & Yang, S. L. (2016). Decadal morphological evolution of the Yangtze Estuary in response to river input changes and estuarine engineering projects. *Geomorphology*, *265*, 12–23. https://doi.org/10.1016/j.geomorph.2016.04.022

Luijendijk, A., Hagenaars, G., Ranasinghe, R., Baart, F., Donchyts, G., & Aarninkhof, S. (2018). The State of the World's Beaches. *Scientific Reports*, *8*(1). https://doi.org/10.1038/s41598-018-24630-6

Luijendijk, A. P., Ranasinghe, R., de Schipper, M. A., Huisman, B. A., Swinkels, C. M., Walstra, D. J., & Stive, M. J. (2017). The initial morphological response of the Sand Engine: A process-based modelling study. *Coastal Engineering*, *119*(November 2016), 1–14. https://doi.org/10.1016/j.coastaleng.2016.09.005

Maan, D. C., van Prooijen, B. C., & Wang, Z. B. (2018). Progradation speed of tide-dominated tidal flats decreases stronger than linearly with decreasing sediment availability and linearly with sea level rise. *Geophysical Research Letters*, 2018GL079933. https://doi.org/10.1029/2018GL079933

Manning, A. J., Baugh, J. V., Spearman, J. R., Pidduck, E. L., & Whitehouse, R. J. (2011). The settling dynamics of flocculating mud-sand mixtures: Part 1-Empirical algorithm development. *Ocean Dynamics*, *61*(2-3), 311–350. https://doi.org/10.1007/s10236-011-0394-7

Marciano, R., Wang, Z. B., Hibma, A., De Vriend, H. J., & Defina, A. (2005). Modeling of channel patterns in short tidal basins. *Journal of Geophysical Research: Earth Surface*, *110*(1), 1–13. https://doi.org/10.1029/2003JF000092

Marijs, K., & Parée, E. (2004). *Nauwkeurigheid vaklodingen Westerschelde en -monding* (tech. rep.). RIKZ.

McCave, F. N. (1973). Mud in the North Sea. *E.D. Goldberg, (ed.) North Sea Science*, (November), 75–100. https://doi.org/10.13140/2.1.1575.7769

Meiliand, E., Alfian, D., & Huhn, K. (2011). Sediment grain-size distribution analysis at the shallow sandy shelf of the North Sea using multivariate geostatistics. *Proce-*

dia Environmental Sciences, *7*, 317–322. https://doi.org/10.1016/j.proenv.2011.07.055

Mengual, B., Hir, P. L., Cayocca, F., & Garlan, T. (2017). Modelling fine sediment dynamics: Towards a common erosion law for fine sand, mud and mixtures. *Water (Switzerland)*, *9*(8). https://doi.org/10.3390/w9080564

Mentaschi, L., Vousdoukas, M. I., Pekel, J. F., Voukouvalas, E., & Feyen, L. (2018). Global long-term observations of coastal erosion and accretion. *Scientific Reports*, *8*(1), 1–11. https://doi.org/10.1038/s41598-018-30904-w

Migniot, C. (1968). Étude Des Propriétés Physiques De Différents Sédiments Très Fins Et De Leur Comportement Sous Des Actions Hydrodynamiques. *La Houille Blanche*, (7), 591–620. https://doi.org/10.1051/lhb/1968041

Migniot, C. (1989). Tassement et rhéologie des vases. Deuxième partie. *La Houille Blanche*, (2), 95–112. https://doi.org/10.1051/lhb/1989006

Milliman, J. D., & Syvitski, J. P. (1992). Geomorphic/tectonic control of sediment discharge to the ocean: the importance of small mountainous rivers. *Journal of Geology*, *100*(5), 525–544. https://doi.org/10.1086/629606

Milliman, J. D., & Farnsworth, K. L. (2011). *River Discharge to the Coastal Ocean*. Cambridge University Press. https://doi.org/10.1017/CBO9780511781247

Milliman, J. D., & Meade, R. H. (1983). World-Wide Delivery of River Sediment to the Oceans. *The Journal of Geology*, *91*(1), 1–21. https://doi.org/10.1086/628741

Minderhoud, P. S., Coumou, L., Erban, L. E., Middelkoop, H., Stouthamer, E., & Addink, E. A. (2018). The relation between land use and subsidence in the Vietnamese Mekong delta. *Science of the Total Environment*, *634*, 715–726. https://doi.org/10.1016/j.scitotenv.2018.03.372

Mitchener, H., & Torfs, H. (1996). Erosion of mud/sand mixtures. *Coastal Engineering*, *29*(1-2), 1–25. https://doi.org/10.1016/S0378-3839(96)00002-6

Monge-Ganuzas, M., Cearreta, A., & Evans, G. (2013). Morphodynamic consequences of dredging and dumping activities along the lower Oka estuary (Urdaibai Biosphere Reserve, southeastern Bay of Biscay, Spain). *Ocean and Coastal Management*, *77*, 40–49. https://doi.org/10.1016/j.ocecoaman.2012.02.006

Mora, C., McKenzie, T., Gaw, I. M., Dean, J. M., von Hammerstein, H., Knudson, T. A., Setter, R. O., Smith, C. Z., Webster, K. M., Patz, J. A., & Franklin, E. C. (2022). Over half of known human pathogenic diseases can be aggravated by climate change. *Nature Climate Change*, *12*(September). https://doi.org/10.1038/s41558-022-01426-1

Mueller, P., Ladiges, N., Jack, A., Schmiedl, G., Kutzbach, L., Jensen, K., & Nolte, S. (2019). Assessing the long-term carbon-sequestration potential of the semi-natural salt marshes in the European Wadden Sea. *Ecosphere*, *10*(1). https://doi.org/10.1002/ecs2.2556

Mulder, H. P. J. (1995). De droge dichtheid als functie van het slibgehalte t.b.v. een sedimentbalans.

Naumann, G., Cammalleri, C., Mentaschi, L., & Feyen, L. (2021). Increased economic drought impacts in Europe with anthropogenic warming. *Nature Climate Change*, *11*(6), 485–491. https://doi.org/10.1038/s41558-021-01044-3

Nederhoff, C. M., Smits, B. P., & Wang, Z. B. (2017). *KPP Waddenzee Kennisontwikkeling morfologie en baggerhoeveelheden: Data analyse hypsometrie en getij* (tech. rep.). Deltares. Delft.

Netzband, A., Reincke, H., & Bergemann, M. (2002). The River Elbe: A case study for the ecological and economical chain of sediments. *Journal of Soils and Sediments*, *2*(3), 110–116.

Nicholls, R. J., & Cazenave, A. (2010). Sea-level rise and its impact on coastal zones. *Science*, *328*(5985), 1517–1520. https://doi.org/10.1126/science.1185782

Nienhuis, J. H., Ashton, A. D., Edmonds, D. A., Hoitink, A. J., Kettner, A. J., Rowland, J. C., & Törnqvist, T. E. (2020). Global-scale human impact on delta morphology has led to net land area gain. *Nature*, *577*(7791), 514–518. https://doi.org/10.1038/s41586-019-1905-9

Nolte, S., Koppenaal, E. C., Esselink, P., Dijkema, K. S., Schuerch, M., De Groot, A. V., Bakker, J. P., & Temmerman, S. (2013). Measuring sedimentation in tidal marshes: A review on methods and their applicability in biogeomorphological studies. *Journal of Coastal Conservation*, *17*(3), 301–325. https://doi.org/10.1007/s11852-013-0238-3

Nordstrom, K. F., & Jackson, N. L. (2012). Physical processes and landforms on beaches in short fetch environments in estuaries, small lakes and reservoirs: A review. *Earth-Science Reviews*, *111*(1-2), 232–247. https://doi.org/10.1016/j.earscirev.2011.12.004

Oost, A. P. (1995). *Dynamics and sedimentary development, of the Dutch Wadden Sea with emphasis on the Frisian Inlet. A study of the barrier islands, ebb-tidal deltas, inlets and drainage basins.* [PhD thesis]. Utrecht University.

Park, N. W., & Jang, D. H. (2014). Comparison of geostatistical kriging algorithms for intertidal surface sediment facies mapping with grain size data. *The Scientific World Journal*, *2014*. https://doi.org/10.1155/2014/145824

Partheniades, E. (1965). Erosion and deposition of cohesive soils. *Journal of the Hydraulics Division*, *91*(1), 105–139.

Pearson, S. (2022). *Sediment Pathways on Ebb-Tidal Deltas. New Tools and Techniques for Analysis* [PhD thesis]. Delft University of Technology. https://doi.org/https://doi.org/10.4233/uuid:c2fe811c-dc2e-4e1f-bb0c-dc43f11cd1eb

Pearson, S. G., Verney, R., van Prooijen, B. C., Tran, D., Hendriks, E. C., Jacquet, M., & Wang, Z. B. (2021). Characterizing the Composition of Sand and Mud Suspensions in Coastal and Estuarine Environments Using Combined Optical and Acoustic Measurements. *Journal of Geophysical Research: Oceans*, *126*(7), 1–23. https://doi.org/10.1029/2021JC017354

Pedersen, J. B., & Bartholdy, J. (2006). Budgets for fine-grained sediment in the Danish Wadden Sea. *Marine Geology*, *235*(1-4 SPEC. ISS.), 101–117. https://doi.org/10.1016/j.margeo.2006.10.008

Perluka, R., Wiegmann, E., Jordans, R., & Swart, L. (2006). *Opnametechnieken Waddenzee* (tech. rep.). Rijkswaterstaat.

Piekhaar, R., & Kort, M. (1983). *Haringvliet monding - Sedimentatieonderzoek 1970-1981* (tech. rep.). Rijkswaterstaat Deltadienst. The Hague.

Pierik, H. J., Leuven, J. R. F. W., Busschers, F. S., Hijma, M. P., & Kleinhans, M. G. (2023). Depth‐limiting resistant layers restrict dimensions and positions of estuarine channels and bars. *The Depositional Record*, *9*(2), 213–232. https://doi.org/10.1002/dep2.184

Pietrzak, J. D., de Boer, G. J., & Eleveld, M. A. (2011). Mechanisms controlling the intra-annual mesoscale variability of SST and SPM in the southern North Sea. *Continental Shelf Research*, *31*(6), 594–610. https://doi.org/10.1016/j.csr.2010.12.014

Pörtner, H. O., Scholes, R. J., Agard, J., Archer, E., Arneth, A., Bai, X., Barnes, D., Burrows, M., Chan, L., Cheung, W. L., Diamond, S., Donatti, C., Duarte, C., Eisenhauer, F., Foden, W., Gasalla, M. A., Handa, C., Hickler, T., Hoegh-Guldberg, O., … Ngo, H. T. (2021). Scientific outcome of the IPBES-IPCC co-sponsored workshop on biodiversity and climate change. *IPEBS secretariat, Bonn, Germany*. https://doi.org/10.5281/zenodo.4659158.IPBES

Pörtner, H. O., Scholes, R. J., Arneth, A., Barnes, D. K., Burrows, M. T., Diamond, S. E., Duarte, C. M., Kiessling, W., Leadley, P., Managi, S., McElwee, P., Midgley, G., Ngo, H. T., Obura, D., Pascual, U., Sankaran, M., Shin, Y. J., & Val, A. L. (2023). Overcoming the coupled climate and biodiversity crises and their societal impacts. *Science (New York, N.Y.)*, *380*(6642), eabl4881. https://doi.org/10.1126/science.abl4881

Postma, H. (1954). *Hydrography of the Dutch Wadden Sea: a study of the relations between water movement, the transport of suspended materials and the production of organic matter* [PhD thesis]. Rijksuniversiteit Groningen.

Prandle, D., Loch, S. G., & Player, R. (1993). Tidal Flow through the Straits of Dover. *Journal of Physical Oceanography*, *23*(1), 23–37. https://doi.org/10.1175/1520-0485(1993)023<0023:TFTTSO>2.0.CO;2

Puls, W., Heinrich, H., & Mayer, B. (1997). Suspended particulate matter budget for the German Bight. *Marine Pollution Bulletin*, *34*(6), 398–409. https://doi.org/10.1016/S0025-326X(96)00161-0

Raff, J. L., Goodbred, S. L., Pickering, J. L., Sincavage, R. S., Ayers, J. C., Hossain, M. S., Wilson, C. A., Paola, C., Steckler, M. S., Mondal, D. R., Grimaud, J. L., Grall, C. J., Rogers, K. G., Ahmed, K. M., Akhter, S. H., Carlson, B. N., Chamberlain, E. L., Dejter, M., Gilligan, J. M., … Williams, L. A. (2023). Sediment delivery to sustain the Ganges-Brahmaputra delta under climate change and anthropogenic impacts. *Nature Communications*, *14*(1), 1–13. https://doi.org/10.1038/s41467-023-38057-9

Rahdarian, A., Bryan, K. R., & Van Der Wegen, M. (2022). On the Influence of Antecedent Morphology on Development of Equilibrium Bathymetry in Estuaries Past and Future. *Journal of Geophysical Research: Earth Surface*, *127*(8), 1–18. https://doi.org/10.1029/2022JF006621

Ranasinghe, R., Duong, T. M., Uhlenbrook, S., Roelvink, D., & Stive, M. (2013). Climate-change impact assessment for inlet-interrupted coastlines. *Nature Climate Change*, *3*(1), 83–87. https://doi.org/10.1038/nclimate1664

Ridderinkhof, H. (1988). Tidal and residual flows in the Western Dutch Wadden Sea I: Numerical model results. *Netherlands Journal of Sea Research*, *22*(1), 1–21. https://doi.org/10.1016/0077-7579(88)90049-X

Ridderinkhof, W., de Swart, H. E., van der Vegt, M., Alebregtse, N. C., & Hoekstra, P. (2014). Geometry of tidal inlet systems: A key factor for the net sediment transport in tidal inlets. *Journal of Geophysical Research: Oceans*, *119*(10), 6988–7006. https://doi.org/10.1002/2014JC010226

Rijkswaterstaat. (1998). Sedimentatlas Waddenzee (CD-Rom). https://svn.oss.deltares.nl/repos/openearthrawdata/trunk/rijkswaterstaat/

Rijkswaterstaat. (2023). Vaklodingen bathymetry request page [Dataset]. www.rijkswaterstaat.nl/formulieren/contactformulier-servicedesk-data

Rosati, J. D. (2005). Concepts in sediment budgets. *Journal of Coastal Research*, *21*(2), 307–322. https://doi.org/10.2112/02-475A.1

Rough years ahead. (2023). *Nature Climate Change*, *13*(7), 589–589. https://doi.org/10.1038/s41558-023-01745-x

Roughan, M. (2021). Gaussian_mixture_model.m, MATLAB Central File Exchange. Retrieved June 14, 2021, from https://www.mathworks.com/matlabcentral/fileexchange/24867-gaussian%7B%5C_%7Dmixture%7B%5C_%7Dmodel-m

Sanford, L. P., & Halka, J. P. (1993). Assessing the paradigm of mutually exclusive erosion and deposition of mud, with examples from upper Chesapeake Bay. *Marine Geology*, *114*(1-2), 37–57. https://doi.org/10.1016/0025-3227(93)90038-W

Schindler, R. J., Parsons, D. R., Ye, L., Hope, J. A., Baas, J. H., Peakall, J., Manning, A. J., Aspden, R. J., Malarkey, J., Simmons, S., Paterson, D. M., Lichtman, I. D., Davies, A. G., Thorne, P. D., & Bass, S. J. (2015). Sticky stuff: Redefining bedform prediction in modern and ancient environments. *Geology*, *43*(5), 399–402. https://doi.org/10.1130/G36262.1

Schoorl, H. (1999). *De convexe kustboog Texel-Vlieland-Terschelling: bijdragen tot de kennis van het westelijk Waddengebied en de eilanden Texel, Vlieland en Terschelling: 1. Het westelijk Waddengebied en het eiland Texel tot circa 1550 (in Dutch)*. Pirola.

Schoorl, H. (2000a). *De convexe kustboog Texel-Vlieland-Terschelling: bijdragen tot de kennis van het westelijk Waddengebied en de eilanden Texel, Vlieland en Terschelling: 2. Het Westelijk Waddengebied en het Eiland van Texel vanaf circa 1550 (in Dutch)*. Pirola.

Schoorl, H. (2000b). *De convexe kustboog Texel-Vlieland-Terschelling: bijdragen tot de kennis van het westelijk Waddengebied en de eilanden Texel, Vlieland en Terschelling: 3. Vlieland (in Dutch)*. Pirola.

Schoorl, H. (2000c). *De convexe kustboog Texel-Vlieland-Terschelling: bijdragen tot de kennis van het westelijk Waddengebied en de eilanden Texel, Vlieland en Terschelling: 4. Terschelling (in Dutch)*. Pirola.

Schoorl, H. (1973). *Zeshonderd Jaar Water en Land: bijdrage tot de historische geoen hydrografie van de Kop van Noord-Holland in de periode 1150-1750 (in Dutch)*. Wolters-Noordhoff.

Schrijvershof, R. A., van Maren, D. S., Torfs, P. J. J. F., & Hoitink, A. J. F. (2023). A Synthetic Spring-Neap Tidal Cycle for Long-Term Morphodynamic Models. *Journal of Geophysical Research: Earth Surface*, *128*(3). https://doi.org/10.1029/2022JF006799

Schwanghart, W. (2022). Experimental (Semi-) Variogram, MATLAB Central File Exchange. Retrieved February 2, 2022, from https://www.mathworks.com/matlabcentral/fileexchange/20355-experimental-semi-variogram

Sievers, J., Milbradt, P., Ihde, R., Valerius, J., Hagen, R., & Plüß, A. (2021). An integrated marine data collection for the German Bight - Part 1: Subaqueous geomorphology and surface sedimentology (1996-2016). *Earth System Science Data*, *13*(8), 4053–4065. https://doi.org/10.5194/essd-13-4053-2021

Singer, A., Bijleveld, A. I., Hahner, F., Holthuijsen, S. J., Hubert, K., Kerimoglu, O., Kleine Schaars, L., Kröncke, I., Lettmann, K. A., Rittweg, T., Scheiffarth, G., van der Veer, H. W., & Wurpts, A. (2023). Long-term response of coastal macrofauna communities to de-eutrophication and sea level rise mediated habitat changes (1980s versus 2018). *Frontiers in Marine Science*, *9*(February), 1–20. https://doi.org/10.3389/fmars.2022.963325

Smits, B., Vroom, J., van Weerdenburg, R. J. A., & Colina Alonso, A. (2022). *Morfologie en Onderhoud Vaargeul Boontjes. Deltares report 11208040-004-ZKS-0004* (tech. rep.). Deltares. Delft, the Netherlands.

Soulsby, R. L., & Clarke, S. (2005). *Bed Shear-stresses Under Combined Waves and Currents on Smooth and Rough Beds (TR 137)* (tech. rep.). HR Wallingford.

Spearman, J. R., Manning, A. J., & Whitehouse, R. J. (2011). The settling dynamics of flocculating mud and sand mixtures: Part 2-numerical modelling. *Ocean Dynamics*, *61*(2-3), 351–370. https://doi.org/10.1007/s10236-011-0385-8

Sundermann, J. (1993). Suspended particulate matter in the North Sea: field observations and model simulations. *Philosophical Transactions of the Royal Society of London. Series A: Physical and Engineering Sciences*, *343*(1669), 423–430. https://doi.org/10.1098/rsta.1993.0056

Syvitski, J. P. M., Vo, C. J., Kettner, A. J., & Green, P. (2005). Impact of human on the flux of terrestrial sediment to the global coastal ocean. *Science*, *308*(April), 376–381.

Syvitski, J. P., Kettner, A. J., Overeem, I., Hutton, E. W., Hannon, M. T., Brakenridge, G. R., Day, J., Vörösmarty, C., Saito, Y., Giosan, L., & Nicholls, R. J. (2009). Sinking deltas due to human activities. *Nature Geoscience*, *2*(10), 681–686. https://doi.org/10.1038/ngeo629

Tejedor, A., Longjas, A., Zaliapin, I., & Foufoula-Georgiou, E. (2015). Delta channel networks: 2. Metrics of topologic and dynamic complexity for delta comparison, physical inference, and vulnerability assessment. *Water Resources Research*, *51*(6), 4019–4045. https://doi.org/10.1002/2014WR016604

Temmerman, S., Meire, P., Bouma, T. J., Herman, P. M., Ysebaert, T., & De Vriend, H. J. (2013). Ecosystem-based coastal defence in the face of global change. *Nature*, *504*(7478), 79–83. https://doi.org/10.1038/nature12859

Terwindt, J., & Breusers, H. (1972). Experiments on the Origin of Flaser, Lenticular and Sand-Clay Alternating Bedding. *Sedimentology*, *19*, 85–97. https://doi.org/https://doi.org/10.1111/j.1365-3091.1972.tb00237.x

Timmerman, A., Haasnoot, M., Middelkoop, H., Bouma, T., & McEvoy, S. (2021). Ecological consequences of sea level rise and flood protection strategies in shallow coastal systems: A quick-scan barcoding approach. *Ocean and Coastal Management*, *210*, 105674. https://doi.org/10.1016/j.ocecoaman.2021.105674

Toimil, A., Losada, I. J., Álvarez-Cuesta, M., & Le Cozannet, G. (2023). Demonstrating the value of beaches for adaptation to future coastal flood risk. *Nature Communications*, *14*(1), 1–11. https://doi.org/10.1038/s41467-023-39168-z

Torfs, H. (1995). *Erosion of mud/sand mixtures* [PhD thesis]. University of Leuven.

Torfs, H., Mitchener, H., Huysentruyt, H., & Toorman, E. (1996). Settling and consolidation of mud/sand mixtures. *Coastal Engineering*, *29*(1-2), 27–45. https://doi.org/10.1016/S0378-3839(96)00013-0

UNESCO. (2020). *UNESCO Marine World Heritage: Custodians of the globe's blue carbon assets*.

van der Spek, A. J. (1995). Reconstruction of tidal inlet and channel dimensions in the Frisian Middelzee, a former tidal basin in the Dutch Wadden Sea. *Tidal signatures in modern and ancient sediments*, (January 1995), 239–258. https://doi.org/10.1002/9781444304138.ch16

van der Wal, D., van Kessel, T., Eleveld, M. A., & Vanlede, J. (2010a). Spatial heterogeneity in estuarine mud dynamics. *Ocean Dynamics*, *60*(3), 519–533. https://doi.org/10.1007/s10236-010-0271-9

van der Wal, D., Wielemaker-van den Dool, A., & Herman, P. M. (2010b). Spatial synchrony in intertidal benthic algal biomass in temperate coastal and estuarine ecosystems. *Ecosystems*, *13*(2), 338–351. https://doi.org/10.1007/s10021-010-9322-9

van der Wegen, M., & Roelvink, J. A. (2008). Long-term morphodynamic evolution of a tidal embayment using a two-dimensional, process-based model. *Journal of Geophysical Research*, *113*(C3), C03016. https://doi.org/10.1029/2006JC003983

van Alphen, J. S. (1990). A mud balance for Belgian-Dutch coastal waters between 1969 and 1986. *Netherlands Journal of Sea Research*, *25*(1-2), 19–30. https://doi.org/10.1016/0077-7579(90)90005-2

van Dreumel, P. F. (1995). *Slib- en zandbeweging in het noordelijk Deltabekken in de periode 1982-1992 (in Dutch)* (tech. rep.). Ministerie van Verkeer en Waterstaat, Directie Zuid-Holland, Afdeling Watersysteemkennis. Rotterdam.

van Kessel, T., Spruyt-de Boer, A., van der Werf, J., Sittoni, L., van Prooijen, B. C., & Winterwerp, H. (2012). *Bed module for sand-mud mixtures. Deltares report 1200327-000-ZKS-0013* (tech. rep.). Delft, the Netherlands.

van Ledden, M. (2003). *Sand-mud segregation in estuaries and tidal basins* [PhD thesis]. Delft University of Technology.

van Ledden, M., van Kesteren, W. G., & Winterwerp, J. C. (2004a). A conceptual framework for the erosion behaviour of sand-mud mixtures. *Continental Shelf Research*, *24*(1), 1–11. https://doi.org/10.1016/j.csr.2003.09.002

van Ledden, M., Wang, Z. B., Winterwerp, H., & de Vriend, H. (2006). Modelling sand-mud morphodynamics in the Friesche Zeegat. *Ocean Dynamics*, *56*(3-4), 248–265. https://doi.org/10.1007/s10236-005-0055-9

van Ledden, M., Wang, Z. B., Winterwerp, H., & de Vriend, H. (2004b). Sand-mud morphodynamics in a short tidal basin. *Ocean Dynamics*, *54*(3-4), 385–391. https://doi.org/10.1007/s10236-003-0050-y

van Maren, D. S., Colina Alonso, A., Engels, A., Vandenbruwaene, W., de Vet, P. L., Vroom, J., & Wang, Z. B. (2023). Adaptation timescales of estuarine systems

to human interventions. *Frontiers in Earth Science*, *11*(February), 1–18. https://doi.org/10.3389/feart.2023.1111530

van Maren, D. S., Oost, A. P., Wang, Z. B., & Vos, P. C. (2016). The effect of land reclamations and sediment extraction on the suspended sediment concentration in the Ems Estuary. *Marine Geology*, *376*, 147–157. https://doi.org/10.1016/j.margeo.2016.03.007

van Maren, D. S., Vroom, J., Fettweis, M., & Vanlede, J. (2020). Formation of the Zeebrugge coastal turbidity maximum: The role of uncertainty in near-bed exchange processes. *Marine Geology*, *425*(April), 106186. https://doi.org/10.1016/j.margeo.2020.106186

van Maren, D. S., Winterwerp, J. C., & Vroom, J. (2015). Fine sediment transport into the hyper-turbid lower Ems River: the role of channel deepening and sediment-induced drag reduction. *Ocean Dynamics*, *65*(4), 589–605. https://doi.org/10.1007/s10236-015-0821-2

van Raaphorst, W., Philippart, C. J., Smit, J. P., Dijkstra, F. J., & Malschaert, J. F. (1998). Distribution of suspended particulate matter in the North Sea as inferred from NOAA/AVHRR reflectance images and in situ observations. *Journal of Sea Research*, *39*(3-4), 197–215. https://doi.org/10.1016/S1385-1101(98)00006-9

van Rijn, L. C. (1993). *Principles of Sediment Transport in Rivers, Estuaries and Coastal Seas*. Aqua Publications.

van Rijn, L. C., Riethmueller, R., & Barth, R. (2018). *Erodibility of Sand-Mud mixtures* (tech. rep.). https://www.leovanrijn-sediment.com/papers/Reporterodibilitymudsand2018.pdf

van Rijn, L. C. (2020). Erodibility of Mud-Sand Bed Mixtures. *Journal of Hydraulic Engineering*, *146*(1), 1–19. https://doi.org/10.1061/(ASCE)HY.1943-7900.0001677

van Rijn, L. C. (2007a). Unified View of Sediment Transport by Currents and Waves. I: Initiation of Motion, Bed Roughness, and Bed-Load Transport. *Journal of Hydraulic Engineering*, *133*(7), 761–775. https://doi.org/10.1061/(asce)0733-9429(2007)133:7(761)

van Rijn, L. C. (2007b). Unified View of Sediment Transport by Currents and Waves. II: Suspended Transport. *Journal of Hydraulic Engineering*, *133*(6), 668–689. https://doi.org/10.1061/(asce)0733-9429(2007)133:6(668)

van Rijn, L. C., & Barth, R. (2019). Settling and consolidation of soft mud-sand layers. *Journal of Waterway, Port, Coastal and Ocean Engineering*, *145*(1). https://doi.org/10.1061/(ASCE)WW.1943-5460.0000483

van Roomen, M., Laursen, K., van Turnhout, C., van Winden, E., Blew, J., Eskildsen, K., Günther, K., Hälterlein, B., Kleefstra, R., Potel, P., Schrader, S., Luerssen, G., & Ens, B. J. (2012). Signals from the Wadden sea: Population declines dominate among waterbirds depending on intertidal mudflats. *Ocean and Coastal Management*, *68*, 79–88. https://doi.org/10.1016/j.ocecoaman.2012.04.004

van Straaten, L. M. J. U., & Kuenen, P. H. (1957). Accumulation of Fine Grained Sediments in the Dutch Wadden Sea. *Geologie en Mijnbouw*, *19*(1954), 329–354.

van Weerdenburg, R., Pearson, S. G., van Prooijen, B., Laan, S., Elias, E., Tonnon, P.-K., & Wang, Z. B. (2021). Field measurements and numerical modelling of wind-driven exchange flows in a tidal inlet system in the Dutch Wadden Sea. *Ocean*

and Coastal Management, *215*(October), 105941. https://doi.org/10.1016/j.ocecoaman.2021.105941

Vermeersen, B. L., Slangen, A. B., Gerkema, T., Baart, F., Cohen, K. M., Dangendorf, S., Duran-Matute, M., Frederikse, T., Grinsted, A., Hijma, M. P., Jevrejeva, S., Kiden, P., Kleinherenbrink, M., Meijles, E. W., Palmer, M. D., Rietbroek, R., Riva, R. E., Schulz, E., Slobbe, D. C., … Van Der Wegen, M. (2018). Sea-level change in the Dutch Wadden Sea. *Geologie en Mijnbouw/Netherlands Journal of Geosciences*, *97*(3), 79–127. https://doi.org/10.1017/njg.2018.7

Vollmer, M., Guldberg, M., Maluck, M., Marrewijk, D., & Schlicksbier, G. (2001). *Landscape and Cultural Heritage in the Wadden Sea Region – Project Report. Wadden Sea Ecosystem No. 12.* (tech. rep.). Common Wadden Sea Secretariat. Wilhelmshaven, Germany.

Vörösmarty, C. J., Meybeck, M., Fekete, B., Sharma, K., Green, P., & Syvitski, J. P. (2003). Anthropogenic sediment retention: Major global impact from registered river impoundments. *Global and Planetary Change*, *39*(1-2), 169–190. https://doi.org/10.1016/S0921-8181(03)00023-7

Vousdoukas, M. I., Ranasinghe, R., Mentaschi, L., Plomaritis, T. A., Athanasiou, P., Luijendijk, A., & Feyen, L. (2020). Sandy coastlines under threat of erosion. *Nature Climate Change*, *10*(3), 260–263. https://doi.org/10.1038/s41558-020-0697-0

Vroom, J., de Vries, B., Dankers, P., & van Maren, D. S. (2022). *Cumulatieve effecten baggeren en verspreiden op habitattype H1130 in het Eems estuarium. Deel 1: Abiotische effecten* (tech. rep.). Deltares. Delft, the Netherlands.

Wahl, T., Haigh, I. D., Woodworth, P. L., Albrecht, F., Dillingh, D., Jensen, J., Nicholls, R. J., Weisse, R., & Wöppelmann, G. (2013). Observed mean sea level changes around the North Sea coastline from 1800 to present. *Earth-Science Reviews*, *124*, 51–67. https://doi.org/10.1016/j.earscirev.2013.05.003

Walling, D. E., & Webb, B. W. (1996). Erosion and sediment yield: A global overview. Series of Proceedings and Reports-Intern Assoc Hydrological Sciences. *IAHS-AISH Publication*, *236*(236), 3–19.

Wang, Y., Yu, Q., & Gao, S. (2014a). Modeling interrelationships between morphological evolution and grain-size trends in back-barrier tidal basins of the East Frisian Wadden Sea. *Geo-Marine Letters*, *34*(1), 37–49. https://doi.org/10.1007/s00367-013-0349-8

Wang, Y., Yu, Q., Gao, S., & Flemming, B. (2014b). Modeling the effect of progressive grain-size sorting on the scale dependence of back-barrier tidal basin morphology. *Continental Shelf Research*, *91*, 26–36. https://doi.org/10.1016/j.csr.2014.09.006

Wang, Z. B., Hoekstra, P., Burchard, H., Ridderinkhof, H., de Swart, H. E., & Stive, M. J. F. (2012). Morphodynamics of the Wadden Sea and its barrier island system. *Ocean and Coastal Management*, *68*, 39–57. https://doi.org/10.1016/j.ocecoaman.2011.12.022

Wang, Z. B., & van der Spek, A. J. F. (2015). Importance of mud for morphological response of tidal basins to sea-level rise. In J. C. P. Wang, J.D. Rosati (Ed.), *The proceedings of the coastal sediments 2015* (pp. 11–14). WORLD SCIENTIFIC. https://doi.org/10.1142/9789814689977_0208

Wang, Z. B., van Maren, D. S., Ding, P. X., Yang, S. L., van Prooijen, B. C., de Vet, P., Winterwerp, J. C., de Vriend, H. J., Stive, M. J. F., & He, Q. (2015). Human impacts on morphodynamic thresholds in estuarine systems. *Continental Shelf Research*, *111*, 174–183. https://doi.org/10.1016/j.csr.2015.08.009

Wang, Z. B., Elias, E. P. L., Van der Spek, A. J. F., & Lodder, Q. (2018). Sediment budget and morphological development of the Dutch Wadden Sea: impact of accelerated sea-level rise and subsidence until 2100. *Netherlands Journal of Geosciences — Geologie en Mijnbouw*, 1–32.

Wehrmann, A. (2016). Wadden Sea. https://doi.org/10.1007/978-94-007-6238-1_143

Weilbeer, H., & Uliczka, I. (2019). *Unterbringung von Baggergut in den Bereich der Ausschließlichen Wirtschaftszone AWZ. BAW-report B3955030610003* (tech. rep.). Bundesanstalt für Wasserbau (BAW).

Wiegmann, E., Perluka, R., Oude Elberink, S., & Vogelzang, J. (2005). *Vaklodingen: de inwintechnieken en hun combinaties. Vergelijking tussen verschillende inwintechnieken en de combinaties ervan. Rapportnummer AGI-2005-GSMH-012* (tech. rep.). Rijkswaterstaat.

Wijnberg, K. M. (1995). *Morphologic Behavior of a Barred Coast over a Period of Decades* [PhD thesis]. Utrecht University.

Willemsen, P. W., Smits, B. P., Borsje, B. W., Herman, P. M., Dijkstra, J. T., Bouma, T. J., & Hulscher, S. J. (2022). Modeling Decadal Salt Marsh Development: Variability of the Salt Marsh Edge Under Influence of Waves and Sediment Availability. *Water Resources Research*, *58*(1), 1–23. https://doi.org/10.1029/2020WR028962

Williams, J. R., Dellapenna, T. M., & Lee, G.-h. (2013). Shifts in depositional environments as a natural response to anthropogenic alterations: Nakdong Estuary, South Korea. *Marine Geology*, *343*, 47–61. https://doi.org/10.1016/j.margeo.2013.05.010

Williams, J. R., Dellapenna, T. M., Lee, G.-h., & Louchouarn, P. (2014). Sedimentary impacts of anthropogenic alterations on the Yeongsan Estuary, South Korea. *Marine Geology*, *357*, 256–271. https://doi.org/10.1016/j.margeo.2014.08.004

Winterwerp, J. C. (2007). On the sedimentation rate of cohesive sediment. *7th International conference on Estuarine and coastal fine sediments dynamics, Gloucester Point, Virginia, USA*, *8*, 209–226. http://dx.doi.org/10.1016/S1568-2692(07)80014-3

Winterwerp, J. C., & van Kesteren, W. G. M. (2004). *Introduction to the physics of cohesive sediment in the marine environment*. Elsevier.

Winterwerp, J. C., van Kessel, T., van Maren, D. S., & van Prooijen, B. C. (2021, December). *Fine sediment in open water: from fundamentals to modeling* (Vol. 55). WORLD SCIENTIFIC. https://doi.org/10.1142/12473

Winterwerp, J. C., & Wang, Z. B. (2013). Man-induced regime shifts in small estuaries - I: Theory. *Ocean Dynamics*, *63*(11-12), 1279–1292. https://doi.org/10.1007/s10236-013-0662-9

Yang, S. L., Li, H., Ysebaert, T., Bouma, T. J., Zhang, W. X., Wang, Y. Y., Li, P., Li, M., & Ding, P. X. (2008). Spatial and temporal variations in sediment grain size in tidal wetlands, Yangtze Delta: On the role of physical and biotic controls. *Estuarine,*

Coastal and Shelf Science, *77*(4), 657–671. https://doi.org/10.1016/j.ecss.2007.10.024

Yang, S. L., Milliman, J. D., Li, P., & Xu, K. (2011). 50,000 dams later: Erosion of the Yangtze River and its delta. *Global and Planetary Change*, *75*(1-2), 14–20. https://doi.org/10.1016/j.gloplacha.2010.09.006

Yao, P., Hu, Z., Su, M., Chen, Y., & Ou, S. (2018). Erosion Behavior of Sand-silt Mixtures: The Role of Silt Content. *Journal of Coastal Research*, *85*(October), 1171–1175. https://doi.org/10.2112/SI85-235.1

Ysebaert, T., Meire, P., Herman, P. M., & Verbeek, H. (2002). Macrobenthic species response surfaces along estuarine gradients: Prediction by logistic regression. *Marine Ecology Progress Series*, *225*(June 2014), 79–95. https://doi.org/10.3354/meps225079

Yu, Q., Wang, Y., Flemming, B., & Gao, S. (2014). Scale-dependent characteristics of equilibrium morphology of tidal basins along the Dutch-German North Sea Coast. *Marine Geology*, *348*, 63–72. https://doi.org/10.1016/j.margeo.2013.12.005

Zagwijn, W. H. (1986). *Nederland in het Holoceen* (tech. rep.). Rijks Geologische Dienst. Haarlem.

Zhou, Z., Liu, Q., Fan, D., Coco, G., Gong, Z., Möller, I., Xu, F., Townend, I., & Zhang, C. (2021). Simulating the role of tides and sediment characteristics on tidal flat sorting and bedding dynamics. *Earth Surface Processes and Landforms*, *46*(11), 2163–2176. https://doi.org/10.1002/esp.5166

Zhou, Z., Wu, Y., Fan, D., Wu, G., Luo, F., Yao, P., Gong, Z., & Coco, G. (2022). Sediment sorting and bedding dynamics of tidal flat wetlands: Modeling the signature of storms. *Journal of Hydrology*, *610*(December 2021), 127913. https://doi.org/10.1016/j.jhydrol.2022.127913

Zhu, Z., Vuik, V., Visser, P. J., Soens, T., van Wesenbeeck, B., van de Koppel, J., Jonkman, S. N., Temmerman, S., & Bouma, T. J. (2020). Historic storms and the hidden value of coastal wetlands for nature-based flood defence. *Nature Sustainability*, *3*(10), 853–862. https://doi.org/10.1038/s41893-020-0556-z

Zijl, F., Verlaan, M., & Gerritsen, H. (2013). Improved water-level forecasting for the Northwest European Shelf and North Sea through direct modelling of tide, surge and non-linear interaction Topical Collection on the 16th biennial workshop of the Joint Numerical Sea Modelling Group (JONSMOD) in Bre. *Ocean Dynamics*, *63*(7), 823–847. https://doi.org/10.1007/s10236-013-0624-2

Zwarts, L. (2004). *Bodemgesteldheid en mechanische kokkelvisserij in de Waddenzee. Rapport RIZA/2004.028* (tech. rep.). RIZA, Ministerie van Verkeer en Waterstaat.

Appendices

A

SUPPORTING INFORMATION FOR CHAPTER 3

This appendix has been submitted as supporting information for the following article:

Colina Alonso, A., van Maren, D. S., Oost, A. P., Esselink, P., Hagen, R., Kösters, F., Bartholdy, J., Bijleveld, A. I., & Wang, Z. B. (conditionally accepted). A mud budget of the Wadden Sea and its implications for sediment management.

Table A.1: Mud sedimentation in the basins (excluding salt marshes). These results are derived from our calculations based on 20 years of observations (1996–2015), except for those of basins 37–39 which are based on literature (Pedersen & Bartholdy, 2006). We account for an uncertainty range of 40% total in every basin.

Basin number	**Basin name**	S_{mud} **[ton/year]**
1	Marsdiep	159,050
2	Eijerlandse Gat	-15,940
3	Vlie	656,710
4	Borndiep	119,734
5	Pinkegat	13,621
6	Zoutkamperlaag	89,730
7	Eilanderbalg	358
8	Lauwers	-7,576
9	Schild	-7,552
10	Ems-Dollard	532,559
11	Osterems	346,286
12	Norderneyer Seegat	274,429
13	Wichter Ee	53,533
14	Accumer Ee	454,713
15	Otzumer Balje	298,239
16	Harle	144,641
17	Blaue Balje	69,667
18	Jade / Jadebusen	670,928
19	Weser	723,582
20	Robinbalje	370,039
21	Westertill / Nordertill	278,510
22	Elbe	930,934
23	Schatzkammer	46,596
24	Neufahrwasser	92,097
25	Flackstrom	26,010
26	Piep / Meldorfer Bucht	671,972
27	Wesselburener Loch	224,575
28	Eidermündung	59,612
29	Tümlauer Bucht	4,892
30	Norderhever- Heverstrom	148,405
31	Rummeloch West	3,038
32	Hoogeloch	1,678
33	Süderaue	161,320
34	Norderaue	33,980
35	Hörnum Tief	149,491
36	Lister Tief	118,661
37	Jyvre Dyb	6,200
38	Knude Dyb	16,870
39	Graadyb	28,150

Table A.2: Mud sedimentation in the Wadden Sea salt marshes, specified for eight sections and the three salt marsh types. The basin numbers refer to the bordering subdivision of the Wadden Sea, as specified in Figure 3.1. We also show the areal extent of the marshes and the average surface elevation change (SEC). We account for an uncertainty range of 40% in the salt marsh sinks.

Section name	Basin numbers	Marsh type	Area [km²]	SEC [mm/year]	S_{mud} [ton/year]
Netherlands	1-7	barrier	43.55	3.2	28,848
Netherlands	1-7	foreland	22.35	17.0	277,364
Ems-Dollard	9-10	barrier	7.40	2.8	4,258
Ems-Dollard	8-10	foreland	13.95	9.7	98,780
Ems-Dollard	10	foreland	11.85	6.5	65,242
Ems-Dollard	10	hallig	0.50	3.0	1,276
Lower Saxony	11-17	barrier	28.95	2.8	16,660
Lower Saxony	11-17	foreland	21.75	18.2	323,924
Jade	18	barrier	3.20	2.8	1,841
Jade	18	foreland	17.95	17	229,320
Weser	19-21	barrier	1.65	3.5	1,195
Weser	19-21	foreland	12.15	16	174,960
Elbe	22-26	barrier	3.05	3.7	2,349
Elbe	22-26	foreland	37.85	2.6	106,837
Schleswig-Holstein	27-35	barrier	23.55	2.8	13,650
Schleswig-Holstein	27-35	foreland	50.90	5.6	260,776
Schleswig-Holstein	27-35	hallig	21.75	2.2	30,735
Denmark	36-39	barrier	46.20	2.8	70,603
Denmark	36-39	foreland	25.20	5.6	129,107

A

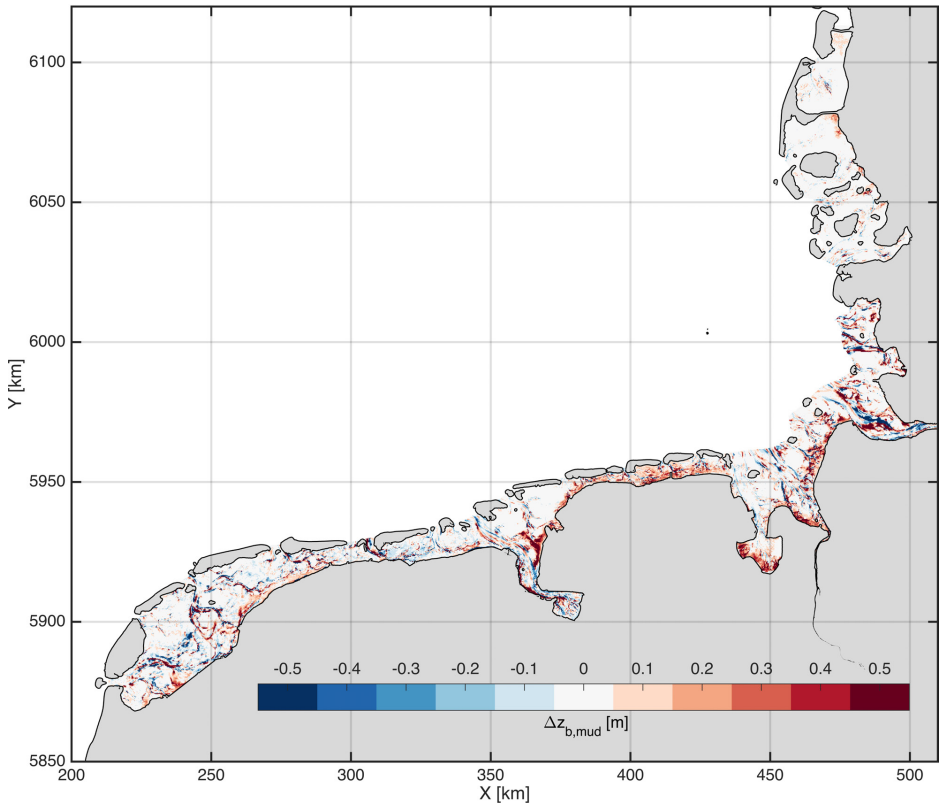

Figure A.1: Mud deposition in the Wadden Sea basins. Red colors indicate net deposition, blue colors net erosion. Net sedimentation and erosion volumes (ΔV) are calculated by subtracting measured bathymetries. These volumes are multiplied with the volumetric mud fraction in the bed to obtain the volumetric contribution of mud (ΔV_{mud}). The calculations are performed for the period 1996–2015 (assuming that the upper bed sediment remains constant within this period) and exclude deposition on the salt marshes. Most mud deposition takes place on the intertidal flats, especially those connected to the mainland coast.

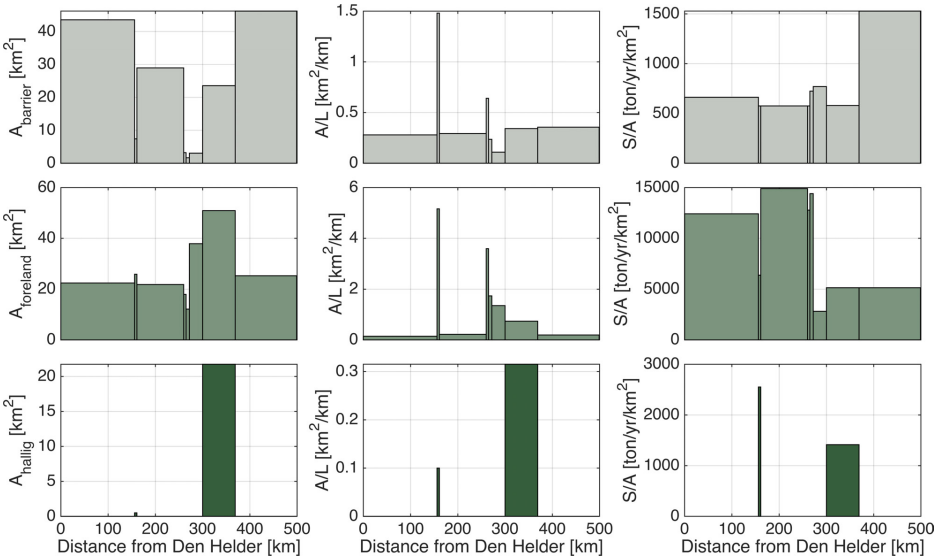

Figure A.2: Salt marsh extent and sinks in the Wadden Sea. Salt marsh types are divided into barrier (connected to the barrier islands in the lee of a dune ridge), foreland (on the mainland coasts of the Netherlands, Germany and Denmark) and hallig (which have developed on a remnant part of the historic mainland, and are not protected by a seawall). Plots on the left column show the total area of the three types of marsh, plotted against the distance form Den Helder (i.e., following the Wadden Sea coast from the West, moving East and North). The middle plots show the area extent per length along the Wadden Sea coast. The right plots show the total mud sinks on the marshes, per km^2 (note the differences in y-axes between the different marsh types). While barrier and foreland salt marshes have a similar total area, the mud budget is much more influenced by the development of the foreland marshes, since accretion rates (and thus also mud deposition) is up to 20–30 times larger.

B

SUPPORTING INFORMATION FOR CHAPTER 4

B.1. MODEL SET-UP

This appendix contains the supporting information for Chapter 4, providing additional information about the numerical model set-up. Model files have been added to a separate repository (https://doi.org/10.4121/21431427). Figure B.1 provides an overview of the model set-up. Table B.1 summarizes the main numerical Delft3D settings (see also Lesser et al., 2004). The initial sediment composition and the suspended mud concentration at the boundary are based on Wadden Sea sediment data (from the *Sediment Atlas* and *SIBES* data sets, see Colina Alonso et al., 2021, 2022) and suspended sediment concentration measurements in the North Sea (*MWTL* data).

This appendix has been published as supporting information for the following article in *Journal of Geophysical Research: Earth Surface*:

Colina Alonso, A., van Maren, D. S., van Weerdenburg, R. J. A., Huismans, Y. & Wang, Z. B. (2023). Morphodynamic modeling of tidal basins: The role of sand-mud interaction. *Journal of Geophysical Research: Earth Surface, 128*, e2023JF007391. [Link]

Table B.1: Numerical Delft3D settings

Parameter	Value	Description
Δt	30	Computational timestep [s]
R	W	Type of bottom friction formulation [-]
ThTrLyr	0.1	Thickness of the transport layer [m]
MxNULyr	20	Number of underlayers [-]
ThUnLyr	1	Thickness of each underlayer [m]

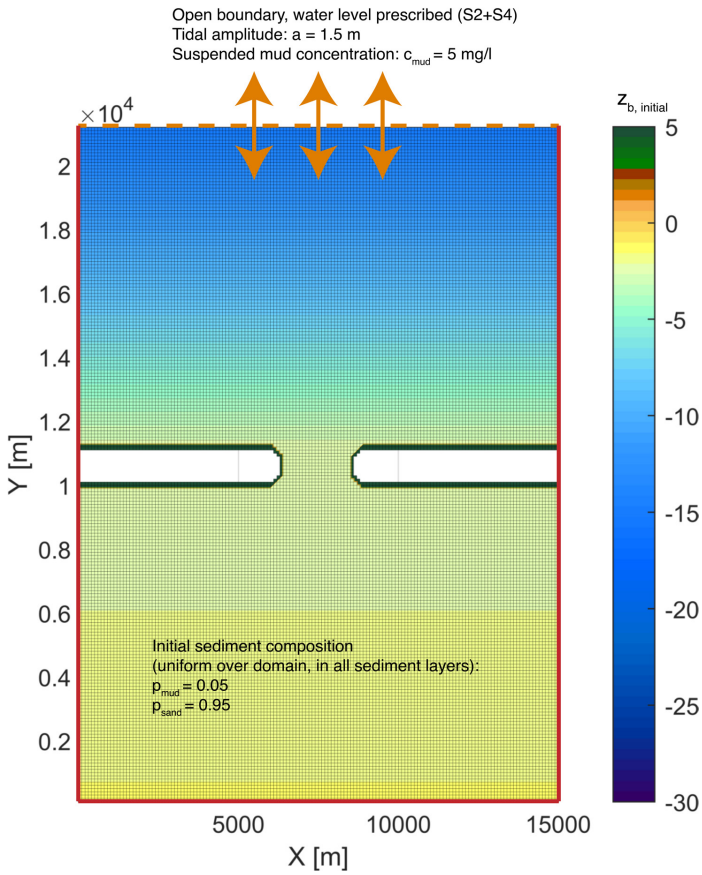

Figure B.1: Overview of the model set-up, showing the initial bathymetry, closed boundaries (red lines), open boundary (orange dashed line) and the computational grid (for both flow and wave computations, with a resolution of 100 $\times$ 100 m.)

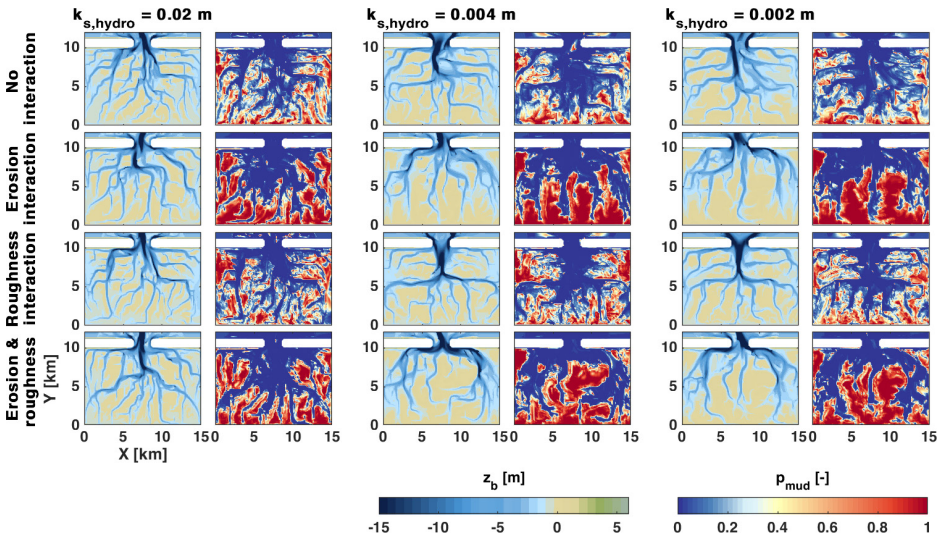

Figure B.2: Modeled morphological evolution (50 years) of a synthetic tidal basin for a range of roughness and sand-mud interaction settings. In all scenarios, the critical bed shear stress for mud erosion (τ_e) is set to 0.5 Pa. The left plots show the computed bed levels and the right plots the mud content of the upper bed (0.1 m).

B.2. SENSITIVITY ANALYSIS: BEDFORM ROUGHNESS

A sensitivity analysis is performed of the modeled morphodynamic evolution to the bedform roughness. This is done by performing simulations for all sand-mud interaction scenarios with a varying total roughness height of $k_{s,hydro}$ = 0.02 m (representing the predominantly sandy bedforms found in the Wadden Sea), $k_{s,hydro}$ = 0.004 m and $k_{s,hydro}$ = 0.002 m. The bedform-related roughness height is used in the hydrodynamic calculations, whereas the morphological calculations only make use of the skin friction (which is much smaller and only varies within the different sand-mud interaction mechanisms), since the water-bed exchange processes are determined by the processes in a thin layer above the bed (Winterwerp et al., 2021).

Figure B.2 shows that the modeled morphodynamic evolution is only limitedly influenced by the choice for $k_{s,hydro}$. In general, the bathymetry becomes smoother with a decreasing $k_{s,hydro}$, and smaller shoals tend to merge into larger ones. However, these differences are much smaller than those that are caused by the sand-mud interaction settings and the choice for τ_e. This is also reflected in the hypsometry and the development of (sandy and muddy) intertidal areas under varying roughness settings (Figure B.3). Also with smaller $k_{s,hydro}$ values, the bimodality of the mud content can only be reproduced when accounting for sand-mud interaction in the model (Figure B.4).

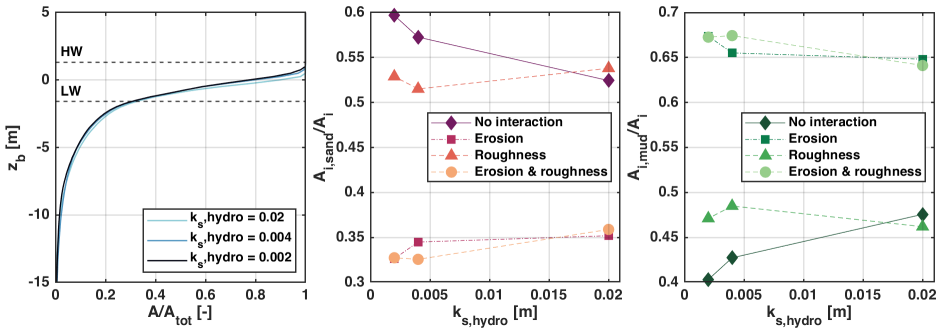

Figure B.3: Average hypsometry for each $k_{s,hydro}$ scenario (left panel) and development of the sandy (middle panel) and muddy (right panel) intertidal areas depending on the bottom roughness.

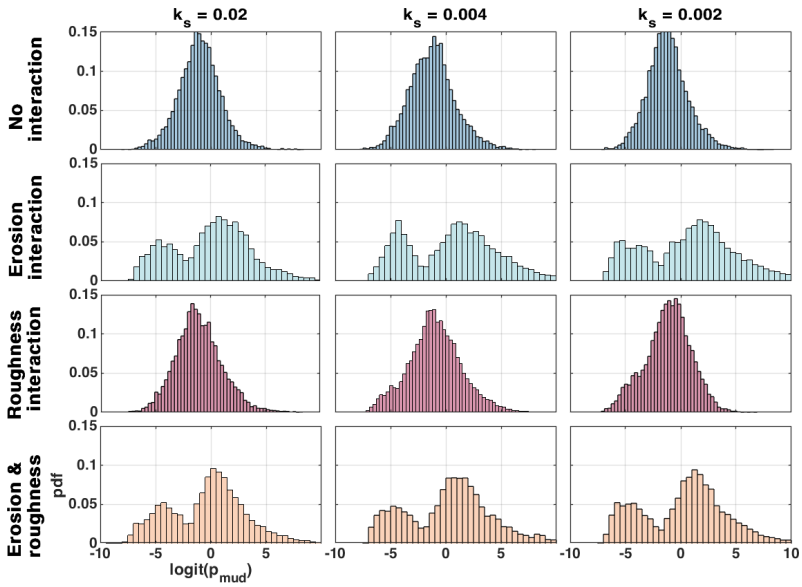

Figure B.4: Distribution of the (logit-transformed) mud content in the upper sediment bed of the numerical models for different $k_{s,hydro}$ and sand-mud interaction settings.

C

SUPPORTING INFORMATION FOR CHAPTER 5

C.1. WADDEN SEA (DELFT3D FM) NUMERICAL MODEL

The numerical model of the Wadden Sea set-up by van Weerdenburg et al. (2021) allows us to study the local hydrodynamics and corresponding sediment dynamics in the Dutch Wadden Sea. The model was used to simulate tides and calculated tide averaged sand concentrations. The model is set-up in Delft3D Flexible Mesh (FM). We used a model bathymetry that was based on bathymetric surveys from 2014 to 2017, representing recent bed levels. Water level boundary conditions prescribed at the boundaries were derived from the DCSMv6-ZUNOv4 model with Kalman filtering of the northwest European shelf (Zijl et al., 2013; van Weerdenburg et al., 2021). Instantaneous near-bed suspended concentrations of sand were calculated by a sand transport model which assumes that sediment concentrations in the water column are determined by local conditions (valid for sand). This transport model is based on van Rijn (2007a, 2007b), and is explained in more detail by Grasmeijer et al. (2022). Calculations were performed using a sand fraction with $D_{50} = 250$ μm. Figures C.1 and C.2 show the model schematization.

C.2. SCHEMATIZED TIDAL INLET (DELFT3D 4) NUMERICAL MODEL

A schematized model of a tidal inlet was set up for this study. The tidal inlet is located between two barrier islands and south of these there is a basin of 15 $\times$ 10 km. The computational grid consists of squares of 100 m $\times$ 100 m. The model has one open boundary, which is the open sea boundary in the North. Here, a tidal water level variation is pre-

This appendix has been published as supporting information for the following article in *Geophysical Research Letters*:

Colina Alonso, A., van Maren, D. S., Herman, P. M. J., van Weerdenburg, R. J. A., Huismans, Y., Holthuijsen, S. J., Govers, L. L., Bijleveld, A. I., & Wang, Z. B. (2022). The existence and origin of multiple equilibria in sand-mud sediment beds. *Geophysical Research Letters, 49*, e2022GL101141. [Link]

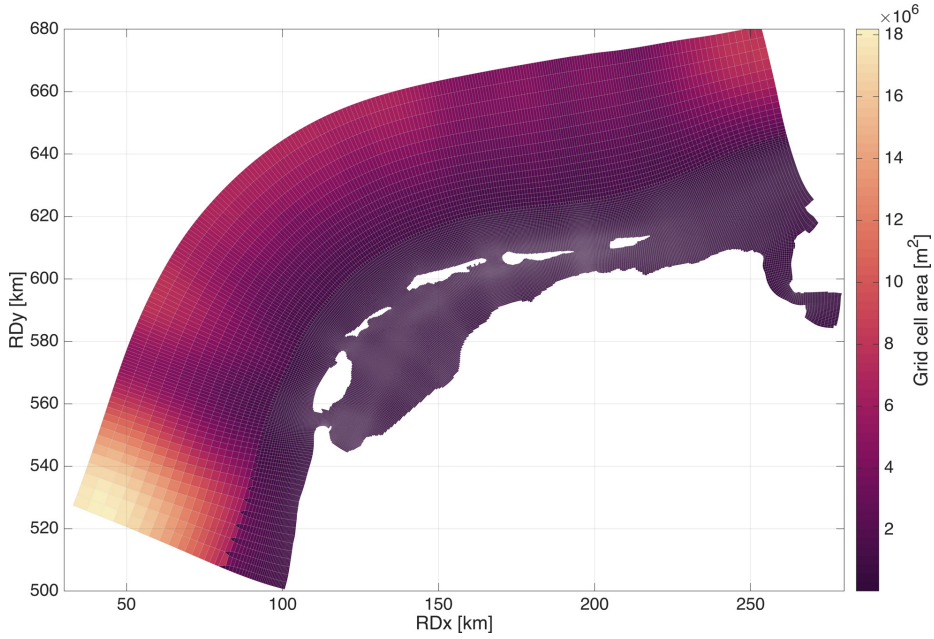

Figure C.1: Computational grid of the Wadden Sea Delft3D FM model

scribed consisting of an S2 tidal signal set to 1.35 m (ϕ = 0) and an S4 tidal signal of 0.15 m (ϕ = 180°). The maximum amplitude of the water level variation is 1.5 m. A wave model (Delft3D-WAVE) is coupled to the Delft3D-FLOW model to simulate locally generated wind waves. The wind conditions are such that there is alternating periods with mild, moderate and moderately strong winds from multiple directions. Mild and moderate winds are mainly coming from the southwest, whereas moderately strong winds are comping from the north-western direction. The bed shear stresses under combined currents and waves are calculated according to Soulsby and Clarke (2005).

The initial topography is a gradually sloping bed (see Figure C.3) with a uniform sediment composition (p_{sand} = 0.95, p_{mud} = 0.05). The dynamics of two sediment fractions are modeled, namely one sand fraction (median sediment diameter D_{50} of 250 μm) and one mud fraction (settling velocity w_s = 0.25 mm/s, critical shear stress for erosion τ_e = 0.25 Pa). The mud concentration at the offshore open boundary is set to 5 mg/l and the sand concentration at the boundary is at local equilibrium. Sand-mud erosion interaction is accounted for using the formulations by van Ledden (2003), in which non-cohesive sediment transport is calculated with van Rijn (1993) transport formulations, and cohesive sediment transport with the Partheniades-Krone formulation (Partheniades, 1965). We work with a stratified bed with on top an active transport layer of 0.1 m. Below the transport layer, 20 Eulerian sediment layers of 1 m thickness are prescribed. Initially, all bed layers have the same sediment composition. The model is run for 50 years, to simulate long-term basin evolution. Figure C.4 shows the bathymetry after this simulation period.

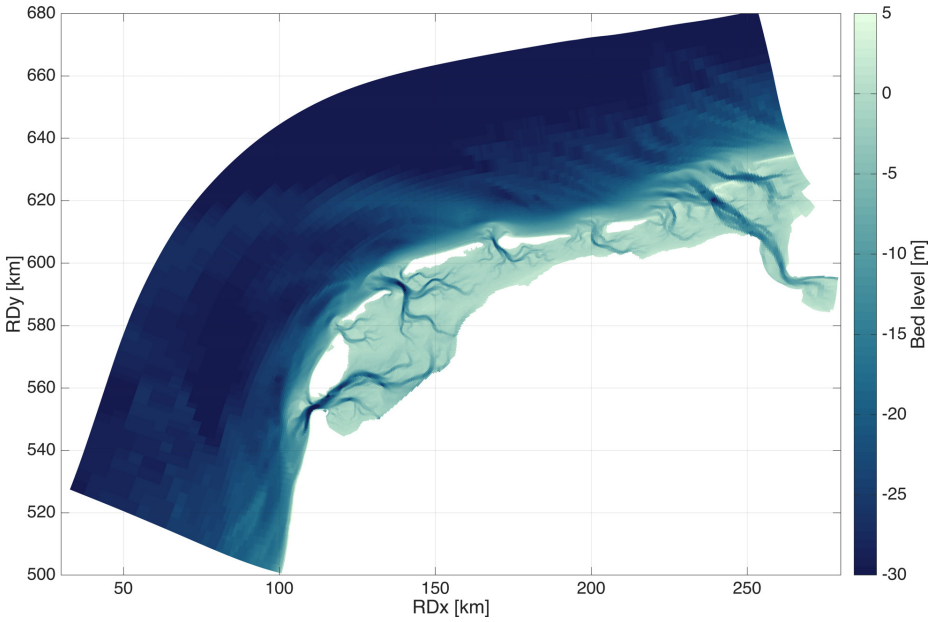

Figure C.2: Bathymetry of the Wadden Sea Delft3D FM model

The main parameter settings are summarized in Table C.1.

C.3. SUSPENDED SEDIMENT CONCENTRATIONS IN THE WADDEN SEA

Within the long-term monitoring program of the Dutch Ministry of Transport (*MWTL*), suspended suspended sediment concentrations in the Wadden Sea have been regularly measured since 1973. Measurements have been carried out in over 50 stations on a monthly to bimonthly basis, although currently only 10 station are still actively measured. Shipboard measurements are performed in the channels, where water samples (with a fixed volume) are taken at 1 m water depth, after which the suspended matter is filtered with a fiberglass filter. Next, remaining salt is being removed and the filters are dried and weighted to determine the remaining sediment mass (and thus the suspended sediment concentration in mg/l).

This data gives insight in the overall trends of the sediment concentrations in the Dutch Wadden Sea. Figure C.5 shows the long-term averaged suspended sediment concentrations. Since concentrations are measured close to the water surface in relatively deep areas (depth $>$ 5 m), the observed suspended sediment is assumed to be mainly mud. In general, concentrations tend to increase in eastward direction, with the highest concentrations found in the Ems Estuary. The average near-surface mud concentration in the Wadden Sea is 67 mg/l. Following a Rouse profile, the near-bed mud concentrations are assumed to be 2–3 times higher.

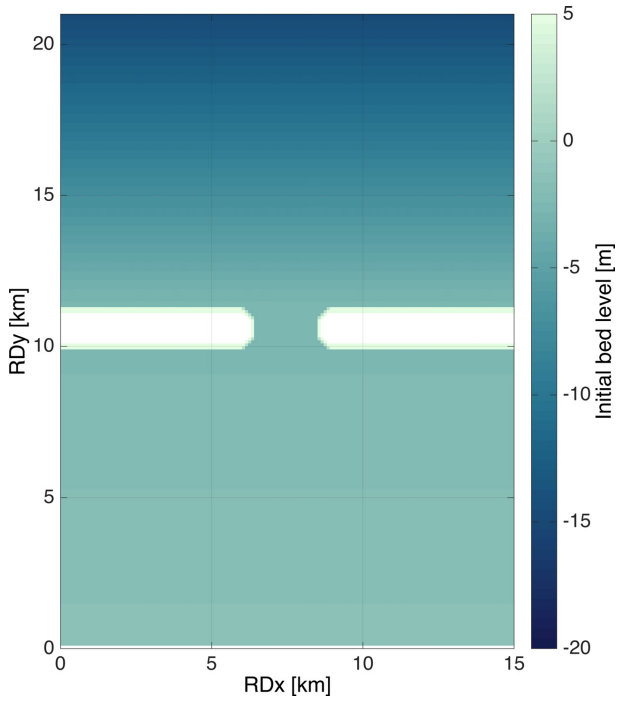

Figure C.3: Initial bathymetry of the schematized tidal basin model

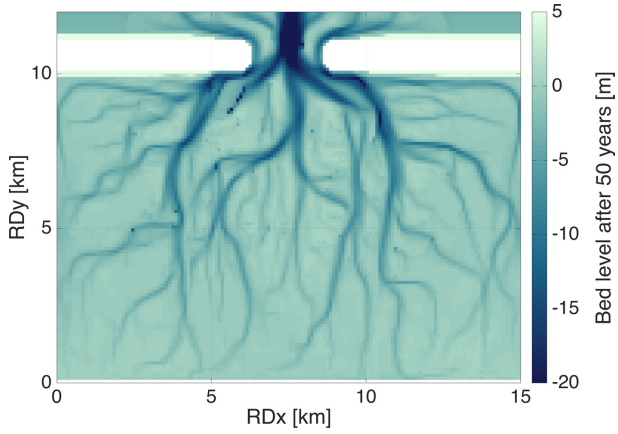

Figure C.4: Bathymetry after simulating 50 years of evolution of the schematized tidal basin model

Table C.1: Model parameter settings

Parameter	Value	Description
Δt	30	Computational timestep [s]
Roumet	W	Type of bottom friction formulation [-]
$k_{s,sand}$	6e-4	Nikuradse roughness height for sand [m]
$k_{s,silt}$	6e-5	Nikuradse roughness height for mud [m]
MorFac	50	Morphological scale factor [-]
MorStt	720	Spin-up interval for start of morphological changes [min]
D_{50}	250	Median grain diameter of sand [μm]
w_s	2.5e-4	Settling velocity of mud [m/s]
τ_e	0.25	Critical bed shear stress for erosion of mud [N/m^2]
M	1e-4	Erosion parameter [m/s]
$p_{mud,crit}$	0.3	Critical mud content for cohesive behavior [-]
ThTrLyr	0.1	Thickness of the transport layer [m]
MxNULyr	20	Number of underlayers [-]
ThUnLyr	1	Thickness of each underlayer [m]

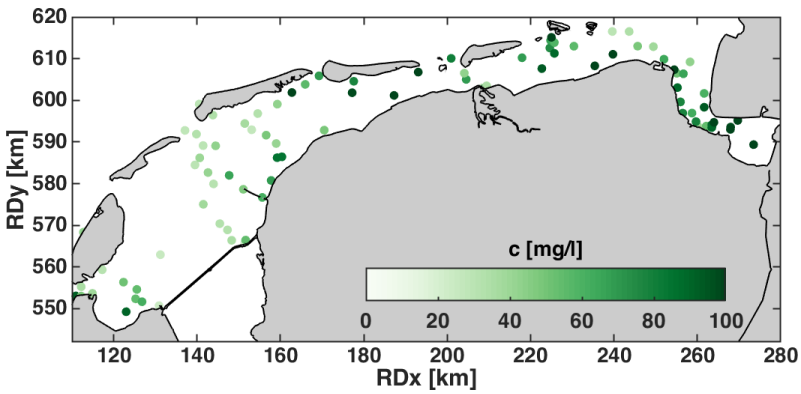

Figure C.5: Suspended sediment concentrations in the Wadden Sea, based on long-term average of the *MWTL* data

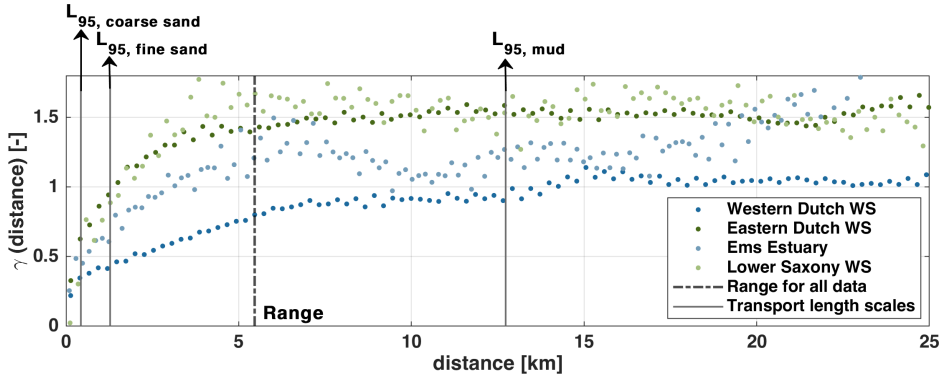

Figure C.6: Autocorrelation of p_{mud} in the bed (based on sediment samples) and 95 percentile length scales (L_{95}) of sediment transport per sediment class. γ assesses the average decrease in similarity between two random variables (p_{mud}) as the distance between the variables increases. Individual semivariograms are calculated following Schwanghart (2022) and the overall range is calculated using ArcGIS Pro software.

C.4. SEDIMENT TRANSPORT LENGTH SCALES AND VARIOGRAM OF p_{mud}

The length scale associated with sediment transport can be defined as:

$$L = \frac{hu}{w_s}, \tag{C.1}$$

in which h is the depth, u the depth-averaged velocity and w_s the settling velocity of the corresponding sediment type. This is also the spatial scale over which deposition (D_{sand}, D_{mud}) can take place. The 95 percentile transport length scales of coarse and fine sand are in the order of 400–1,400 m, whereas for mud this is about 13 km (showing that mud can be transported over much larger distances). The variogram of p_{mud} shows the inter-dependency of the observed mud content as a function of distance. Variograms were calculated for 4 sub-areas (Western Dutch WS, Eastern Dutch WS, Ems Estuary and Lower Saxony WS) following Schwanghart (2022). In addition, the range of the entire data set was calculated, which shows the distance at which the data are no longer spatially correlated (5,464 m). This range is much larger than the 95 percentile transport spatial scales associated with D_{sand}, showing that transport of sand is limited, which validates the assumption of correlation between D_{sand} and the local values of p_{mud}. On the other hand, transport of mud can take place over much larger scales, which explains why D_{mud} is does not necessarily depend on the local conditions, and why a direct correlation with the local p_{mud} was not found.

C.5. RELATION BETWEEN p_{mud} AND c_{sand}

The relation between the near-bed suspended sand concentration (c_{sand}) and the local mud content in the sediment bed (p_{mud}) was studied in two ways:

- First, the relation was studied for the Wadden Sea, by calculating tide-averaged

near-bed sand concentrations with a numerical model and comparing these with the measured bed composition (see Chapter 5).

- In addition, this relation was studied for a generalized case with a numerical model of a schematized tidal inlet. In this model we simulated hydrodynamics, sand-mud sediment transport and morphodynamic evolution, enabling us to compare the modeled suspended sand/mud concentrations with the modeled bed composition.

We found that the relation between c_{sand} and p_{mud} can be schematized with a sigmoidal fit. We used one fit to summarize the findings of both models. This relation is as follows:

$$c_{sand} = \frac{1.8}{(1 + e^{(400 * p_{mud})})^{0.1}} + 0.004 \tag{C.2}$$

ACKNOWLEDGEMENTS

When I started my PhD, I was thrilled to embark on this new adventure, but I also feared it would be a somehow lonely ride. Luckily, I look back on a journey full of companionship, which I am tremendously grateful for. Even more, this thesis would have not been the same — and probably wouldn't have been there at all — without all the people that have surrounded me in the past years, both professionally and personally.

To start with, I would like to thank my promotors Zheng Bing Wang and Bas van Maren. Wang, thank you for your guidance and for the trust you have put in me since I started working on my MSc. thesis with you. I knew I could always rely on the critical and constructive point of view you bring to the table. Your ability to pinpoint fundamental issues within seconds will never cease to amaze me. I am also incredibly grateful for the freedom you have given me to shape this research my way. Bas, I truly don't know where to start. You have been an expert advisor, daily supervisor, strategic counsellor and a mentor all in one. Thank you for teaching and encouraging me to maintain a balance between pragmatism and perfectionism. Besides this being a great help in finishing a PhD in time, I think I will benefit from it the rest of my life. Thank you for your enthusiasm towards my work, for helping me solve problems that I could not have solved myself, for the thorough reviews on everything I've written, and also for the many fun chats we've had. I truly mean it when I say I couldn't have wished for a better supervisor.

To Bram van Prooijen and Peter Herman: Bram, back in 2018 you introduced me to the world of coastal research during my first NCK-days. It was then when I realized doing a PhD might really be something I would like. Thank you for this, and for always transmitting so much contagious enthusiasm (whether it's about sediment dynamics, conferences or songs we have written for graduating PhD students). You created a great atmosphere in the lab. Peter, I vividly remember the first piece of advice you gave me four years ago: you suggested to me not to be too goal oriented and to allow myself to wonder and see where my research would end up (even though this might be nowhere). As you probably noticed back then, this goes fully against my nature — not knowing where I'm going and why I'm going there secretly frightens me — but I have tried my best to do so. Our bimodality work really took some wondering, but looking back, this is the part of the thesis that I am most proud of and that I enjoyed most working on. Many, many thanks for your guidance.

I also want to thank those who directly and indirectly contributed to my research through paper-collaborations and reviews. Sander Holthuijsen, Allert Bijleveld and Laura Govers, thank you for your enthusiasm towards my research and for making it possible to work with the SIBES data. Edwin Elias, many thanks for sharing your immense knowledge on sediment budgets and for your critical point of view that one can always trust

on. Albert Oost, thank you for setting up the initial mud budget with me. What started as a relatively small project has now turned into a chapter of this thesis and a publication. Frank Kösters, Robert Lepper and Jesper Bartholdy, your contributions through data & knowledge of the Wadden Sea have been invaluable and I want to thank you for a very pleasant collaboration. Ymkje Huismans, thank you for looking for the interfaces between Deltares projects and my PhD research with me, starting fruitful collaborations that have led to multiple papers. And of course, also Bert Jagers, thank you for patiently answering all of my Delft3D questions and for making the changes to the source code possible. I also want to thank the reviewers of my publications for their efforts: it wasn't always easy and we did not always agree, but eventually my work has absolutely benefited from your point of view. Also many thanks to the independent members of my committee, Mathijs van Ledden, Maarten Kleinhans, Sergio Fagherazzi, Qing He, Stefan Aarninkhof and Ad Reniers for their time, efforts and interest.

I have spent most of my PhD days in the Waterlab, surrounded by amazing colleagues who, simply put, made it so much more fun. To my paranymphs, Jill and Clàudia: I am so happy I got to do this with both of you by my side and I am immensely grateful for your friendship the past years. Jill, you are amazing: fun, trustworthy, hardworking, positive, and always keeping an eye on others. I am in absolute awe of your strength (both mentally and physically!). I also want to thank you and Erik for one of the best parties we've had as a group. I had so much fun, and so much dancing talent was unlocked and discovered that evening. Clàudia, thank you for being my Spanish secure base in the lab. Besides being incredibly multi-talented and hardworking, you have an amazing ability to self reflect. I'm sure you will do great things and I hope I will be not too far away to celebrate all of your successes (and to simply have breakfast together every once in a while). Patricia and Alejandra, thank you for filling our office with warmth and kindness. Patri, you have shown us that one can be sensitive and caring, while also being very, very powerful. Thank you for setting this example, I wish everybody could learn this from you. Ale, your fight for justice is inspiring. Thank you for being our joint ethical compass or a supportive cheerleader when we most needed one. Nici and Lodewijk: thank you for your guidance (especially when I was still a PhD rookie) and for checking up on how I was doing. A simple "Vind je het nog leuk?" (up to the very last moment) meant a lot. Stuart, thank you being such an awesome colleague and friend since the first time we met. I really admire how you always seem to find the time and energy to help others. You have the ability to make us feel heard and supported, and you're the best Coastal Engineering ambassador any university could wish for. Matt, thank you for the good vibes, sarcastic jokes and Modern Family imitations. We've missed you here. Kifayath, thank you for the calmness you transmit in our office. Kshitiz, thank you for having the loudest laugh of the lab. Your positive energy radiates through the office walls. To the fish tank: Jelle, Chit, Jianwei and Shelby: you guys have created an amazing atmosphere. Thank you so much for your kindness, silly jokes and for your support (in good and bad times; I especially loved how you were always up for celebrating successes together). I am in awe of your dedication and hard work combined with fun. Xin, you made me laugh a lot. Wim, thank you for the many inspiring talks during our lunches. I hope you will still teach me how to make seitan one day. Thank you also to the new ones (Kieran, Eki and Amber;

it feels like you have always been here) to the ones that left already a while ago (Yorick, Erik, Viktor, Gonzalo, Merel, Irene, Marco, Zeinab, Maria; you have been great examples on how to be a researcher and a lab member) and to those that I did not work directly with, but who absolutely contributed to the good vibes (Laura, Nina, Kees, Erik, Astrid, Claire, Chantal, Pieter). Also many thanks to my coastal colleagues on the 3rd floor. A special shoutout to those that I went to conferences with. Su, Paul, Jakob, Floris, Gijs, Anne, Christa and all the others: I had an amazing time abroad with you. And not to forget, Otti and Inge, thank you for your administrative support throughout the entire PhD process.

While working on my PhD at the TU Delft, I have had the privilege to work for Deltares. I want to thank my managers, Dirk-Jan Walstra, Bob Hoogendoorn and now Bart Grasmeijer, for their trust and flexibility. You have given me the opportunity to collaborate with incredibly smart and talented people on challenging projects in which my PhD findings were directly put into practice. This has been invaluable for my PhD progress, as well as for my personal growth. I also want to thank my AMO colleagues for everything they have taught me, for their interest in what I do, and especially for making me feel part of the team even though I was only there one day a week. Also a big thank you to my colleagues from ESD, for allowing me into their muddy world. A special thanks goes out to Roy, for being my fellow sand-mud enthusiast and for all the fun chats we've had over the past years. I already look forward to reading your thesis.

I am lucky that there is also a significant part of my life filled with people that have absolutely nothing to do with research, but who have been a fundamental part of my spare time. To my friends (who I will not mention by name, simply because I'm afraid I will forget someone): you have been the best distraction I could have wished for. Thank you for showing interest in what I do, and especially for subsequently reminding me there is so much more in life. I am tremendously grateful for the love and support of my family. Maria, bedankt dat je me erop wijst dat dingen ook anders (lees: relaxter) kunnen. Zonder jouw relativerende vermogen en de bijbehorende adviezen ("druk maken is voor compressors") zou het leven een stuk ingewikkelder zijn. Ik ben onwijs trots op alles wat je tot nu hebt bereikt en hoe je je blijft ontwikkelen. Papá y mamá, mil gracias por vuestro apoyo y por creer en mí. Mamá, desde pequeña me enseñaste a trabajar duro. Sin esta ética de trabajo no hubiese terminado nunca la tesis. Papá, gracias por tus consejos (aunque no siempre me guste admitirlo, te suelo hacer caso) y en especial por enseñarme a disfrutar resolviendo problemas complejos en lugar de temerlos. En tenslotte ook René: dit werk is ook zeker mede dankzij jou mogelijk gemaakt. Bedankt voor je liefde, steun, je zorgen, voor het meedenken, voor dat je me altijd uitdaagt om de beste versie van mezelf te zijn én om me op zo veel mogelijk vlakken te ontwikkelen... maar vooral dank je wel dat je het leven zo waanzinnig veel leuker maakt.

Ana Colina Alonso
Rotterdam, January 21st, 2024

ABOUT THE AUTHOR

Ana Colina Alonso was born on the 16th of March 1993 in Madrid, Spain. In 2001, she moved to the Netherlands together with her parents and sister. In 2011, she concluded her secondary education (gynasium, vwo) at Van Maerlantlyceum in Eindhoven, after which she moved to Delft to pursue a BSc. in Architecture, Urbanism & the Built Environment. Furthermore, she minored in Civil Engineering and discovered the world of Hydraulic Engineering. Through a MSc. degree of Delft University of Technology, she specialized in Coastal Engineering and graduated *cum laude*. While working on her MSc. thesis at Deltares, she had the opportunity to present her results at the Dutch national conference for coastal research (NCK), where she discovered her strong interest for research. She started her PhD in the Coastal Engineering section at Delft University of Technology in September 2018, and also continued working part-time as a researcher and advisor in the Applied Morphodynamics department at Deltares. Ana lives in Rotterdam together with her partner. In her spare time, she mostly enjoys spending time with friends and family — whether it's during dinners, sports sessions, weekend getaways or year-round ocean swims.

LIST OF PUBLICATIONS

JOURNAL ARTICLES

FIRST AUTHOR

4. **Colina Alonso, A.**, van Maren, D. S., Oost, A. P., Esselink, P., Hagen, R., Kösters, F., Bartholdy, J., Bijleveld, A. I., & Wang, Z. B. (conditionally accepted at *Communications Earth & Environment*). A mud budget of the Wadden Sea and its implications for sediment management. [Chapter 3]

3. **Colina Alonso, A.**, van Maren, D. S., van Weerdenburg, R. J. A., Huismans, Y. & Wang, Z. B. (2023). Morphodynamic modeling of tidal basins: The role of sand-mud interaction. *Journal of Geophysical Research: Earth Surface, 128*, e2023JF007391. [Link, Chapter 4]

2. **Colina Alonso, A.**, van Maren, D. S., Herman, P. M. J., van Weerdenburg, R. J. A., Huismans, Y., Holthuijsen, S. J., Govers, L. L., Bijleveld, A. I., & Wang, Z. B. (2022). The existence and origin of multiple equilibria in sand-mud sediment beds. *Geophysical Research Letters, 49*, e2022GL101141. [Link, Chapter 5]

1. **Colina Alonso, A.**, van Maren, D. S., Elias, E. P. L., Holthuijsen, S. J., & Wang, Z. B. (2021). The contribution of sand and mud to infilling of tidal basins in response to a closure dam. *Marine Geology, 439*, 106544. [Link, Chapter 2]

CO-AUTHOR

1. van Maren, D. S., **Colina Alonso, A.**, Engels, A., Vandenbruwaene, W., de Vet, P. L. M., Vroom J. & Wang, Z. B. (2023). Adaptation timescales of estuarine systems to human interventions. *Frontiers in Earth Science 11*, 1–18 doi: 10.3389/feart.2023.1111530. [Link]

CONFERENCE PROCEEDINGS AND TALKS

FIRST AUTHOR

12. **Colina Alonso, A.**, van Maren, D. S. & Wang, Z. B. (2023). Controls of the sediment composition in tidal systems. INTERCOH 2023, Incheon, South Korea, September 2023.

11. **Colina Alonso, A.**, van Maren, D. S., van Weerdenburg, R. J. A., Huismans, Y. & Wang, Z. B. (2023). Improving morphodynamic modelling using sand-mud interaction and morphologic metrics. NCK Days 2023, Delft, the Netherlands, March 2023.

10. **Colina Alonso, A.**, van Maren, D. S., Herman, P. M. J., & Wang, Z. B. (2022). Factors Controlling the Equilibrium Sediment Composition in Sand-Mud Tidal Basins. 37th International Conference on Coastal Engineering 2022 (ICCE), Sydney, NSW, Australia, December 2022.

9. **Colina Alonso, A.**, Oost, A. P., Esselink, P., Wang, Z. B. & van Maren, D. S. (2022). Findings and Implications of a First Mud Budget for The Wadden Sea. Ocean Sciences Meeting 2022 (OSM), Online Conference due to COVID-19, February 2022.

8. **Colina Alonso, A.**, van Maren, D. S., van Weerdenburg, R. J. A., Huismans, Y., Herman, P. M. J., & Wang, Z. B. (2021). On the large-scale effects of small-scale sand-mud interaction. 7th International Conference on Estuaries and Coasts (ICEC): Anthropocene Coasts, Online Conference due to COVID-19, October 2021.

7. **Colina Alonso, A.**, van Maren, D. S., Herman, P. M. J., van Weerdenburg, R. J. A., Huismans, Y., & Wang, Z. B. (2021). Feedback loops arising from sand-mud interaction cause bimodal mud contents. INTERCOH 2021, Delft, the Netherlands, September 2021.
    - ***Awarded 1st Place - INTERCOH Ray Krone Award***

6. **Colina Alonso, A.**, van Maren, D. S., Elias, E. P. L., Holthuijsen, S. J., & Wang, Z. B. (2021). The contribution of sand and mud to infilling of the Western Wadden Sea. NCK Days 2021, Online Conference due to COVID-19, March 2021.

5. **Colina Alonso, A.**, Oost, A. P., Esselink, P., Wang, Z. B., van Kessel, T. & van Maren, D. S. (2021). Towards a Mud Budget for the Trilateral Wadden Sea. NCK Days 2021, Online Conference due to COVID-19, March 2021.
    - ***Keynote Speaker***

4. **Colina Alonso, A.**, van Maren, D. S., Wang, Z. B. & Herman, P. M. J. (2020). Understanding sand-mud interaction and its large-scale impact on tidal basins. NCK Days 2020, cancelled due to COVID-19.

3. **Colina Alonso, A.**, van Maren, D. S., Wang, Z. B. & Herman, P. M. J. (2019). Towards an understanding of sand-mud segregation in tidal basins. 11th River, Coastal and Estuarine Morphodynamics Symposium (RCEM), Auckland, New Zealand, November 2019.

2. **Colina Alonso, A.**, van Maren, D. S., Wang, Z. B. & Herman, P. M. J. (2019). Analysing the large-scale impact of the Afsluitdijk on the sediment patterns in the Western Wadden Sea. NCK Days 2019, Enkhuizen, the Netherlands, March 2019.
    - ***Awarded Best Poster Presentation***

1. **Colina Alonso, A.** Wang, Z. B., van Prooijen, B. C., Walstra, D. J. R., Tonnon, P. K. & de Vet, P. L. M. (2018). Unravelling the mechanisms behind the morphodynamic evolution of the Haringvliet ebb-tidal delta. NCK Days 2018, Haarlem, the Netherlands, March 2018.

CO-AUTHOR

5. van Weerdenburg, R. J. A., **Colina Alonso, A.**, van Maren, D. S., van Rijn, L. C., Boechat Albernaz, M. & Huismans, Y. (2023). Flume modelling to investigate the erosion of sand-mud mixtures under currents and waves in the laboratory and in Delft3D. NCK Days 2023, Delft, the Netherlands, March 2023.

4. Naidoo, J., Elmilady, H. M., **Colina Alonso, A.**, Dastgheib, A. & van der Wegen, M. (2023). Development of tidal flats under sea level rise. NCK Days 2023, Delft, the Netherlands, March 2023.

3. Vroom, J., Smits, B. P., van Weerdenburg, R. J. A., **Colina Alonso, A.**, de Vries, J. & Lofvers, E. (2023). What are the causes for the unexpected high dredging volumes in the navigation channel Boontjes in the Wadden Sea? NCK Days 2023, Delft, the Netherlands, March 2023.

2. Huismans, Y., Huisman, B., **Colina Alonso, A.**, van der Vegt, H. & van der Wegen, M. (2020). Sediment management in the Western Scheldt: the morphodynamic response to sediment disposal in deep pits. NCK Days 2021, cancelled due to COVID-19.

1. Groenewegen, M. Q. T., de Vries, S., **Colina Alonso, A.**, Abraimi, R., Tonnon, P.K & Aarninkhof, S. G. J. (2020). Morphological development of the Bollen van de Ooster: A potential hazard for Goeree-Overflakkee? NCK Days 2021, cancelled due to COVID-19.

SCIENTIFIC REPORTS

FIRST AUTHOR

4. **Colina Alonso, A.**, Smits, B.P. & Vroom, J. (2021). Stijging *Baggerhoeveelheden Vaargeul Boontjes.* Deltares rapport 11206799-007-ZKS-0001. Delft, the Netherlands.

3. **Colina Alonso, A.**, van Weerdenburg, R.J.A., van Maren, D.S. & Huismans, Y. (2020). *Modelling sand-mud interaction in Delft3D.* Deltares report 11205286-010-ZWS-0001. Delft, the Netherlands.

2. **Colina Alonso, A.** (2020). *Evolutie van het bodemslib in de Waddenzee.* Deltares rapport 11205229-001-ZKS-0003. Delft, the Netherlands.

1. **Colina Alonso, A.** (2018). *Morphodynamics of the Haringvliet ebb-tidal delta: Unravelling the Mechanisms behind its Morphological Evolution.* MSc thesis. Delft University of Technology, Faculty of Civil Engineering and Geosciences. [Link].

CO-AUTHOR

7. van Weerdenburg, R. J. A., **Colina Alonso, A.** & van Maren, D. S. (2024). *Modelling sand-mud dynamics in Delft3D.* MUSA report 11204950-TKI-MUSA-04. Delft, the Netherlands.

6. Smits, B., Vroom, J., van Weerdenburg, R. J. A., & **Colina Alonso, A**. (2022). *Morfologie en Onderhoud Vaargeul Boontjes.* Deltares rapport 11208040-004-ZKS-0004. Delft, the Netherlands.

5. Elias, E. P. L., **Colina Alonso, A.** & van Maren, D. S. (2021). *Morfologische veranderingen Eems-Dollard en Groninger Wad.* Deltares rapport 11203742-000. Delft, the Netherlands.

4. Oost, A. P., **Colina Alonso, A.**, Esselink, P., Wang, Z. B., van Kessel, T. & van Maren, D. S. (2021). *Where Mud Matters. Towards a Mud Balance for the Trilateral Wadden Sea Area: Mud supply, transport and deposition.* Published by the Wadden Academy, report 2021-02.

3. Huismans, Y., van der Vegt, H., Huisman, B. J. A. & **Colina Alonso, A.** (2021). Westerschelde : storten in diepe putten. Technische rapportage: mesoschaal morfologische ontwikkelingen rond de Put van Hansweert 2021. Deltares rapport 1210301-015-ZKS-0011. Delft, the Netherlands.

2. van der Wegen, M., Schrijvershof, R. A., **Colina Alonso, A.**, Broekema, Y. B., Kranenburg, W. M. & Huisman, B. J. A. (2021). *Hydrodynamics in the pits of Borssele and Hansweert: data-analysis and Delft3D-FM modeling 2021.* Deltares report 1210301-015-ZKS-0007. Delft, the Netherlands.

1. Van Rijn, L. C., **Colina Alonso, A**. & Manning, A. J., (2020). *Literature review on sand and mud.* TKI MUSA report 11204950-001-ZKS-0002.

Photograph of the Wadden Sea - by Kevin Krautgartner